

DEEP INELASTIC SCATTERING BY QUANTUM LIQUIDS

BY

ALEKSANDAR BELIĆ

**Dipl., University of Belgrade, 1985
M.S., University of Illinois, 1987**

THESIS

**Submitted in partial fulfillment of the requirements
for the degree of Doctor of Philosophy in Physics
in the Graduate College of the
University of Illinois at Urbana-Champaign, 1992**

Urbana, Illinois

UNIVERSITY OF ILLINOIS AT URBANA-CHAMPAIGN

THE GRADUATE COLLEGE

JANUARY 1992

WE HEREBY RECOMMEND THAT THE THESIS BY

ALEKSANDAR BELIĆ

ENTITLED DEEP INELASTIC SCATTERING

BY QUANTUM LIQUIDS

BE ACCEPTED IN PARTIAL FULFILLMENT OF THE REQUIREMENTS FOR

THE DEGREE OF DOCTOR OF PHILOSOPHY

V.R. Pcedipde

Director of Thesis Research

A.C. Anderson

Head of Department

Committee on Final Examination†

V.R. Pcedipde

Chairperson

J.K. Lamb

J.M. Maul

M. Stone

† Required for doctor's degree but not for master's.

DEEP INELASTIC SCATTERING BY QUANTUM LIQUIDS

Aleksandar Belić, Ph. D.

Department of Physics

University of Illinois at Urbana-Champaign, 1992

Vijay R. Pandharipande, Advisor

The impulse approximation and the related concept of the scaling of the dynamic structure function $S(\mathbf{k}, \omega)$ at large k and ω have played a dominant role in the analysis of the deep inelastic neutron scattering by quantum liquids. These concepts are reviewed along with the prevalent approximations to treat final state interactions neglected in the impulse approximation.

At large momentum transfers it is convenient to express the dynamic structure function $S(\mathbf{k}, \omega)$ as the sum of a part symmetric about $\omega = k^2/2m$ and an antisymmetric part. The latter is zero in the impulse approximation, and its leading contribution is given by $(m/k)^2 J_1(y)$, where $y \equiv (m/k)(\omega - k^2/2m)$ is the usual scaling variable. The integrals of $J_1(y)$, weighted with y , y^3 and y^5 in liquid ${}^4\text{He}$ are calculated using sum-rules. Polynomial expansions are used to construct models of $J_1(y)$ which appear to be in qualitative agreement with the observed antisymmetric part at large values of k .

Next, we study the dynamic structure function $S(\mathbf{k}, \omega)$ of Bose liquids in the asymptotic limit $k, \omega \rightarrow \infty$ at constant y , using the orthogonal correlated basis of Feynman phonon states. This approach has been traditionally and successfully used to study $S(\mathbf{k}, \omega)$ at small k, ω , and it appears possible to develop it further to obtain a unified theory of $S(\mathbf{k}, \omega)$ at all k and ω . In this thesis, we prove within this approach that $S(\mathbf{k}, \omega)$ scales exactly in the $k, \omega \rightarrow \infty$ limit, as is well known. It is also shown that, within a very good approximation, the scaling function $J(y)$ is determined solely by the static structure function $S(q)$ of the liquid. In contrast, the traditional approach to determining $S(\mathbf{k}, \omega)$ at large k, ω is based on the impulse approximation; $J_{IA}(y)$ is solely determined by the momentum distribution $n(q)$ of

the particles in the liquid. In weakly interacting systems, where the impulse approximation is exact, the $J(y)$ calculated from the Feynman phonon basis is identical to $J_{IA}(y)$. The $J(y)$ of liquid ${}^4\text{He}$ is calculated using this theory and the experimental $S(q)$. It is quite similar to the $J_{IA}(y)$ obtained from the theoretical $n(q)$ of liquid ${}^4\text{He}$. A number of technical developments in orthogonal correlated basis theories are also reported.

Finally, we develop the orthogonal correlated basis formalism that is suitable for studying the dynamic structure function $S(\mathbf{k}, \omega)$ of Fermi liquids in the asymptotic limit $k, \omega \rightarrow \infty$ at constant y .

This thesis is dedicated to
Vesna
whose love, care and diligence
made it all possible.

Acknowledgements

It is a pleasure to thank my advisor, Vijay Pandharipande, for his patient guidance and support throughout the course of my graduate studies. His insights were both invaluable and inspiring.

I have benefited from the discussions with Professors. S. J. Chang, R. O. Simmons, M. Stone, and D. Pines. I wish to thank Professor M. Raether for the support during the past six and a half years, and Professor S. Milošević for steering me into this line of research.

The friendship and assistance of Fong Liu, Hrabri Rajić, Daniel Lewart, and Clovis Wotzasek was instrumental in surviving Urbana. Additional thanks go to my colleagues J. Carrubba, C. Gutleben, T. Issaevitch, R. Loucks, B. MacGibbon, J. Martinez, T. Schlagel, to my neighbors Petrovs and Sigurjonssons, and friends Boško, Agica, Obrad and Zorica for the nice times we have spent together.

This research was supported in part by U. S. Department of Energy, Division of Material Sciences grant DE-AC02-76ER01198, and the National Science Foundation grant PHY-89-21025.

Contents

Chapter

1	Introduction	1
2	Basic notions of non-relativistic deep inelastic scattering	3
2.1	Scattering experiments	3
2.2	y -scaling	6
2.3	Impulse approximation (IA)	7
2.4	Theories of final states effects	9
2.4.1	Convolution approach	9
2.4.2	Gersh series	12
2.4.3	Sum-rule arguments	17
2.4.4	Correlated basis approach	21
3	Antisymmetric part of $S(\mathbf{k}, \omega)$ of liquid ${}^4\text{He}$	23
3.1	Calculation of the y^m moments of $J(y)$ and $J_1(y)$	24
3.1.1	The proof of equation (3.8)	27
3.2	Evaluation of the antisymmetric part of $S(\mathbf{k}, \omega)$ of liquid ${}^4\text{He}$	30
3.3	Conclusions	33

4	Correlated basis theory of $S(k, \omega)$ in the scaling limit	36
4.1	CB states and their properties	36
4.1.1	Diagonal CB matrix elements	39
4.1.2	Off-diagonal CB matrix elements	42
4.2	Orthogonalization of CB states	47
4.2.1	Gram-Schmidt orthogonalization procedure	49
4.2.2	Löwdin transformation and its properties	49
4.2.3	Fantoni-Pandharipande scheme of orthogonalization	55
4.3	OCB matrix elements in scaling limit	58
4.4	OCBPT of $S(k, \omega)$	62
4.5	Scaling property of $S(k, \omega)$	64
5	Calculation of the scaling function of the Bose liquid at $T=0$	66
5.1	Calculation of the scaling function	66
5.2	Proof of the Ward identity	74
5.3	Discussion	78
5.4	Numerical results	82
5.5	Conclusions	84
6	Correlated basis theory of $S(k, \omega)$ for Fermi systems	86
6.1	The choice of the CB states	86
6.2	CB matrix elements and their properties	89
6.3	OCBPT of $S(k, \omega)$ for Fermi systems and its y -scaling property	91
	Bibliography	94
	Vita	98

Chapter 1

Introduction

In the last few years there has been a growing interest in the possibilities for experimental determination of single-particle momentum distributions in non-relativistic many-body systems by means of inelastic neutron scattering at large momentum transfers¹⁻¹¹. This interest was generated by the advent of pulsed-neutron sources that made possible measurements with substantially larger momentum transfers than before. For example, in the case of liquid ⁴He a momentum transfer of 20-30Å⁻¹ was achieved¹¹, which is much larger than the rms momentum of atoms in the liquid of $\sim 1.6\text{\AA}^{-1}$. If it is assumed that at such large momentum transfers the potentials between the atoms in the liquid are negligible compared to the large kinetic energy of the struck atom, the deep inelastic response is completely determined by the initial single-particle momentum distribution. This assumption is known as the impulse approximation (IA)^{12,13}. At large momentum transfers k , the IA response $S(\mathbf{k}, \omega)$ exhibits the phenomenon of y -scaling, i.e. the combination $\frac{k}{m}S(\mathbf{k}, \omega)$ depends solely upon the scaling variable¹² $y = \frac{m}{k}(\omega - \frac{k^2}{2m})$ and not separately on upon k and ω . However, the y -scaling property of the deep inelastic response is more general than the IA in the sense that it may hold even when the IA fails.

If the IA is valid, the momentum distribution can be extracted from the deep inelastic

response in a model-independent way. This gives rise to the exciting possibility that the momentum distribution is a directly observable quantity. If this were true not only would we be able to check the accuracy of our calculations and more reliably determine interparticle potentials, but also to test fundamental physical ideas such as bose condensation or the existence of the sharp fermi surface!

Unfortunately, in the most interesting cases, such as ^4He , ^3He , and nuclear matter, there is a strong repulsive short-ranged component in the interparticle potential which is not negligible compared to the recoil kinetic energy even for the large momentum transfers achieved in recent experiments. Thus the IA must be corrected to account for interaction of the recoiling particle with the surrounding medium. These corrections are called final state interaction (FSI) corrections^{13–33}. Clearly, it would be desirable to develop an analytic, first-principles theory of the dynamic structure function at large momentum transfers, in order to understand the FSI. In this thesis we develop such a theory based on the orthogonal correlated basis formalism^{34,35}, and apply it to the case of a quantum liquid at zero temperature.

The thesis is organized as follows. In Ch.2 we introduce the formalism of deep inelastic scattering, the concept of y -scaling, and IA, and then review various proposed theories of FSI. In Ch.3 we show how the leading antisymmetric correction to the asymptotic dynamic structure function (DSF) $S(\mathbf{k},\omega)$ can be estimated using sum rules³⁶. In Ch.4 the deep inelastic response of the bose liquid at zero temperature is formulated³⁷ in terms of orthogonal correlated basis theory, which is then used to prove the y -scaling in that case. Ch.5 deals with the explicit calculation³⁷ of the scaling function of the bose liquid at $T = 0$, and of the ^4He in particular. Finally, Ch.6 extends the formalism developed in Ch.4 to the case of a zero temperature fermi liquid, including the proof of y -scaling.³⁸

Chapter 2

Basic notions of non-relativistic deep inelastic scattering

In this chapter we will formally develop concepts of deep inelastic scattering, y -scaling, IA and review existing theories of FSI.

2.1 Scattering experiments

Inelastic scattering experiments have been a very useful tool in our efforts to investigate and understand properties of the many-body systems. In a typical scattering experiment the bound state of N interacting particles, i.e. the target, is bombarded with probes which, during the scattering process, transfer momentum \mathbf{k} and energy ω to it. If the coupling of the probes to the constituents of the target is weak, Born approximation^{39,40} is applicable and the differential cross section for the process in which final state of the target is not observed is proportional to the dynamic structure function (DSF) $S(\mathbf{k}, \omega)$ of the system.

Various types of probes (electrons, neutrons, x-rays, ...) have been used over the years to study wide variety of many-body systems (solids, liquids, atoms, nuclei, nucleons, ...) with considerable success^{41–44}. Furthermore, by choosing appropriate values for momentum

and energy transfers (\mathbf{k}, ω) the experimenter can study particular properties of the many-body system, such as collective modes or single particle dynamics.

In this thesis we will focus on the deep inelastic neutron scattering (DINS) from quantum liquids at zero temperature¹⁻¹¹. Initially the target is assumed to be a bound state of atoms containing nuclei such as ^4He with zero spin. The spin of the neutron can be ignored in this case, but we will keep track of it nonetheless in order to make the generalization to the case of scatterers with nonzero spin straightforward. Our starting point is the observation that the interaction between neutron and nucleus is short ranged, the radius of interaction being $a \sim 1\text{fm} = 10^{-5}\text{\AA}$. In typical DINS experiment neutrons of incident energy $E \sim 1\text{eV}$ are used which corresponds to the initial momentum $p \sim 20\text{\AA}^{-1}$, so that the inequality $pa \ll 1$ is satisfied by several orders of magnitude. Under such conditions neutron-nucleus scattering is isotropic, with the total cross section $\sigma = 4\pi b^2$, where b is the scattering length. Following the beautiful idea due to Fermi⁴⁵, we introduce the pseudopotential

$$U(\mathbf{r} - \mathbf{r}_j) = \frac{4\pi b}{2m} \delta(\mathbf{r} - \mathbf{r}_j) \quad (2.1)$$

to describe the interaction of neutron at \mathbf{r} with a nucleus at \mathbf{r}_j , where m is the reduced mass of neutron and a nucleus. It is easy to check that in Born approximation the scattering length b_B for potential (2.1) has precisely the exact value b :

$$b_B^2 = \frac{1}{4\pi} \sigma_B = \frac{1}{4\pi} \int d^2\Omega_{\mathbf{k}} \frac{m^2}{4\pi^2} \left| \int d^3r e^{-i\mathbf{k}\cdot\mathbf{r}} U(\mathbf{r}) \right|^2 = \frac{m^2}{4\pi^2} \left(\frac{4\pi b}{2m} \right)^2 = b^2. \quad (2.2)$$

Thus this potential gives the correct description of neutron-atom scattering at eV energies in the Born approximation, and is meant to be used with it only. The total interaction potential of neutron with the target is

$$H_{\text{int}}(\mathbf{r}) = \frac{4\pi b}{2m} \sum_j \delta(\mathbf{r} - \mathbf{r}_j) = \frac{4\pi b}{2m} \rho(\mathbf{r}), \quad (2.3)$$

where $\rho(\mathbf{r})$ is the density. For the initial and final states of neutron we use $V^{-1/2} e^{i\mathbf{p}\cdot\mathbf{r}} \eta_\lambda$ and $V^{-1/2} e^{i\mathbf{p}'\cdot\mathbf{r}} \eta_{\lambda'}$, where V is the quantization volume and η_λ 's are spin wave functions,

so that the matrix element of H_{int} for a transition with the target states $|i\rangle$ and $|f\rangle$ is

$$\frac{1}{V} \int d^3r e^{-i\mathbf{p}'\cdot\mathbf{r}} \eta_{\lambda'}^\dagger \langle f | H_{\text{int}}(\mathbf{r}) | i \rangle e^{i\mathbf{p}\cdot\mathbf{r}} \eta_\lambda = \frac{4\pi b}{2mV} \delta_{\lambda\lambda'} \langle f | \rho_{\mathbf{k}}^\dagger | i \rangle, \quad (2.4)$$

where $\mathbf{k} = \mathbf{p} - \mathbf{p}'$ is the momentum transfer to the target, and

$$\rho_{\mathbf{k}} = \sum_i e^{-i\mathbf{k}\cdot\mathbf{r}_i} \quad (2.5)$$

is Fourier component of the density. The transition rate from an initial state $|i, \mathbf{p}\lambda\rangle$ to a final state $|f, \mathbf{p}'\lambda'\rangle$ is given by the golden rule⁴⁶ as

$$T_{i\rightarrow f} = 2\pi |\langle f, \mathbf{p}'\lambda' | H_{\text{int}} | i, \mathbf{p}\lambda \rangle|^2 \delta(\omega - E_f + E_i), \quad (2.6)$$

where E_i and E_f are target energies and $\omega = (p^2 - p'^2)/2m$ is the energy lost by neutron, i.e. the energy transfer to the target. Typically DINS experiments do not resolve the final state of the target $|f\rangle$ nor the final polarization of the neutron λ' , while the initial state of neutron is usually unpolarized. At low (ideally zero) temperature the target is initially in its ground state. Under these conditions the cross section for scattering into a final neutron state in an interval $\Delta\mathbf{p}' = V d^3p'/(2\pi)^3$ is obtained by appropriate summations of $T_{i\rightarrow f}$ and dividing by the incident neutron flux $v_{\text{rel}}/V = p/mV$:

$$d^2\sigma = 2\pi \left(\frac{4\pi b}{2mV} \right)^2 \frac{1}{2} \sum_\lambda \sum_{\lambda', f} \delta_{\lambda, \lambda'} \left| \langle f | \rho_{\mathbf{k}}^\dagger | 0 \rangle \right|^2 \delta(\omega - E_f + E_0) \frac{V d^3p' mV}{(2\pi)^3 p}. \quad (2.7)$$

Using $d^3p' = mp' d\omega d\Omega'$ we can express the double differential cross section for neutron scattering into a final solid angle Ω' with an energy loss ω as

$$\frac{d^2\sigma}{d\Omega' d\omega} = \frac{Nb^2 p'}{p} S(\mathbf{k}, \omega), \quad (2.8)$$

where $S(\mathbf{k}, \omega)$ is the dynamic structure function defined as⁴⁷

$$S(\mathbf{k}, \omega) = \frac{1}{N} \sum_f \left| \langle f | \rho_{\mathbf{k}}^\dagger | 0 \rangle \right|^2 \delta(\omega - E_f + E_0). \quad (2.9)$$

2.2 y -scaling

The concept of scaling in physics refers to a situation when a function that normally depends upon several variables, under certain conditions depends only upon their particular combinations that are called scaling variables. In the case of y -scaling the function under consideration is $S(\mathbf{k}, \omega)$ which depends upon two variables. It is convenient to eliminate the energy variable ω in favor of the West scaling variable¹²

$$y \equiv \frac{m}{k}(\omega - \frac{k^2}{2m}), \quad (2.10)$$

and express $S(\mathbf{k}, \omega)$ in terms of the Compton profile⁴¹ $J(\mathbf{k}, y)$

$$J(\mathbf{k}, y) \equiv \frac{k}{m} S(\mathbf{k}, \omega = \frac{k^2}{2m} + \frac{ky}{m}). \quad (2.11)$$

This transformation is motivated by the experimental observation¹⁻¹¹ that, for large k , Compton profile of an isotropic system depends on y alone:

$$J(k, y) \longrightarrow J(y) \quad k \rightarrow \infty. \quad (2.12)$$

This property of the Compton profile is referred to as y -scaling, and $J(y)$ is called scaling function. In terms of $S(\mathbf{k}, \omega)$ the y -scaling property is expressed as

$$\frac{k}{m} S(\mathbf{k}, \omega) \longrightarrow J(y) \quad k, \omega \rightarrow \infty, \text{ at } y = \text{const}. \quad (2.13)$$

It should be stressed that y -scaling is a general property of deep inelastic response of non-relativistic systems in that it is observed and can be theoretically proved in all cases that were studied, regardless of the type of interparticle interaction.

It is less known that $S(\mathbf{k}, \omega)$ obey another scaling law³², which we mention for completeness:

$$\omega S(\mathbf{k}, \omega) \longrightarrow \delta(1-x) \quad k, \omega \rightarrow \infty, \text{ at } x \equiv \frac{k^2}{2m\omega} = \text{const}. \quad (2.14)$$

This is the non-relativistic analog of Bjorken scaling^{48,49}. Since scaling function $\delta(1-x)$ does not depend on the specific properties of the target, no information other than the

mere existence of the scattering centers can be deduced from it. But their existence in the non-relativistic condensed matter systems can be established by direct methods, and hence the concept of Bjorken scaling is not particularly useful in non-relativistic physics. On the contrary, in elementary particle physics the model independent conclusions are desirable, and Bjorken scaling is an important tool in research⁵⁰.

2.3 Impulse approximation (IA)

In order to derive the expression for $S(\mathbf{k}, \omega)$ in IA we write the Hamiltonian of the system as

$$H = H_{IA} + v_I, \quad (2.15)$$

$$H_{IA} = \sum_{i \neq I} \frac{\mathbf{p}_i^2}{2m} + \frac{1}{2} \sum_{i, j \neq I} v_{ij} + \frac{\mathbf{p}_I^2}{2m}, \quad (2.16)$$

$$v_I = \sum_{i \neq I} v_{iI}, \quad (2.17)$$

where I denotes the struck particle. In DINS experiments the momentum \mathbf{p}_I acquires large value of the order of the momentum transfer k , and if the potential v_{ij} is finite then the interaction v_I of recoiling particle with surrounding medium can be regarded as a small perturbation compared to its kinetic energy $p_I^2/2m \sim k^2/2m$. Thus, in zeroth approximation, the struck particle decouples from the rest of the system and recoils as if it was free. This is the IA¹³. The higher terms in the perturbation expansion as well as the case of hard core potentials will be discussed in the next section.

The $S(\mathbf{k}, \omega)$ can be written as

$$S(\mathbf{k}, \omega) = \frac{1}{2\pi N} \int dt e^{i\omega t} \langle 0 | \rho_{\mathbf{k}}(t) \rho_{\mathbf{k}}^\dagger(0) | 0 \rangle = \frac{1}{2\pi N} \sum_{i, j} \int dt e^{i\omega t} \langle 0 | e^{-i\mathbf{k} \cdot \mathbf{r}_i(t)} e^{i\mathbf{k} \cdot \mathbf{r}_j(0)} | 0 \rangle, \quad (2.18)$$

where $\rho_{\mathbf{k}}(t)$, and $\mathbf{r}_i(t)$ are density fluctuation and position operators in the Heisenberg picture. The limits of integration in the Fourier transform integrals are assumed to be $-\infty$

and $+\infty$ throughout this thesis, unless explicitly stated otherwise. The double sum in the above equation can be split in two parts: $i = j$ (the incoherent part) and $i \neq j$ (the coherent part). In DINS $k \gg 2\pi/d$, where d is the average nearest-neighbor distance. As a result the $i \neq j$ (coherent) part can be neglected and we obtain

$$S(\mathbf{k}, \omega) = \frac{1}{2\pi N} \sum_i \int dt e^{i\omega t} \langle 0 | e^{-i\mathbf{k}\cdot\mathbf{r}_i(t)} e^{i\mathbf{k}\cdot\mathbf{r}_i(0)} | 0 \rangle. \quad (2.19)$$

The assumption of IA is that struck particle recoils freely. The Heisenberg operator of the position $\mathbf{r}_i(t)$ for the free particle can be expressed in terms of Schrödinger operators \mathbf{r}_i and \mathbf{p}_i as

$$\mathbf{r}_i(t) = \mathbf{r}_i + \frac{t}{m} \mathbf{p}_i, \quad (2.20)$$

and using the Baker-Hausdorff lemma⁵¹

$$e^A e^B = e^{A+B+\frac{1}{2}C}, \quad C \equiv [A, B] \text{ is a c-number} \quad (2.21)$$

we find

$$\begin{aligned} S_{IA}(\mathbf{k}, \omega) &= \frac{1}{N} \sum_i \langle 0 | \frac{1}{2\pi} \int dt e^{i\omega t} \exp \left\{ -i \frac{\mathbf{k} \cdot \mathbf{p}_i}{m} t - i \frac{k^2}{2m} t \right\} | 0 \rangle \\ &= \frac{1}{N} \sum_i \langle 0 | \delta \left(\omega - \frac{k^2}{2m} - \frac{\mathbf{k} \cdot \mathbf{p}_i}{m} \right) | 0 \rangle = \int \frac{d^3 p}{(2\pi)^3 \rho} n(p) \delta \left(\omega - \frac{k^2}{2m} - \frac{\mathbf{k} \cdot \mathbf{p}}{m} \right), \end{aligned} \quad (2.22)$$

where $n(p)$ is the single-particle momentum distribution, and ρ is average density of the system. From this expression and equation (2.13) we find that the scaling function in IA is

$$J_{IA}(y) = \int \frac{d^3 p}{(2\pi)^3 \rho} n(p) \delta(y - \hat{\mathbf{k}} \cdot \mathbf{p}) \quad (2.23)$$

$$= \frac{1}{(2\pi)^2 \rho} \int_{|y|}^{\infty} dp p n(p). \quad (2.24)$$

Experimentally, one measures the Compton profile and looks for scaling by considering its behavior at fixed y as k increases. If at high k it approaches an k -independent scaling function then, according to the IA prescription (equation (2.24)), it may be possible to obtain $n(p)$ by differentiation:

$$n(p) = - \frac{(2\pi)^2 \rho}{p} \left. \frac{dJ_{IA}(y)}{dy} \right|_{y=p}. \quad (2.25)$$

2.4 Theories of final states effects

There have been several attempts^{13–33} to develop the theory of FSI. In this section we will give an overview of those theories in order to gain some insight into the problems that lie ahead of us as well as to motivate our own approach^{36–38}.

2.4.1 Convolution approach

In the convolution approach $S(\mathbf{k}, \omega)$ is written as a convolution of the IA result $S_{IA}(\mathbf{k}, \omega)$ and the folding function F :

$$S(\mathbf{k}, \omega) = \int d\omega' F(k, \omega - \omega') S_{IA}(\mathbf{k}, \omega'), \quad (2.26)$$

$$F(k, \omega) = \frac{1}{2\pi} \int dt e^{i\omega t} A(k, t). \quad (2.27)$$

There has been an extensive amount of work^{13–20} along these lines, but here we present it in an unified form. Using the notation of the previous section we can define

$$A(k, t) = \frac{\langle 0 | \rho_{\mathbf{k}} e^{-iHt} \rho_{\mathbf{k}}^\dagger | 0 \rangle}{\langle 0 | \rho_{\mathbf{k}} e^{-iH_0 t} \rho_{\mathbf{k}}^\dagger | 0 \rangle}. \quad (2.28)$$

The denominator of this expression, as we have seen, describes the free motion of the struck particle and the uncoupled, fully correlated, motion of the remnant, while the numerator describes the true motion of the whole system. The $|A(k, t)|^2$ represents the probability that the struck particle is moving freely after time t , i.e. that it is in the same momentum state $\mathbf{k} + \mathbf{p}_{\text{initial}}$ at time t after the collision with the neutron, regardless of the motion of the residual system. The amplitude $A(k, t)$ is a complex number which can be written as

$$A(k, t) = e^{-i(V(k, t) - iW(k, t))t}, \quad (2.29)$$

which together with equation (2.27) implies that $W(k, t)$ determines the width of the folding function, while $V(k, t)$ gives the shift in the energy. The probability $P(k, t) = |A(k, t)|^2 = \exp\{-2W(k, t)t\}$ satisfies the decay equation

$$\frac{dP(k, t)}{dt} = -\frac{P(k, t)}{\tau(k, t)}, \quad P(k, 0) = 1, \quad (2.30)$$

where $\tau(k, t)$ is the mean life time of I , i.e. of the state which describes the free recoil of the struck particle. The solution of equation (2.30) is

$$P(k, t) = \exp \left\{ - \int_0^t dt' \tau^{-1}(k, t') \right\}, \quad (2.31)$$

and we obtain

$$W(k, t) = \frac{1}{2t} \int_0^t dt' \tau^{-1}(k, t'). \quad (2.32)$$

In the simplest approximation¹³ $\tau(k, t)$ is independent of t :

$$\tau^{-1}(k, t) = \rho \sigma v, \quad (2.33)$$

where $v = k/m$ is the velocity of the struck atom, and σ is the total cross section for atom-atom scattering. In this approximation the folding function is a Lorentzian:

$$F(k, \omega) = \frac{1}{2\pi\tau} \frac{1}{\omega^2 + 1/4\tau^2}, \quad (2.34)$$

which has unrealistically long tails. It will be shown in subsection 2.4.3 that the DSF obtained with the Lorentzian folding function does not satisfy the ω^2 (kinetic energy) sum-rule.

The failure of the Lorentzian folding function at large ω indicate that the approximation (2.33) for the mean life time is unphysical at small t . Indeed, the density around the recoiling atom is not uniform, but rather given by $\rho g(r)$, where $g(r)$ is the pair distribution function, and the amount of scattering at small t is significantly reduced since $g(r) \approx 0$ for $r \ll \rho^{-1/3}$. Using the classical value $r = vt$ a better, time dependent approximation for the lifetime is obtained¹⁴:

$$\tau^{-1}(k, t) = \rho g(vt) \sigma v, \quad (2.35)$$

so that

$$W(k, t) = \frac{\rho \sigma v}{2t} \int_0^t dt' g(vt'), \quad (2.36)$$

and the resulting folding function does not have long tails. This semi-classical argument has been further developed by assuming that the interaction between atoms at large ω can be approximated by a hard core of radius r_c . One can then introduce impact parameter averaging to obtain¹⁸⁻²⁰:

$$\tau^{-1}(k, t) = \rho v 4\pi \int_0^{r_c} db b g(\sqrt{(vt)^2 + b^2}), \quad (2.37)$$

$$W(k, t) = \rho v \frac{2\pi}{t} \int_0^t dt' \int_0^{r_c} db b g(\sqrt{(vt')^2 + b^2}). \quad (2.38)$$

The effective value of r_c depends upon $\omega \sim k^2/2m$, and the DSF obtained with this approximation is in fair agreement with the available data¹¹ on neutron scattering by liquid ^4He .

If the interparticle potential is weak, the correlation between the particles vanishes and the uniform limit ($g(r) \sim 1$) is reached, so that the expressions (2.35) and (2.37) for $\tau^{-1}(k, t)$ reduce to the simple expression (2.33). At the same time, the total cross section σ also vanishes causing the Lorentzian folding function (2.34) to shrink into δ -function, and the IA is obtained as expected.

Finally, we want to discuss the small y behavior of DSF in the convolution approach. The $S_{IA}(\mathbf{k}, \omega)$ and $J_{IA}(y)$ of Bose liquids at temperatures below the λ -transition temperature have a δ -function contribution at $y = 0$ coming from the atoms in the condensate, and we ask whether the same is true for $J(y)$ in the convolution approach. From equation (2.10) it is clear that the width of $J(y)$ is given by the width of $S(\mathbf{k}, \omega)$ divided by k/m . Because of this division any part of $S(\mathbf{k}, \omega)$ that has a constant width as $k \rightarrow \infty$ will appear as a δ -function peak in $J(y)$. In other words, even if we assume that $S(\mathbf{k}, \omega)$ has a peak at $\omega = k^2/2m$ whose width is finite in the limit $k \rightarrow \infty$, the resulting $J(y)$ will have a δ -function peak at $y = 0$. Thus, in the convolution approach, $J(y)$ will have δ -function peak only if the folding function $F(k, \omega)$ of equation (2.26) has a finite width in the limit

$k \rightarrow \infty$. From the equations (2.33), (2.35) and (2.37) it follows that the width of $F(k, \omega)$ is of order $\tau^{-1} \sim k\sigma$, hence it is governed by the behavior of σ for large k when the eikonal approximation⁵² applies giving

$$\sigma = 4\pi \int_0^\infty \rho d\rho \left[1 - \cos \left(\frac{m}{k} \int_{-\infty}^\infty dz v \left(\sqrt{\rho^2 + z^2} \right) \right) \right]. \quad (2.39)$$

For example, in the case of the inverse power potential $v(r) = \alpha/r^{2n}$, $n > 1$ the above formula gives $\sigma \sim k^{-2/(2n-1)}$ implying $\tau^{-1} \sim k^{(2n-3)/(2n-1)}$, and the asymptotic $J(y)$ can not have a δ -function peak in the convolution approach. The same conclusion holds for the familiar case of the hard sphere interaction which is obtained in the $n \rightarrow \infty$ limit when $\sigma \rightarrow \text{constant}$ at large k and $\tau^{-1} \sim k$. In contrast, the case $n = 1$ is a representative of the weak potential scenario: the potential $v(r) = \alpha/r^2$ is Fourier transformable, and the cosine in equation (2.39) can be expanded to obtain the large k Born approximation result⁵²

$$\sigma = \frac{2\pi m^2}{k^2} \int_0^\infty \rho d\rho \left(\int_{-\infty}^\infty dz v \left(\sqrt{\rho^2 + z^2} \right) \right)^2, \quad (2.40)$$

which gives vanishing width $\tau \sim k^{-1}$ and IA is recovered, as mentioned above.

2.4.2 Gersh series

In another approach²⁵⁻³⁰ the $S(\mathbf{k}, \omega)$ at large k and ω is expanded in powers of m/k :

$$\frac{k}{m} S(\mathbf{k}, \omega) = J(y) + \frac{m}{k} J_1(y) + \left(\frac{m}{k}\right)^2 J_2(y) + \dots \quad (2.41)$$

If the interparticle potential is finite and smooth enough so that its Fourier transform $\tilde{v}(p)$ decreases exponentially in the limit $p \rightarrow \infty$, then it is possible to calculate $J_n(y)$ as a function of $(n+1)$ -body off-diagonal density matrix. Due to the smallness of $\tilde{v}(p)$ at large p , the coherent part of $S(\mathbf{k}, \omega)$ (c.f. equations (2.18) and (2.19)) can be neglected, and the starting point of this calculation is the expression for the incoherent DSF of the spinless

Bose liquid at $T = 0$:

$$S(\mathbf{k}, \omega) = -\frac{1}{\pi} \text{Im} \langle 0 | e^{-i\mathbf{k}\cdot\mathbf{r}_1} [\omega - H + E_0 + i\eta]^{-1} e^{i\mathbf{k}\cdot\mathbf{r}_1} | 0 \rangle \quad (2.42)$$

$$= -\frac{1}{\pi} \text{Im} \sum_{l=0}^{\infty} \langle 0 | e^{-i\mathbf{k}\cdot\mathbf{r}_1} [\omega - H_{IA} + E_0 + i\eta]^{-1} (v_1 [\omega - H_{IA} + E_0 + i\eta]^{-1})^l e^{i\mathbf{k}\cdot\mathbf{r}_1} | 0 \rangle, \quad (2.43)$$

where we have split the Hamiltonian in two pieces as in equations (2.15)-(2.17), and η is a positive infinitesimal. The eigenstates of H_{IA} are written as $|\mathbf{p}, n\rangle \equiv |\mathbf{p}\rangle_1 |n\rangle_{N-1}$, where $|\mathbf{p}\rangle$ is a plane wave state of the struck particle, and $|n\rangle$ are eigenstates for $N-1$ background particles with energies E_{N-1}^n . They are used as intermediate states to obtain

$$\begin{aligned} S(\mathbf{k}, \omega) = & -\frac{1}{\pi} \text{Im} \left\{ \sum_{\mathbf{p}, n} |\langle 0 | \mathbf{p}, n \rangle|^2 \langle \mathbf{p} + \mathbf{k}, n | [\omega - H_{IA} + E_0 + i\eta]^{-1} | \mathbf{p} + \mathbf{k}, n \rangle \right. \\ & + \sum_{\mathbf{p}, n} \sum_{\mathbf{q}, m} \langle 0 | \mathbf{p}, n \rangle \langle \mathbf{p} + \mathbf{k}, n | [\omega - H_{IA} + E_0 + i\eta]^{-1} | \mathbf{p} + \mathbf{k}, n \rangle \langle \mathbf{p} + \mathbf{k}, n | v_1 | \mathbf{q} + \mathbf{k}, m \rangle \\ & \left. \times \langle \mathbf{q} + \mathbf{k}, m | [\omega - H_{IA} + E_0 + i\eta]^{-1} | \mathbf{q} + \mathbf{k}, m \rangle \langle \mathbf{q}, m | 0 \rangle + \dots \right\}. \quad (2.44) \end{aligned}$$

The expansion (2.44) is known as Gersh series²⁵. Each energy denominator carries the factor m/k in the scaling limit:

$$\begin{aligned} & \langle \mathbf{p} + \mathbf{k}, n | [\omega - H_{IA} + E_0 + i\eta]^{-1} | \mathbf{p} + \mathbf{k}, n \rangle \\ & = \left[\omega - \frac{(\mathbf{p} + \mathbf{k})^2}{2m} - E_{N-1}^n + E_0 + i\eta \right]^{-1} = \frac{m}{k} \left[y - \hat{\mathbf{k}} \cdot \mathbf{p} + O(k^{-1}) + i\eta \right]^{-1}, \quad (2.45) \end{aligned}$$

and l -th term in Gersh series has exactly l of them. On the other hand, under the conditions stated above, the matrix elements $\langle v_1 \rangle$ are finite, i.e. of order $O(k^0)$, so that the expansion (2.44) is indeed an asymptotic series in powers of m/k .

When the interaction contains a hard core, i.e. when the interparticle potential $v(r)$ is divergent enough at small r so that its Fourier transform $\tilde{v}(p)$ is not defined, Gersh series fails. To understand why it happens we will explicitly calculate the term $J_1(y)$, which is the first correction to $J(y)$ obtained in the IA. There are two contribution to J_1 , one coming from the second term in equation (2.44) which we denote $J_{1,1}(y)$, and another one ($J_{1,0}(y)$)

from the $O(k^{-1})$ terms of the energy denominator in the first term of the same equation.

The former contribution is given by

$$J_{1,1}(y) = -\frac{1}{\pi} \text{Im} \sum_{\mathbf{p}, n} \sum_{\mathbf{q}, m} \frac{\langle 0 | \mathbf{p}, n \rangle \langle \mathbf{p} + \mathbf{k}, n | v_1 | \mathbf{q} + \mathbf{k}, m \rangle \langle \mathbf{q}, m | 0 \rangle}{(y - \hat{\mathbf{k}} \cdot \mathbf{p} + i\eta)(y - \mathbf{q} \cdot \hat{\mathbf{k}} + i\eta)}. \quad (2.46)$$

Since the denominator does not depend on labels n and m after the terms of order $O(k^{-1})$ are neglected, it is possible to sum over complete sets of background states to obtain

$$\begin{aligned} J_{1,1}(y) &= -\frac{1}{\pi} \text{Im} \frac{1}{V^2} \sum_{\mathbf{p}, \mathbf{q}} \int d^3 r_1 d^3 r'_1 d^3 r''_1 d^3 r_2 \cdots d^3 r_N \frac{\Psi_0^*(\mathbf{r}_1, \mathbf{r}_2, \dots, \mathbf{r}_N) \Psi_0(\mathbf{r}'_1, \mathbf{r}_2, \dots, \mathbf{r}_N)}{(y - \hat{\mathbf{k}} \cdot \mathbf{p} + i\eta)(y - \mathbf{q} \cdot \hat{\mathbf{k}} + i\eta)} \\ &\quad \times e^{i\mathbf{p} \cdot \mathbf{r}_1} e^{-i(\mathbf{p} + \mathbf{k}) \cdot \mathbf{r}'_1} \sum_{j \neq 1} v(\mathbf{r}'_1 - \mathbf{r}_j) e^{i(\mathbf{q} + \mathbf{k}) \cdot \mathbf{r}'_1} e^{-i\mathbf{q} \cdot \mathbf{r}''_1} \\ &= -\frac{1}{\pi} \text{Im} \frac{1}{V^2} \sum_{\mathbf{p}, \mathbf{q}} \frac{\rho^2}{N} \int d^3 r_1 d^3 r'_1 d^3 r''_1 d^3 r_2 \frac{\rho_2(\mathbf{r}_1, \mathbf{r}_2; \mathbf{r}'_1, \mathbf{r}_2)}{(y - \hat{\mathbf{k}} \cdot \mathbf{p} + i\eta)(y - \mathbf{q} \cdot \hat{\mathbf{k}} + i\eta)} \\ &\quad \times e^{i\mathbf{p} \cdot (\mathbf{r}_1 - \mathbf{r}'_1)} e^{i\mathbf{q} \cdot (\mathbf{r}'_1 - \mathbf{r}''_1)} v(\mathbf{r}'_1 - \mathbf{r}_2), \end{aligned} \quad (2.47)$$

where we have introduced the two-body density matrix

$$\rho_2(\mathbf{x}_1, \mathbf{x}_2; \mathbf{y}_1, \mathbf{y}_2) \equiv \frac{N(N-1)}{\rho^2} \int d^3 r_3 \cdots d^3 r_N \Psi_0^*(\mathbf{x}_1, \mathbf{x}_2, \mathbf{r}_3, \dots, \mathbf{r}_N) \Psi_0(\mathbf{y}_1, \mathbf{y}_2, \mathbf{r}_3, \dots, \mathbf{r}_N). \quad (2.48)$$

Next, we change variables $\mathbf{r}_1 = \mathbf{r}''_1 + \mathbf{s} + \mathbf{r}_2$, $\mathbf{r}'_1 = \mathbf{r}''_1 + \mathbf{u} + \mathbf{r}_2$ and perform the trivial \mathbf{r}_2 integration to obtain

$$\begin{aligned} J_{1,1}(y) &= -\frac{1}{\pi} \text{Im} \rho \int d^3 r''_1 d^3 s d^3 u \rho_2(\mathbf{r}''_1 + \mathbf{s}, 0; \mathbf{r}''_1, 0) v(\mathbf{r}''_1 + \mathbf{u}) \\ &\quad \times \int \frac{d^3 p}{(2\pi)^3} \frac{e^{i\mathbf{p} \cdot (\mathbf{s} - \mathbf{u})}}{y - \hat{\mathbf{k}} \cdot \mathbf{p} + i\eta} \int \frac{d^3 q}{(2\pi)^3} \frac{e^{i\mathbf{q} \cdot \mathbf{u}}}{y - \mathbf{q} \cdot \hat{\mathbf{k}} + i\eta}. \end{aligned} \quad (2.49)$$

Integrations over \mathbf{p} and \mathbf{q} are performed using

$$\begin{aligned} \int \frac{d^3 p}{(2\pi)^3} \frac{e^{i\mathbf{p} \cdot \mathbf{a}}}{y - \hat{\mathbf{k}} \cdot \mathbf{p} + i\eta} &= \int_{-\infty}^{\infty} \frac{dp_{\parallel}}{2\pi} \frac{e^{ip_{\parallel} a_{\parallel}}}{y - p_{\parallel} + i\eta} \int \frac{d^2 p_{\perp}}{(2\pi)^2} e^{i\mathbf{p}_{\perp} \cdot \mathbf{a}_{\perp}} \\ &= -\delta^2(\mathbf{a}_{\perp}) e^{iy a_{\parallel}} \int_{-\infty}^{\infty} \frac{dp_{\parallel}}{2\pi} \frac{e^{ip_{\parallel} a_{\parallel}}}{p_{\parallel} - i\eta} = -i \delta^2(\mathbf{a}_{\perp}) \theta(a_{\parallel}) e^{iy a_{\parallel}}, \end{aligned} \quad (2.50)$$

where parallel and normal components are defined with respect to the direction of \mathbf{k} , and after renaming $s_{\parallel} \rightarrow s$ and $u_{\parallel} \rightarrow u$ we get

$$J_{1,1}(y) = \frac{\rho}{\pi} \int_{-\infty}^{\infty} ds \sin(ys) \int d^3 r \rho_2(\mathbf{r} + s\hat{\mathbf{k}}, 0; \mathbf{r}, 0) \int_0^s du v(\mathbf{r} + u\hat{\mathbf{k}}). \quad (2.51)$$

In order to obtain the other contribution $J_{1,0}(y)$ we expand the energy denominator (2.45):

$$\begin{aligned} & \langle \mathbf{p} + \mathbf{k}, n | [\omega - H_{IA} + E_0 + i\eta]^{-1} | \mathbf{p} + \mathbf{k}, n \rangle \\ &= \frac{m}{k} [y - \hat{\mathbf{k}} \cdot \mathbf{p} + i\eta]^{-1} + \left(\frac{m}{k}\right)^2 \left(\frac{p^2}{2m} + E_{N-1}^n - E_0\right) [y - \hat{\mathbf{k}} \cdot \mathbf{p} + i\eta]^{-2} + O(k^{-3}), \end{aligned} \quad (2.52)$$

and substitute into the first term of equation (2.44). The result

$$J_{1,0}(y) = -\frac{1}{\pi} \text{Im} \sum_{\mathbf{p}, n} \frac{|\langle 0 | \mathbf{p}, n \rangle|^2}{(y - \hat{\mathbf{k}} \cdot \mathbf{p} + i\eta)^2} \left(\frac{p^2}{2m} + E_{N-1}^n - E_0\right) \quad (2.53)$$

can be further simplified using

$$\langle \mathbf{p}, n | \frac{p^2}{2m} + E_{N-1}^n - E_0 | 0 \rangle = \langle \mathbf{p}, n | H_{IA} - H | 0 \rangle = -\langle \mathbf{p}, n | v_1 | 0 \rangle \quad (2.54)$$

to obtain

$$J_{1,0}(y) = -\frac{1}{\pi} \text{Im} \frac{d}{dy} \sum_{\mathbf{p}, n} \frac{\langle 0 | \mathbf{p}, n \rangle \langle \mathbf{p}, n | v_1 | 0 \rangle}{y - \hat{\mathbf{k}} \cdot \mathbf{p} + i\eta}. \quad (2.55)$$

Further calculation is similar to that of $J_{1,1}(y)$:

$$\begin{aligned} J_{1,0}(y) &= -\frac{1}{\pi} \text{Im} \frac{d}{dy} \frac{1}{V} \sum_{\mathbf{p}} \int d^3 r_1 d^3 r'_1 d^3 r_2 \dots d^3 r_N \frac{\Psi_0^*(\mathbf{r}_1, \mathbf{r}_2, \dots, \mathbf{r}_N) \Psi_0(\mathbf{r}'_1, \mathbf{r}_2, \dots, \mathbf{r}_N)}{y - \hat{\mathbf{k}} \cdot \mathbf{p} + i\eta} \\ &\quad \times e^{i\mathbf{p} \cdot (\mathbf{r}_1 - \mathbf{r}'_1)} \sum_{j \neq 1} v(\mathbf{r}'_1 - \mathbf{r}_j) \\ &= -\frac{1}{\pi} \text{Im} \frac{d}{dy} \frac{1}{V} \sum_{\mathbf{p}} \frac{\rho^2}{N} \int d^3 r_1 d^3 r'_1 d^3 r_2 \frac{\rho_2(\mathbf{r}_1, \mathbf{r}_2; \mathbf{r}'_1, \mathbf{r}_2)}{y - \hat{\mathbf{k}} \cdot \mathbf{p} + i\eta} e^{i\mathbf{p} \cdot (\mathbf{r}_1 - \mathbf{r}'_1)} v(\mathbf{r}'_1 - \mathbf{r}_2) \\ &= -\frac{1}{\pi} \text{Im} \frac{d}{dy} \rho \int d^3 r d^3 s \rho_2(\mathbf{r} + \mathbf{s}, 0; \mathbf{r}, 0) v(\mathbf{r}) \int \frac{d^3 p}{(2\pi)^3} \frac{e^{i\mathbf{p} \cdot \mathbf{s}}}{y - \hat{\mathbf{k}} \cdot \mathbf{p} + i\eta} \\ &= \frac{1}{\pi} \text{Im} \frac{d}{dy} i\rho \int_0^\infty ds e^{iys} \int d^3 r \rho_2(\mathbf{r} + s\hat{\mathbf{k}}, 0; \mathbf{r}, 0) v(\mathbf{r}) \\ &= -\frac{\rho}{\pi} \int_0^\infty ds s \sin(ys) \int d^3 r \rho_2(\mathbf{r} + s\hat{\mathbf{k}}, 0; \mathbf{r}, 0) v(\mathbf{r}), \end{aligned} \quad (2.56)$$

and we find²⁵

$$\begin{aligned} J_1(y) &= J_{1,0}(y) + J_{1,1}(y) \\ &= \frac{\rho}{\pi} \int_0^\infty ds \sin(ys) \int d^3 r \rho_2(\mathbf{r} + s\hat{\mathbf{k}}, 0; \mathbf{r}, 0) \int_0^s du [v(\mathbf{r} + u\hat{\mathbf{k}}) - v(\mathbf{r})]. \end{aligned} \quad (2.57)$$

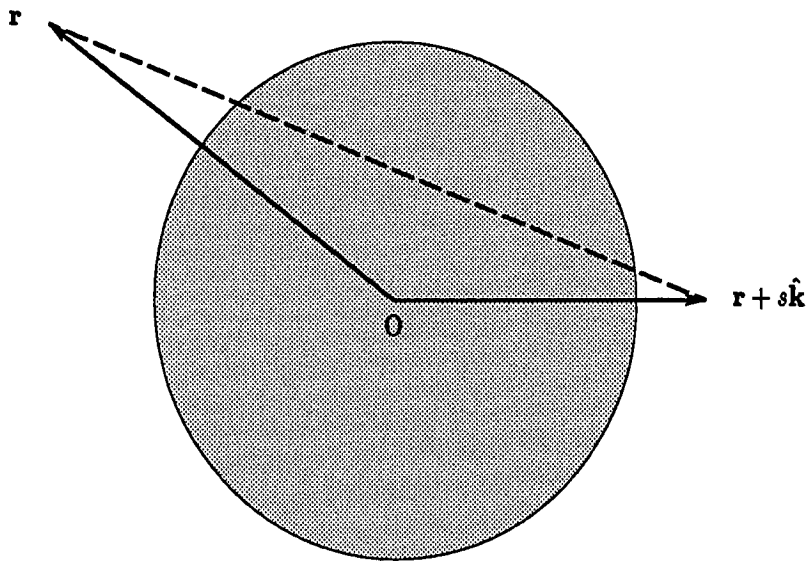


Figure 2.1: $J_1(y)$ of equation (2.57) diverges when the path of u -integration (dashed line) passes through the hard core region (shaded area).

It is easy to see that formula (2.57) does not apply to hard core systems. The analysis of the integrand shows that in this case the points defined by vectors \mathbf{r} and $\mathbf{r} + s\hat{\mathbf{k}}$ can not be near the origin due to the presence of the exact two-body density matrix $\rho_2(\mathbf{r} + s\hat{\mathbf{k}}, 0; \mathbf{r}, 0)$ that becomes vanishingly small when its first or second pair of arguments are close. However, apart from this restriction, their position can be arbitrary. In particular, it may happen that the straight line that connects those two points, along which the u integral in equation (2.57) is taken, passes near the origin, as is shown in Figure 2.1. The hard core potential $v(r)$ takes on large values in the region $r \rightarrow 0$ (shaded area), and this causes the u integral to diverge. The reason for this failure of Gersh series is that the decomposition (2.15)-(2.17) of the Hamiltonian is not physical when the interparticle potential has hard core. Indeed, the nonperturbed Hamiltonian (2.16) decouples the recoiling particle from the rest of the system, and its eigenstates $|\mathbf{p}, n\rangle$, which are used as intermediate states in the perturbation

expansion, do not take into account strong short range correlations that would normally prevent the struck particle from entering the hard core region of background particles.

Thus, when interparticle potential contains a hard core the Gersh series for $S(\mathbf{k}, \omega)$ diverges term by term, and an infinite resummation must be performed to make it finite. The result of this resummation amounts to replacing the bare interaction (2.17) with the T-matrix t , which is defined by the relation⁵³

$$t = v_1 + v_1[\omega - H_{IA} + E_0 + i\eta]^{-1}t. \quad (2.58)$$

However, the T-matrix is k -dependent, and the analysis of series (2.44) is not feasible without the explicit numerical calculation of t .²⁹ The general analysis is still possible in the somewhat unphysical case of the hard sphere interparticle potential

$$v(r) = \begin{cases} \infty & r < r_c \\ 0 & r > r_c \end{cases}, \quad (2.59)$$

since T-matrix for the scattering of hard spheres grows linearly with k , as was pointed out by Weinstein and Negele³⁰. It is obvious that the power counting that led to IA in the case of smooth Fourier transformable potential fails. For example, the second term in equation (2.44) contains two energy denominators and one T-matrix, hence it is of order $O(k^{-1})$ as is the IA term. Thus, Weinstein and Negele conclude that the $S(\mathbf{k}, \omega)$ of hard sphere gas y -scales, but the scaling function is not given by IA.

2.4.3 Sum-rule arguments

The ω^n weighted moments of DSF

$$S_n(k) \equiv \int_0^\infty d\omega \omega^n S(\mathbf{k}, \omega) \quad (2.60)$$

of the many-body system at zero temperature can be obtained if the ground state wave function is known, using the relation

$$S_n(k) = \frac{1}{N} \langle 0 | \rho_{\mathbf{k}} [H, \rho_{\mathbf{k}}^\dagger]_n | 0 \rangle, \quad (2.61)$$

where

$$[H, \rho_{\mathbf{k}}^\dagger]_n \equiv \underbrace{[H, \dots, [H, \rho_{\mathbf{k}}^\dagger] \dots]}_{n\text{-times}} \quad (2.62)$$

is a short hand notation for the n -times nested commutator. Although this relation, referred to as ω^n sum-rule, is quite well known³⁴, we will present its elementary derivation. From equations (2.9) and (2.60) we have

$$\begin{aligned} S_n(k) &= \frac{1}{N} \sum_f \left| \langle f | \rho_{\mathbf{k}}^\dagger | 0 \rangle \right|^2 (E_f - E_0)^n \\ &= \frac{1}{N} \langle 0 | \rho_{\mathbf{k}} (H - E_0)^n \rho_{\mathbf{k}}^\dagger | 0 \rangle, \end{aligned} \quad (2.63)$$

so that the ω^n sum-rule (2.61) holds if

$$(H - E_0)^n \rho_{\mathbf{k}}^\dagger | 0 \rangle = [H, \rho_{\mathbf{k}}^\dagger]_n | 0 \rangle. \quad (2.64)$$

The last identity can be proven by induction. For $n = 1$ we find

$$(H - E_0) \rho_{\mathbf{k}}^\dagger | 0 \rangle = (H \rho_{\mathbf{k}}^\dagger - \rho_{\mathbf{k}}^\dagger E_0) | 0 \rangle = [H, \rho_{\mathbf{k}}^\dagger] | 0 \rangle, \quad (2.65)$$

and assuming that the identity holds for some $n > 1$ we obtain

$$\begin{aligned} (H - E_0)^{n+1} \rho_{\mathbf{k}}^\dagger | 0 \rangle &= (H - E_0)(H - E_0)^n \rho_{\mathbf{k}}^\dagger | 0 \rangle \\ &= (H - E_0)[H, \rho_{\mathbf{k}}^\dagger]_n | 0 \rangle = (H[H, \rho_{\mathbf{k}}^\dagger]_n - [H, \rho_{\mathbf{k}}^\dagger]_n E_0) | 0 \rangle \\ &= [H, [H, \rho_{\mathbf{k}}^\dagger]_n] | 0 \rangle = [H, \rho_{\mathbf{k}}^\dagger]_{n+1} | 0 \rangle, \end{aligned} \quad (2.66)$$

which finishes the proof of the identity (2.64) and the ω^n sum-rule (2.61).

The moments $S_n(k)$ can be related to the y^m moments of $J_l(y)$ (c.f. equation (2.41))

$$J_l^m \equiv \int_{-k/2}^{\infty} dy y^m J_l(y) \quad (2.67)$$

using the auxiliary set of central moments of $S(\mathbf{k}, \omega)$:

$$\bar{S}_n(k) \equiv \left(\frac{m}{k}\right)^n \int_0^{\infty} d\omega \left(\omega - \frac{k^2}{2m}\right)^n S(\mathbf{k}, \omega). \quad (2.68)$$

Indeed, \bar{S}_n 's and S_n 's are connected by binomial expansion

$$\bar{S}_n(k) = \left(\frac{m}{k}\right)^n \sum_{i=0}^n \binom{n}{i} \left(-\frac{k^2}{2m}\right)^{n-i} S_i(k), \quad (2.69)$$

while from equation (2.41) we get

$$\begin{aligned} \bar{S}_n(k) &= \left(\frac{m}{k}\right)^n \int_{-k/2}^{\infty} \frac{k}{m} dy \left(\frac{k}{m}y\right)^n \frac{m}{k} \left[J(y) + \frac{m}{k} J_1(y) + \dots \right] \\ &= J^n + \frac{m}{k} J_1^n + \dots, \end{aligned} \quad (2.70)$$

so that

$$J^n = \lim_{k \rightarrow \infty} \bar{S}_n(k), \quad (2.71)$$

$$J_1^n = \lim_{k \rightarrow \infty} \frac{k}{m} [\bar{S}_n(k) - J^n], \quad (2.72)$$

etc. In section 3.1 it will be shown that

$$\bar{S}_n(k) = \begin{cases} \frac{1}{n+1} \langle 0 | (p_i)^n | 0 \rangle + O(k^{-2}) & n \text{ even,} \\ O(k^{-1}) & n \text{ odd,} \end{cases} \quad (2.73)$$

where $O(k^{-1})$ and $O(k^{-2})$ terms contain expectation values of the potential and its various derivatives. From equations (2.71)-(2.73) we obtain

$$J^n = \begin{cases} \frac{1}{n+1} \langle 0 | (p_i)^n | 0 \rangle & n \text{ even,} \\ 0 & n \text{ odd,} \end{cases} \quad (2.74)$$

$$J_1^n = \begin{cases} 0 & n \text{ even,} \\ O(1) & n \text{ odd.} \end{cases} \quad (2.75)$$

Since from equation (2.23) it follows that

$$\begin{aligned} J_{IA}^n &\equiv \int_{-k/2}^{\infty} dy y^n J_{IA}(y) = \int \frac{d^3 p}{(2\pi)^3 \rho} n(p) (\hat{\mathbf{k}} \cdot \mathbf{p})^n \\ &= \begin{cases} \frac{1}{n+1} \int \frac{d^3 p}{(2\pi)^3 \rho} n(p) p^n & n \text{ even,} \\ 0 & n \text{ odd,} \end{cases} \end{aligned} \quad (2.76)$$

we conclude that

$$\int_{-k/2}^{\infty} dy y^n J(y) = \int_{-k/2}^{\infty} dy y^n J_{IA}(y) \quad (2.77)$$

for all values of n . We also conclude from equation (2.75) that $J_1(y)$ is an odd function. This observations, due to Sears^{31,32}, imply that the asymptotic $J(y)$ is given by $J_{IA}(y)$, and that the leading correction to IA is of order $O(k^{-1})$ and purely antisymmetric in y . This correction too can be estimated using sum-rules³⁶, as will be shown in chapter 3.

As presented above, the Sears' sum-rule argument appears to prove the asymptotic validity of IA in general, regardless of the shape of the interparticle potential $v(r)$. However, we know that such a sweeping statement can not be true since, for one thing, it does not hold in the case of hard sphere gas, according to Weinstein and Negele³⁰. What went wrong is the fact that we tacitly assumed that ω^n sum rules exist for all n , which puts strong constraint on the choice of $v(r)$, making the applicability of the sum-rule argument rather limited. Let us consider, for example, the system interacting with the $1/r$ potential. It is Fourier transformable, and thus IA holds, as was shown in subsection 2.4.2. On the other hand, it is well known that only the first few sum-rules exist for this potential, and Sears' argument is not applicable.

The very step where the above argument may fail is taking the $k \rightarrow \infty$ limit in equation (2.73). The neglected $O(k^{-1})$ and $O(k^{-2})$ terms contain the expectation values of the potential and its various derivatives that appear in $[H, \rho_{\mathbf{k}}^\dagger]_n$ that may fail to exist causing the ω^n sum-rule to diverge. However, in the very important case of the hard core potentials of the Lennard-Jones, type all sum-rules exist, and can be used to estimate the scaling function $J(y)$ and corrections to it, as will be demonstrated in chapter 3.

From equation (2.76) it follows that the first three moments of the scaling function $J(y)$ are

$$\int_{-\infty}^{\infty} dy J(y) = 1, \quad (2.78)$$

$$\int_{-\infty}^{\infty} dy y J(y) = 0, \quad (2.79)$$

$$\int_{-\infty}^{\infty} dy y^2 J(y) = \frac{2m}{3} E_k, \quad (2.80)$$

where E_k is the ground state kinetic energy per particle. We now show that the scaling function obtained from the Lorentzian folding function (equation (2.34)) in the convolution approach does not satisfy the kinetic energy sum-rule (2.80). From equations (2.26) and (2.34) we find

$$J(y) = \int_{-k/2}^{\infty} dy' \frac{1}{2\pi\rho\sigma} \frac{1}{(y-y')^2 + 1/4\rho^2\sigma^2} J_{IA}(y'), \quad (2.81)$$

and obtain

$$\int_{-\infty}^{\infty} dy y^2 J(y) = \int_{-k/2}^{\infty} dy' \frac{1}{2\pi\rho\sigma} J_{IA}(y') \int_{-\infty}^{\infty} dy \frac{y^2}{(y-y')^2 + 1/4\rho^2\sigma^2} = \infty. \quad (2.82)$$

Thus, the Lorentzian folding function indeed has the unrealistically long tails, which causes the divergence of the kinetic energy sum-rule.

2.4.4 Correlated basis approach

All the theories mentioned above start from the IA that takes into account the interactions in the initial state of the target, and try to improve upon it by incorporating the effects of FSI. This procedure gets more and more difficult as k decreases and the FSI become more important. In contrast the response at small k and ω is easily treated by using Feynman phonon states⁵⁴. In particular the orthogonal correlated basis (OCB) formalism^{34,35} based on Feynman's ideas is quite successful^{55,56} in explaining the observed $S(k, \omega)$ at $k \lesssim 2\text{\AA}^{-1}$. The small and large k methods have different starting points; the momentum distribution $n(q)$ is the main input for the IA, while the OCB formalism uses the static structure function $S(q)$ as the main input. The $S(q)$ and $n(q)$ are not unrelated. For example, if one uses the Jastrow wave function^{57,58}

$$\Psi_J = \prod_{i<j} f_J(r_{ij}), \quad (2.83)$$

to approximate the ground state, then the $S(q)$ (i.e. the pair distribution function $g(r)$) determines³⁴ $f_J(r)$ and hence $n(q)$. However it is not clear that there exists a one to one correspondence between the $S(q)$ and $n(q)$ of a general Bose ground state wave function.

In principle the OCB formalism can be used to study $S(\mathbf{k}, \omega)$ at all k and ω , however the calculations⁵⁵ become technically complicated as k increases. In the present work we show that, by using analogs of Ward identities^{59,60} in orthogonal correlated basis perturbation theories (OCBPT), it is possible to calculate the $S(\mathbf{k}, \omega)$ in the scaling limit, and thus extend this low k method to the $k \rightarrow \infty$ limit.

Chapter 3

Antisymmetric part of $S(\mathbf{k}, \omega)$ of liquid ${}^4\text{He}$

In this chapter we study the ω^n sum-rules $S_n(k)$ (equation (2.61)) of the hard core quantum liquid at zero temperature, and use them to estimate the antisymmetric part of $S(\mathbf{k}, \omega)$ ³⁶. In subsection 2.4.4 it was argued that ω^n sum-rules exist for all n if the interparticle potential is smooth and has a strongly repulsive core. It was also shown that the y^m moments of the functions $J_l(y)$ that appear in the expansion (2.41) can be evaluated from $S_n(k)$. In section 3.1 we prove that the y^m moments of $J(y)$ are the same as those of $J_{IA}(y)$ (equation (2.76)), and obtain explicit expressions for the y^m moments of $J_1(y)$ which is an antisymmetric function of y . In principle, the function $J_1(y)$ is completely determined by its y^m moments. However, the numerical evaluation of these moments becomes difficult as m increases. In section 3.2 we compute the first three odd moments of the function $J_1(y)$ of the liquid ${}^4\text{He}$. These are used to estimate its shape by means of the orthogonal polynomial expansion, and the results are compared to the observed antisymmetric part of $S(\mathbf{k}, \omega)$. Finally, the brief summary is given in section 3.3.

In order to simplify the notation we use the system of units in which $\hbar^2/2m = 1$, or, equivalently, $\text{\AA}^{-2} = 6.06K$ in the case of the liquid ${}^4\text{He}$, throughout this chapter.

3.1 Calculation of the y^m moments of $J(y)$ and $J_1(y)$

The ω^n sum-rule $S_n(k)$ (equation (2.61)) contains the n -fold commutator $[H, \rho_{\mathbf{k}}^\dagger]_n$. It is straightforward to calculate this commutator for the first few n 's:

$$[H, \rho_{\mathbf{k}}^\dagger]_1 = \sum_{\mathbf{i}} e^{i\mathbf{k}\cdot\mathbf{r}_i} (k^2 + 2\mathbf{k} \cdot \mathbf{p}_i) \quad (3.1)$$

$$[H, \rho_{\mathbf{k}}^\dagger]_2 = \sum_{\mathbf{i}} e^{i\mathbf{k}\cdot\mathbf{r}_i} \left\{ (k^2 + 2\mathbf{k} \cdot \mathbf{p}_i)^2 - 2k \sum_{j(\neq i)} \left(\frac{1}{i} \partial_{z,i} v_{ij} \right) \right\} \quad (3.2)$$

$$\begin{aligned} [H, \rho_{\mathbf{k}}^\dagger]_3 = & \sum_{\mathbf{i}} e^{i\mathbf{k}\cdot\mathbf{r}_i} \left\{ (k^2 + 2\mathbf{k} \cdot \mathbf{p}_i)^3 + k^3 \left[-6 \sum_{j(\neq i)} \left(\frac{1}{i} \partial_{z,i} v_{ij} \right) \right. \right. \\ & + k^2 \left[-8 \sum_{j(\neq i)} \left(\left(\frac{1}{i} \partial_{z,i} \right)^2 v_{ij} \right) - 12 \sum_{j(\neq i)} \left(\frac{1}{i} \partial_{z,i} v_{ij} \right) \left(\frac{1}{i} \partial_{z,i} \right) \right] \\ & \left. \left. + k \left[2 \sum_{j(\neq i)} \left(\frac{1}{i} \partial_{z,i} (D_{ij} v_{ij}) \right) \right] \right\} \quad (3.3) \end{aligned}$$

$$\begin{aligned} [H, \rho_{\mathbf{k}}^\dagger]_4 = & \sum_{\mathbf{i}} e^{i\mathbf{k}\cdot\mathbf{r}_i} \left\{ (k^2 + 2\mathbf{k} \cdot \mathbf{p}_i)^4 + k^5 \left[-12 \sum_{j(\neq i)} \left(\frac{1}{i} \partial_{z,i} v_{ij} \right) \right. \right. \\ & + k^4 \left[-32 \sum_{j(\neq i)} \left(\left(\frac{1}{i} \partial_{z,i} \right)^2 v_{ij} \right) - 48 \sum_{j(\neq i)} \left(\frac{1}{i} \partial_{z,i} v_{ij} \right) \left(\frac{1}{i} \partial_{z,i} \right) \right] \\ & + k^3 \left[-24 \sum_{j(\neq i)} \left(\left(\frac{1}{i} \partial_{z,i} \right)^3 v_{ij} \right) - 64 \sum_{j(\neq i)} \left(\left(\frac{1}{i} \partial_{z,i} \right)^2 v_{ij} \right) \left(\frac{1}{i} \partial_{z,i} \right) \right. \\ & \left. \left. - 48 \sum_{j(\neq i)} \left(\frac{1}{i} \partial_{z,i} v_{ij} \right) \left(\frac{1}{i} \partial_{z,i} \right)^2 + 8 \sum_{j(\neq i)} \left(\frac{1}{i} \partial_{z,i} (D_{ij} v_{ij}) \right) \right] \right. \\ & + k^2 \left[12 \sum_{j,m(\neq i)} \left(\frac{1}{i} \partial_{z,i} v_{ij} \right) \left(\frac{1}{i} \partial_{z,i} v_{im} \right) + 12 \sum_{j(\neq i)} \left(\left(\frac{1}{i} \partial_{z,i} \right)^2 (D_{ij} v_{ij}) \right) \right. \\ & \left. \left. + 16 \sum_{j(\neq i)} \left(\frac{1}{i} \partial_{z,i} (D_{ij} v_{ij}) \right) \left(\frac{1}{i} \partial_{z,i} \right) \right] \right. \\ & + k \left[-4 \sum_{j,m(\neq i)} \left(\left(\frac{1}{i} \partial_{z,i} \right) \nabla_i v_{ij} \cdot \nabla_i v_{im} \right) - 4 \sum_{j,m(\neq i)} \left(\left(\frac{1}{i} \partial_{z,i} \right) \nabla_m v_{im} \cdot \nabla_m v_{mj} \right) \right. \\ & \left. \left. - 2 \sum_{j(\neq i)} \left(\frac{1}{i} \partial_{z,i} ((D_{ij})^2 v_{ij}) \right) \right] \right\}, \quad (3.4) \end{aligned}$$

where $\partial_{z,i} \equiv \hat{\mathbf{k}} \cdot \nabla_i$ and

$$D_{ij}v_{ij} \equiv (\nabla_i^2 v_{ij}) + (\nabla_i v_{ij}) \cdot \nabla_i + (\nabla_j^2 v_{ij}) + (\nabla_j v_{ij}) \cdot \nabla_j. \quad (3.5)$$

From equations (3.1)-(3.4) we observe that the dominant terms in the $k \rightarrow \infty$ are those that do not contain the potential v_{ij} . The leading corrections are given by the terms containing only one v_{ij} , while the terms containing two v 's are negligible at large k for the following reason. In the n -fold commutator $[H, \rho_{\mathbf{k}}^\dagger]_n = [T + V, \rho_{\mathbf{k}}^\dagger]_n$ the powers of k appear as a result of commuting of T with $e^{i\mathbf{k}\cdot\mathbf{r}_i}$. Hence, the leading term of the commutator $[H, \rho_{\mathbf{k}}^\dagger]_n$ in the $k \rightarrow \infty$ limit is

$$[T, \rho_{\mathbf{k}}^\dagger]_n = \sum_i e^{i\mathbf{k}\cdot\mathbf{r}_i} (k^2 + 2\mathbf{k} \cdot \mathbf{p}_i)^n, \quad (3.6)$$

which does not depend on v_{ij} . Similarly the next leading term is a sum of n terms, each containing one v and $n - 1$ T 's:

$$\sum_{m=0}^{n-1} \underbrace{[T, \dots, [T, [V, [T, \dots, [T, \rho_{\mathbf{k}}^\dagger] \dots]]]}_{\substack{m \text{ times} \\ n-m-1 \text{ times}}}. \quad (3.7)$$

We neglect the terms containing two or more v 's, and call this approximation the "1 v " approximation. Equations (3.1) - (3.4) can be generalized to the arbitrary n to obtain

$$[H, \rho_{\mathbf{k}}^\dagger]_n = \sum_i e^{i\mathbf{k}\cdot\mathbf{r}_i} \{ (k^2 + 2\mathbf{k} \cdot \mathbf{p}_i)^n + \{n\} \}, \quad (3.8)$$

in 1 v approximation. The $\{n\}$ is defined as

$$\{n\} \equiv \sum_{m=2}^n \binom{n}{m} k^{2(n-m)} (-1)^m \sum_{i=1}^{m-1} (-2k)^i \sum_{j=1}^i \binom{m}{j-1} \binom{m-j}{m-i} K_{i-j+1; m-i-1; j-1}, \quad (3.9)$$

where

$$K_{a;b;c} \equiv \sum_{j(\neq i)} \{ (\frac{1}{i} \partial_{z,i})^a [(D_{ij})^b v_{ij}] (\frac{1}{i} \partial_{z,i})^c \}, \quad (3.10)$$

and the powers of the operator D_{ij} are defined as the repeated application of equation (3.5).

The proof of the equation (3.8) is given in the subsection 3.1.1.

From equations (2.61) and (3.8) we obtain

$$S_n(k) = \frac{1}{N} \langle 0 | \sum_{i,j} e^{i\mathbf{k} \cdot \mathbf{r}_{ij}} [(k^2 + 2\mathbf{k} \cdot \mathbf{p}_i)^n + \{n\}] | 0 \rangle. \quad (3.11)$$

It was explained in section 2.3 that the coherent $i \neq j$ terms in the double sum above are exponentially small in the $k \rightarrow \infty$ limit, and thus can be neglected to obtain

$$S_n(k) = \langle 0 | [(k^2 + 2\mathbf{k} \cdot \mathbf{p}_i)^n + \{n\}] | 0 \rangle. \quad (3.12)$$

On the other hand, from the equations (2.60) and (2.68) we obtain

$$S_n(k) = \sum_{m=0}^n \binom{n}{m} k^{2(n-m)} (2k)^m \bar{S}_m(k). \quad (3.13)$$

Equations (3.9), (3.12) and (3.13) are solved to obtain

$$\begin{aligned} \bar{S}_n(k) &= \langle 0 | (p_{z,i})^n | 0 \rangle + (-1)^n \sum_{i=1}^{n-1} (-2k)^i \sum_{j=1}^i \binom{n}{j-1} \binom{n-j}{n-i} K_{i-j+1; n-i-1; j-1} \\ &= \begin{cases} \frac{1}{n+1} \langle 0 | (p_i)^n | 0 \rangle + O(k^{-2}) & n \text{ even,} \\ \frac{1}{2k} (-1)^{\frac{n+1}{2}} \sum_{m=1}^{n-1} (n-m) \binom{n}{m-1} \\ \quad \times \sum_{j(\neq i)} \langle 0 | (\partial_{z,i}^{n-m} v(r_{ij})) \partial_{z,i}^{m-1} | 0 \rangle + O(k^{-2}) & n \text{ odd,} \end{cases} \end{aligned} \quad (3.15)$$

in accordance with equation (2.73). It was shown in subsection 2.4.4 that the y^m moments of the functions J_l can be found from the central moments $\bar{S}_n(k)$. Using equations (2.71), (2.72) and (3.15) we find that the moments of the $J(y)$ are the same as those of the $J_{IA}(y)$ (equation (2.76)) and that the moments of $J_1(y)$ are given by

$$J_1^n = \begin{cases} 0 & n \text{ even,} \\ (-1)^{\frac{n+1}{2}} \sum_{m=1}^{n-1} (n-m) \binom{n}{m-1} \sum_{j(\neq i)} \langle 0 | (\partial_{z,i}^{n-m} v(r_{ij})) \partial_{z,i}^{m-1} | 0 \rangle & n \text{ odd.} \end{cases} \quad (3.16)$$

To obtain the moments of $J_{l \geq 2}(y)$ from equation (3.14) the terms of order $O(k^{-2})$ and higher are needed. However, equation (3.14) was obtained in $1v$ approximation and we can

easily convince ourselves that the neglected terms of the commutator $[H, \rho_{\mathbf{k}}^\dagger]_n$ that contain two or more v 's do contribute to these orders, so that the moments of $J_{i \geq 2}(y)$ can not be determined from equation (3.14).

3.1.1 The proof of equation (3.8)

We will prove equation (3.8) by induction. First, we observe that it accounts for all $1v$ terms in equations (3.1)-(3.4), i.e. it holds for $n = 1, \dots, 4$. Next, we assume that it holds for some number n . For $[H, \rho_{\mathbf{k}}^\dagger]_{n+1}$ we find

$$\begin{aligned} [H, \rho_{\mathbf{k}}^\dagger]_{n+1} &= [H, [H, \rho_{\mathbf{k}}^\dagger]_n] = \left[T + V, \sum_{\mathbf{i}} e^{i\mathbf{k} \cdot \mathbf{x}_i} [(k^2 + 2\mathbf{k} \cdot \mathbf{p}_i)^n + \{n\}] \right] \\ &= \sum_{\mathbf{i}} e^{i\mathbf{k} \cdot \mathbf{x}_i} \left\{ (k^2 + 2\mathbf{k} \cdot \mathbf{p}_i)^{n+1} + (k^2 + 2\mathbf{k} \cdot \mathbf{p}_i)\{n\} \right. \\ &\quad \left. + [T, \{n\}] + [V, (k^2 + 2\mathbf{k} \cdot \mathbf{p}_i)^n] + [V, \{n\}] \right\}. \end{aligned} \quad (3.17)$$

The last term in the curly bracket contains the potential v_{ij} twice and is discarded in the $1v$ approximation. Thus, in order to finish the proof of the equation (3.8), we have to show that

$$\{n+1\} = (k^2 + 2\mathbf{k} \cdot \mathbf{p}_i)\{n\} + [T, \{n\}] + [V, (k^2 + 2\mathbf{k} \cdot \mathbf{p}_i)^n]. \quad (3.18)$$

We denote the right-hand side of the above equation as RHS and obtain

$$\begin{aligned} \text{RHS} &= \sum_{m=2}^n \binom{n}{m} k^{2(n-m)} (-1)^m \sum_{i=1}^{m-1} (-2k)^i \sum_{j=1}^i \binom{m}{j-1} \binom{m-j}{m-i} \\ &\quad \times \left\{ (k^2 + 2\mathbf{k} \cdot \mathbf{p}_i) K_{i-j+1; m-i-1; j-1} + [T, K_{i-j+1; m-i-1; j-1}] \right\} \\ &\quad + \sum_{m=1}^n \binom{n}{m} k^{2(n-m)} (2k)^m \left[V, \left(\frac{1}{i} \partial_{z,i} \right)^m \right] \\ &= \sum_{m=2}^n \binom{n}{m} k^{2(n-m)} (-1)^m \sum_{i=1}^{m-1} (-2k)^i \sum_{j=1}^i \binom{m}{j-1} \binom{m-j}{m-i} \\ &\quad \times \left\{ k^2 K_{i-j+1; m-i-1; j-1} + 2k [K_{i-j+2; m-i-1; j-1} + K_{i-j+1; m-i-1; j}] + K_{i-j+1; m-i; j-1} \right\} \\ &\quad + \sum_{m=1}^n \binom{n}{m} k^{2(n-m)} (2k)^m \sum_{j=1}^m \binom{m}{j-1} K_{m-j+1; 0; j-1} \end{aligned} \quad (3.19)$$

We note that the last term in equation (3.19) can be written as a sum of $m = 1$ part and $m \neq 1$ part which can be added to the fourth term as $i = m$ part. Also, we substitute

$$\binom{n}{m} = \binom{n+1}{m} - \frac{n}{n+1-m} \binom{n}{m} \quad (3.20)$$

into the first term of equation (3.19) and obtain

$$\begin{aligned} \text{RHS} &= \sum_{m=2}^{n+1} \binom{n+1}{m} k^{2(n+1-m)} (-1)^m \sum_{i=1}^{m-1} (-2k)^i \sum_{j=1}^i \binom{m}{j-1} \binom{m-j}{m-i} K_{i-j+1; m-i-1; j-1} \\ &- (-1)^{n+1} \sum_{i=1}^n (-2k)^i \sum_{j=1}^i \binom{n+1}{j-1} \binom{n-j+1}{n-i+1} K_{i-j+1; n-i; j-1} \\ &- \sum_{m=2}^n \frac{n}{n+1-m} \binom{n}{m} k^{2(n-m+1)} (-1)^m \sum_{i=1}^{m-1} (-2k)^i \\ &\quad \times \sum_{j=1}^i \binom{m}{j-1} \binom{m-j}{m-i} K_{i-j+1; m-i-1; j-1} \\ &+ \sum_{m=2}^n \binom{n}{m} k^{2(n-m)} (-1)^m \sum_{i=1}^{m-1} (-1)^i (2k)^{i+1} \\ &\quad \times \sum_{j=1}^i \binom{m}{j-1} \binom{m-j}{m-i} [K_{i-j+2; m-i-1; j-1} + K_{i-j+1; m-i-1; j}] + \\ &- \sum_{m=2}^n \binom{n}{m} k^{2(n-m)} (-1)^m \sum_{i=1}^m (-2k)^i \sum_{j=1}^i \binom{m}{j-1} \binom{m-j}{m-i} K_{i-j+1; m-i; j-1} \\ &+ \binom{n}{1} k^{2(n-1)} 2k \binom{m}{0} K_{1; 0; 0} \end{aligned} \quad (3.21)$$

The first term on the right-hand side of equation (3.21) is equal to $\{n+1\}$, while the $m = 2$ part of the third term and the last term cancel each other. We shift the variables $m \rightarrow m+1$ in the remainder of the third term, $i \rightarrow i-1$ in the fourth term, and $i \rightarrow i-1$, $j \rightarrow j-1$ in the fifth one, and obtain

$$\begin{aligned} &\text{RHS} - \{n+1\} = \\ &= - \sum_{m=2}^{n-1} \frac{m+1}{n-m} \binom{n}{m+1} k^{2(n-m)} (-1)^{m+1} \sum_{i=1}^m (-2k)^i \\ &\quad \times \sum_{j=1}^i \binom{m+1}{j-1} \binom{m-j+1}{m-i+1} K_{i-j+1; m-i; j-1} \end{aligned}$$

$$\begin{aligned}
& - (-1)^n \sum_{i=1}^n (-2k)^i \sum_{j=1}^i \binom{n+1}{j-1} \binom{n-j+1}{n-i+1} K_{i-j+1;n-i;j-1} \\
& - \sum_{m=2}^n \binom{n}{m} k^{2(n-m)} (-1)^m \left\{ -2k \binom{m}{0} \binom{m-1}{m-1} K_{1;m-1;0} + \sum_{i=2}^m (-2k)^i \right. \\
& \times \left\{ \sum_{j=2}^{i-1} \left[\binom{m}{j-1} \binom{m-j}{m-i+1} + \binom{m}{j-2} \binom{m-j+1}{m-i+1} + \binom{m}{j-1} \binom{m-j}{m-i} \right] \right. \\
& \times K_{i-j+1;m-i;j-1} \\
& + \left[\binom{m}{0} \binom{m-1}{m-i+1} + \binom{m}{0} \binom{m-1}{m-i} \right] K_{i;m-i;0} \\
& \left. \left. + \left[\binom{m}{i-2} \binom{m-i+1}{m-i+1} + \binom{m}{i-1} \binom{m-i}{m-i} \right] K_{1;m-i;i-1} \right\} \right\}. \quad (3.22)
\end{aligned}$$

The second term on the right-hand side of equation (3.22) can be added to the first one as its $m = n$ part. The further simplification is achieved by using the identities

$$\frac{m+1}{n-m} \binom{n}{m+1} = \binom{n}{m}, \quad (3.23)$$

$$\begin{aligned}
& \binom{m}{j-1} \binom{m-j}{m-i+1} + \binom{m}{j-2} \binom{m-j+1}{m-i+1} + \binom{m}{j-1} \binom{m-j}{m-i} \\
& = \binom{m+1}{j-1} \binom{m-j+1}{m-i+1}, \quad (3.24)
\end{aligned}$$

$$\begin{aligned}
& \binom{m}{0} \binom{m-1}{m-i+1} + \binom{m}{0} \binom{m-1}{m-i} = \binom{m}{m-i+1} \\
& = \binom{m+1}{j-1} \binom{m-j+1}{m-i+1} \Big|_{j=1}, \quad (3.25)
\end{aligned}$$

$$\begin{aligned}
& \binom{m}{i-2} \binom{m-i+1}{m-i+1} + \binom{m}{i-2} \binom{m-i}{m-i} = \binom{m+1}{i-1} \\
& = \binom{m+1}{j-1} \binom{m-j+1}{m-i+1} \Big|_{j=i}. \quad (3.26)
\end{aligned}$$

to obtain

$$\text{RHS} - \{n+1\} =$$

$$\begin{aligned}
&= \sum_{m=2}^n \binom{n}{m} k^{2(n-m)} (-1)^m \sum_{i=1}^m (-2k)^i \sum_{j=1}^i \binom{m+1}{j-1} \binom{m-j+1}{m-i+1} K_{i-j+1; m-i; j-1} \\
&\quad - \sum_{m=2}^n \binom{n}{m} k^{2(n-m)} (-1)^m \sum_{i=1}^m (-2k)^i \sum_{j=1}^i \binom{m+1}{j-1} \binom{m-j+1}{m-i+1} K_{i-j+1; m-i; j-1} \\
&= 0, \tag{3.27}
\end{aligned}$$

which finishes the proof of equation (3.8).

3.2 Evaluation of the antisymmetric part of $S(\mathbf{k}, \omega)$ of liquid

${}^4\text{He}$

From equation (3.16) we find that the first few odd moments of $J_1(y)$ are given by

$$J_1^1 = 0, \tag{3.28}$$

$$J_1^3 = \frac{1}{2} \sum_{j(\neq i)} \langle 0 | (\partial_{z,i}^2 v(r_{ij})) | 0 \rangle, \tag{3.29}$$

$$J_1^5 = \sum_{j(\neq i)} \left[\langle 0 | (\partial_{z,i}^4 v(r_{ij})) | 0 \rangle - 5 \langle 0 | (\partial_{z,i}^2 v(r_{ij})) \partial_{z,i}^2 | 0 \rangle \right]. \tag{3.30}$$

The J_1^3 depends only upon the radial distribution function $g(r)$:

$$J_1^3 = \frac{1}{2} \frac{4\pi\rho}{3} \int_0^\infty r^2 dr \left(v''(r) + \frac{2v'(r)}{r} \right) g(r), \tag{3.31}$$

and it has been calculated with realistic potentials and the exact $g(r)$ obtained with the Green's function Monte Carlo (GFMC) method^{61,62}.

It is convenient to define:

$$J_1^5 = A - 5B; \tag{3.32}$$

$$A = \frac{4\pi\rho}{5} \int_0^\infty r^2 dr \left(v^{(IV)}(r) + \frac{4v'''(r)}{r} \right) g(r) \tag{3.33}$$

can be calculated easily from the GFMC $g(r)$. The term B involves gradients of the ground-state wave function, and thus can not be obtained from distribution functions alone. In the

present work we estimate it with the simplest Jastrow approximation^{57,58}

$$\Psi_0 = \prod_{i < j} f_2(r_{ij}), \quad (3.34)$$

for the ground-state wave function of liquid ⁴He. It is then given by

$$B = B_1 + B_2 + B_3, \quad (3.35)$$

$$B_1 = \rho \int d^3r g(r) (\partial_z^2 v(r)) \frac{\partial_z^2 f_2(r)}{f_2(r)}, \quad (3.36)$$

$$B_2 = \rho^2 \int d^3r_{ij} d^3r_{ik} g_3(\mathbf{r}_{ij}, \mathbf{r}_{ik}) (\partial_{z,i}^2 v(r_{ij})) \times \left[\frac{\partial_{z,i}^2 f_2(r_{ik})}{f_2(r_{ik})} + 2 \frac{\partial_{z,i} f_2(r_{ij})}{f_2(r_{ij})} \frac{\partial_{z,i} f_2(r_{ik})}{f_2(r_{ik})} \right], \quad (3.37)$$

$$B_3 = \rho^3 \int d^3r_{ij} d^3r_{ik} d^3r_{il} g_4(\mathbf{r}_{ij}, \mathbf{r}_{ik}, \mathbf{r}_{il}) (\partial_{z,i}^2 v(r_{ij})) \times \frac{\partial_{z,i} f_2(r_{ik})}{f_2(r_{ik})} \frac{\partial_{z,i} f_2(r_{il})}{f_2(r_{il})}. \quad (3.38)$$

It is easy to calculate B_1 exactly, and the superposition approximation⁶³:

$$g_3(\mathbf{r}_{ij}, \mathbf{r}_{ik}) \approx g(r_{ij})g(r_{ik})g(r_{jk}), \quad (3.39)$$

$$g_4(\mathbf{r}_{ij}, \mathbf{r}_{ik}, \mathbf{r}_{il}) \approx g(r_{ij})g(r_{ik})g(r_{il})g(r_{jk})g(r_{jl})g(r_{kl}), \quad (3.40)$$

is used for the three- and four-body distribution functions in B_2 and B_3 . The calculation of B_3 is further approximated by expanding g_4 in powers of short ranged functions $h_{ij} = g(r_{ij}) - 1$:

$$g_4(\mathbf{r}_{ij}, \mathbf{r}_{ik}, \mathbf{r}_{il}) \approx g(r_{ij})g(r_{ik})g(r_{il})[1 + h_{jk} + h_{jl} + h_{kl} + h_{jk}h_{jl} + h_{jk}h_{kl} + h_{jl}h_{kl} + h_{jk}h_{jl}h_{kl}]. \quad (3.41)$$

The three terms 1, h_{jk} , and h_{jl} give zero contribution, the h_{kl} term gives the largest contribution ($\sim -8\text{\AA}^{-6}$), the terms quadratic in h give contributions of order 2.5\AA^{-6} each, and the contribution of the $h_{jk}h_{jl}h_{kl}$ term, expected to be $\sim -1\text{\AA}^{-6}$, is neglected.

Table 3.1: The J_1^3 and J_1^5 in liquid ^4He

Term	Aziz	LJ
J_1^3	12.4\AA^{-4}	10.1\AA^{-4}
J_1^5	198\AA^{-6}	133\AA^{-6}
A	462\AA^{-6}	498\AA^{-6}
B	53\AA^{-6}	73\AA^{-6}
B_1	111\AA^{-6}	126\AA^{-6}
B_2	-57\AA^{-6}	-52\AA^{-6}
B_3	-1\AA^{-6}	-1\AA^{-6}

The calculated values are given in Table 1 for the Aziz⁶⁴ and Lennard-Jones (LJ) models of the interatomic potential. The GFMC $g(r)$ of the Courant group^{61,62} are used. The McMillan⁶⁵ $f_2(r)$:

$$f_2(r) = \exp \left[-\frac{1}{2} \left(\frac{b}{r} \right)^5 \right], \quad (3.42)$$

$$b = 1.17\sigma = 2.99\text{\AA}, \quad (3.42)$$

is used for calculations with the LJ potential, and an optimized $f_2(r)$ obtained by the paired phonon analysis⁶⁶ is used with the Aziz potential.

The calculation of J_1^5 can be significantly improved by considering ground-state wave functions with pair and triplet correlations⁶⁷, and by using exact many-body distribution functions via a Monte Carlo integration of the expectation values. The triplet correlations influence the pair distribution functions and the binding energy by $\sim 10\%$, and assuming that they have a similar effect on J_1^5 , we can expect the present results to change by $\sim 10\%$.

The values of J_1^3 and J_1^5 can be used to test calculations of $J_1(y)$. They can also be

used to construct crude models of $J_1(y)$ as follows. Let $J_1(y)$ be given by:

$$J_1(y) = \sum_{\text{Odd } n} b_n \mathcal{P}_n(y) J_{IA}(y), \quad (3.43)$$

where \mathcal{P}_n are odd polynomials

$$\mathcal{P}_n(y) = \sum_{\text{odd } m < n} \xi_{n,m} y^m, \quad (3.44)$$

obeying the orthogonality condition

$$\langle \mathcal{P}_m | \mathcal{P}_n \rangle \equiv \int_{-\infty}^{+\infty} dy \mathcal{P}_m(y) \mathcal{P}_n(y) J_{IA}(y) = \delta_{m,n}. \quad (3.45)$$

Then from equations (3.43)-(3.45) it follows that

$$b_n = \int_{-\infty}^{+\infty} dy \mathcal{P}_n(y) J_1(y) = \sum_{\text{odd } m < n} \xi_{n,m} J_1^m. \quad (3.46)$$

We have obtained two approximations to $J_1(y)$. In the first $b_{n>3} = 0$ and $b_1 (= 0)$ and b_3 are determined from J_1^1 and J_1^3 , and in the second $b_{n>5} = 0$ and $b_{n \leq 5}$ are determined from $J_1^{n \leq 5}$. The variational⁶⁸ $n(p)$ is used to generate the weight function $J_{IA}(y)$. With the Aziz potential we obtain $b_3 = 4.42$ and $b_{n \neq 3} = 0$ in the first approximation, and $b_3 = 4.42$, $b_5 = 1.83$ and $b_{n \neq 3,5} = 0$ in the second. The two approximations are compared with the antisymmetric part of measured² $S(\mathbf{k}, \omega)$ at $k = 10 \text{ \AA}^{-1}$, divided by $(k/m)^2$ in Figs. 3.1 and 3.2. Although the second approximation (solid line) is clearly better than the first one, it does not completely fit the data; the position of the zero of $J_1(y)$, in particular, is shifted from the experimental value.

3.3 Conclusions

There is a large class of systems (hydrogen atom, for example) such that $S(\mathbf{k}, \omega)$ has divergent ω^n sum-rules for big enough n . On the other hand, in systems with LJ-like interactions these moments exist to all orders due to $\exp(-c/r^5)$ behavior of the many-body distribution functions at small interatomic distances r . The results of the present

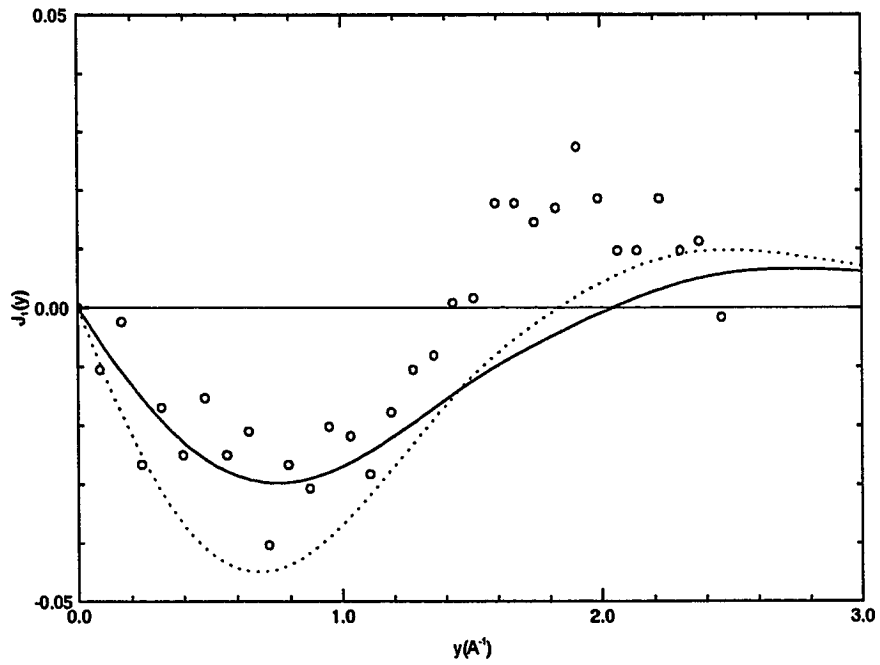


Figure 3.1: The two approximations to $J_1(y)$ calculated with the Aziz potential compared with the antisymmetric part of $(k/m)^2 S(k, \omega)$ measured at $k = 10 \text{ \AA}^{-1}$ from ref. 2.

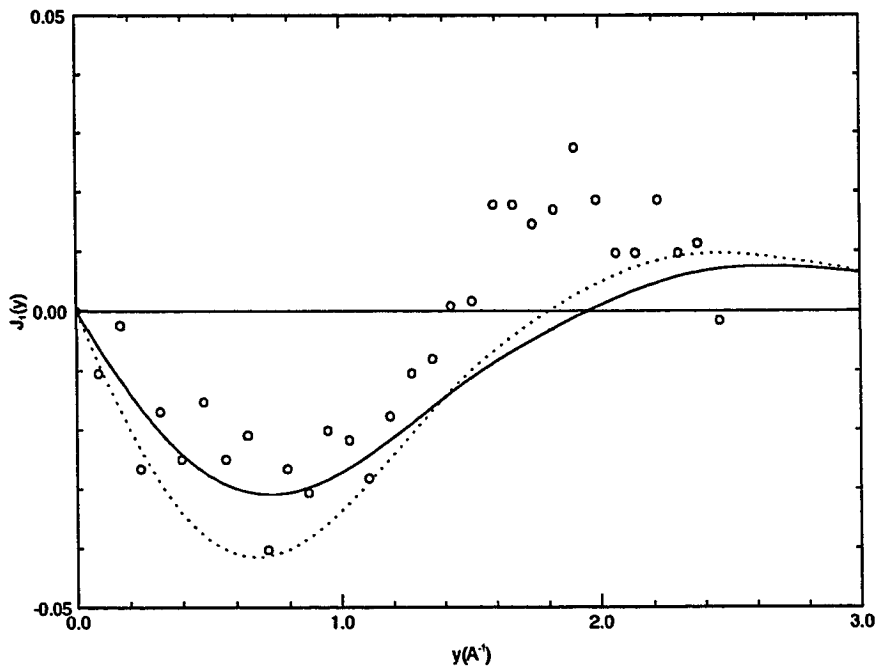


Figure 3.2: The same as in Fig. 3.1, calculated with the LJ potential.

calculations suggest that just the lowest few sum-rules provide a qualitative description of the $J_1(y)$. Few more values of J_1^n for $n = 7, 9, \dots$ may be needed to obtain a quantitative description of the $J_1(y)$. Unfortunately it appears that calculations of $J_1^{n>3}$ are not trivial. For example there is a large cancellation between the leading two-body integrals A and B_1 that contribute to J_1^5 . A wrong negative value of J_1^5 is obtained²⁷ if only the two-body integrals are retained and B_2 and B_3 are neglected. These cancellations appear to persist for higher J_1^n .

The comparison of present results with experimental data suggests that at $k = 10\text{\AA}^{-1}$, the $(m/k)^2 J_1(y)$ gives a large part of the total antisymmetric part of $S(\mathbf{k}, \omega)$, which justifies the use of the series (2.41) at $k > 10\text{\AA}^{-1}$. Although in principle the J_1^n are sensitive to the interatomic potentials, the comparison of values obtained with the Aziz and LJ potentials indicates that the J_1^3 and J_1^5 need to be determined with errors smaller than 10% to study models of interatomic potentials.

Chapter 4

Correlated basis theory of $S(\mathbf{k}, \omega)$ in the scaling limit

In this chapter we formulate the theory³⁷ of $S(\mathbf{k}, \omega)$ of a non-relativistic spinless Bose liquid at zero temperature, in the scaling limit. The main building block of this theory are OCB states. They are obtained from CB states, whose definition and properties are given in section 4.1, using the orthogonalization scheme described in section 4.2. In section 4.3 the general properties of OCB matrix elements in the scaling limit are obtained, and in section 4.4 the general framework of OCBPT of $S(\mathbf{k}, \omega)$ is set up. The y -scaling property of $S(\mathbf{k}, \omega)$ is proved in section 4.5.

4.1 CB states and their properties

In the Correlated Basis (CB) theories of quantum liquids the CB states are defined as^{34,35}:

$$|\mathbf{p}_1, \dots, \mathbf{p}_n\rangle \equiv \frac{G|\mathbf{p}_1, \dots, \mathbf{p}_n\rangle}{[\mathbf{p}_1, \dots, \mathbf{p}_n|G^\dagger G|\mathbf{p}_1, \dots, \mathbf{p}_n\rangle]^{1/2}}, \quad (4.1)$$

where $| \]$ are noninteracting states of the ideal gas, and G is the correlation operator which is usually determined by minimizing the ground state energy

$$E_0 = \langle 0|H|0 \rangle \equiv \frac{\langle 0|G^\dagger H G|0 \rangle}{\langle 0|G^\dagger G|0 \rangle}. \quad (4.2)$$

If, as is often done in the case of Bose liquids⁵⁴, $G|0$ is taken to be equal to the exact ground state $\Psi_0 \equiv |0\rangle$ the condition (4.2) is automatically satisfied, and the Feynman phonon basis is obtained:

$$|p_1, \dots, p_n\rangle = \frac{(\rho_{p_1}^\dagger \cdots \rho_{p_n}^\dagger) |0\rangle}{\langle 0| (\rho_{p_1} \cdots \rho_{p_n}) (\rho_{p_1}^\dagger \cdots \rho_{p_n}^\dagger) |0\rangle^{1/2}}, \quad (4.3)$$

where

$$(\rho_{p_1}^\dagger \cdots \rho_{p_n}^\dagger) \equiv \sum_{\substack{i, \dots, l \\ i \neq \dots \neq l}} \exp[i(p_1 \cdot r_i + \cdots + p_n \cdot r_l)], \quad (4.4)$$

Note that in this notation $\rho_{p_1}^\dagger \cdots \rho_{p_n}^\dagger$ does not equal $(\rho_{p_1}^\dagger \cdots \rho_{p_n}^\dagger)$ with brackets. The simple product of ρ_p^\dagger 's contains terms where particles i, j, \dots in the sum are the same. Such terms are excluded from the product in the brackets by definition (4.4).

For further calculations we need the diagonal and off-diagonal CB matrix elements of the unit operator and the Hamiltonian. They can be expressed in terms of a -body distribution functions³⁴

$$g_a(\mathbf{r}_1, \dots, \mathbf{r}_a) \equiv \frac{N(N-1) \cdots (N-a+1)}{\rho^a} \int d^3r_{a+1} \cdots d^3r_N |\Psi_0(\mathbf{r}_1, \dots, \mathbf{r}_N)|^2. \quad (4.5)$$

We are studying homogeneous isotropic Bose systems (liquids) so that g_a 's depend only upon the distances $r_{ij} \equiv |\mathbf{r}_i - \mathbf{r}_j|$ between the particles in the a -body cluster. For example, the two-body distribution function, that is usually called pair distribution function, depends upon the distance between two particles only:

$$g_2(\mathbf{r}_i, \mathbf{r}_j) = g(r_{ij}) = g_{ij}. \quad (4.6)$$

In the same fashion the three body distribution function is denoted g_{ijk} instead of $g_3(\mathbf{r}_i, \mathbf{r}_j, \mathbf{r}_k)$

etc. Since the interatomic potential in the liquid has finite range and there is no long range order, it follows that if one particle is removed far from the rest of the a -body cluster, then the a -body distribution function reduces to the $(a - 1)$ -body one³⁴:

$$g_a(\mathbf{r}_1, \dots, \mathbf{r}_{a-1}, \mathbf{r}_a) \longrightarrow g_{a-1}(\mathbf{r}_1, \dots, \mathbf{r}_{a-1}) \quad \text{when } r_{ai} \gg \rho^{-1/3} \quad (i = 1, \dots, a - 1). \quad (4.7)$$

In particular, for $a = 2$ we obtain

$$g(r) \longrightarrow 1 \quad \text{when } r \gg \rho^{-1/3}. \quad (4.8)$$

It is useful to express many-body distribution functions g_a in terms of the short range function

$$h(r) \equiv g(r) - 1 \quad (4.9)$$

and the connected parts g_a^c that have the property

$$g_a^c(\mathbf{r}_1, \dots, \mathbf{r}_a) \longrightarrow 0 \quad \text{when any } r_{ij} \gg \rho^{-1/3} \quad (i, j = 1, \dots, a). \quad (4.10)$$

The connected parts become important when all the particles of the a -body cluster are near, that is within the distance $\sim \rho^{-1/3}$ from each other. For the three-body distribution function we have³⁴

$$g_{ijk} = 1 + h_{ij} + h_{ik} + h_{jk} + g_{ijk}^c. \quad (4.11)$$

If the short range function h_{ij} is denoted by a dashed line connecting points i and j

$$h_{ij} = \underset{i}{\circ} \text{---} \text{---} \text{---} \underset{j}{\circ} \quad (4.12)$$

then equation (4.11) can be written as

$$g_{ijk} = 1 + \underset{i}{\circ} \text{---} \text{---} \text{---} \underset{j}{\circ} \quad (4.13)$$

where it is understood that all possible assignments of the labels i, j, k to the end points

(denoted by open circles) of the dashed line are to be taken into account. Similarly, for the four-body function we obtain³⁴

$$\begin{aligned}
 g_{ijkl} = & 1 + \text{---} \circ \text{---} \circ \text{---} \circ \text{---} \circ \text{---} + \text{---} \circ \text{---} \circ \text{---} \circ \text{---} \circ \text{---} \\
 & + \begin{array}{c} \text{---} \circ \text{---} \circ \\ \text{---} \circ \text{---} \circ \end{array} + g_{ijk}^c + g_{ijl}^c + g_{ikl}^c + g_{jkl}^c + g_{ijkl}^c, \quad (4.14)
 \end{aligned}$$

and so on.

We now proceed with the calculation of diagonal and off-diagonal CB matrix elements of the unit operator and the Hamiltonian.

4.1.1 Diagonal CB matrix elements

The normalization of one-phonon state is given by

$$\begin{aligned}
 \langle 0 | \rho_{\mathbf{k}} \rho_{\mathbf{k}}^\dagger | 0 \rangle & \equiv \sum_{i,j} \langle 0 | e^{i\mathbf{k}\cdot\mathbf{r}_{ij}} | 0 \rangle = \text{---} \circ_i \text{---} + \text{---} \overset{\mathbf{k}}{\curvearrowright} \text{---} \text{---} \circ_j \\
 & = N + N(N-1)\rho^2 \int d^3r_1 d^3r_2 e^{i\mathbf{k}\cdot\mathbf{r}_{12}} (g(r_{12}) - 1) = NS(\mathbf{k}), \quad (4.15)
 \end{aligned}$$

where the full line with an arrow pointing from the point i to the point j denotes $e^{i\mathbf{k}\cdot\mathbf{r}_{ij}}$ factor, the full circle with the index denotes multiplication with ρ and volume integration over the coordinate with that index, and the summation over all the indices is assumed.

For the normalization of the two-phonon state we obtain

$$\begin{aligned}
 \langle 0 | (\rho_{\mathbf{p}} \rho_{\mathbf{q}}) (\rho_{\mathbf{p}}^\dagger \rho_{\mathbf{q}}^\dagger) | 0 \rangle & \equiv \sum_{i \neq j} \sum_{l \neq m} \langle 0 | e^{i(\mathbf{p}\cdot\mathbf{r}_{ii} + \mathbf{q}\cdot\mathbf{r}_{jm})} | 0 \rangle \\
 = & \text{---} \circ_i^{\mathbf{p}} \text{---} \circ_j^{\mathbf{q}} + \text{---} \overset{\mathbf{p}-\mathbf{q}}{\curvearrowright} \text{---} \text{---} \circ_j + \text{---} \circ_i^{\mathbf{p}} \text{---} \overset{\mathbf{q}}{\curvearrowright} \text{---} \text{---} \circ_m + \text{---} \overset{\mathbf{p}}{\curvearrowright} \text{---} \text{---} \circ_i \text{---} \overset{\mathbf{q}}{\curvearrowright} \text{---} \text{---} \circ_j
 \end{aligned}$$

$$\begin{aligned}
& + 2 \left(\begin{array}{c} \text{Diagram 1: } i \text{---} j \text{---} m \text{ with arcs } p \text{ (} i \rightarrow j \text{)} \text{ and } q \text{ (} j \rightarrow m \text{)} \\ \text{Diagram 2: } i \text{---} m \text{---} j \text{ with arcs } p \text{ (} i \rightarrow m \text{)} \text{ and } p-q \text{ (} m \rightarrow j \text{)} \\ \text{Diagram 3: } m \text{---} i \text{---} j \text{ with arcs } q \text{ (} m \rightarrow i \text{)} \text{ and } q-p \text{ (} i \rightarrow j \text{)} \\ \text{Diagram 4: } i \text{---} l \text{---} j \text{ with arcs } p \text{ (} i \rightarrow l \text{)} \text{ and } q \text{ (} j \rightarrow m \text{)} \end{array} \right) \\
& + g_{ijk}^c \text{ terms} + g_{ijkl}^c \text{ terms. \tag{4.16}
\end{aligned}$$

It was mentioned earlier that the distribution functions of the liquid depend only upon the differences of the coordinates $r_{ij} = |\mathbf{r}_i - \mathbf{r}_j|$ so that an integration over one of the particle coordinates can be carried out in every connected piece of diagrams in equation (4.16). Such integration gives the factor $\Omega = N/\rho$, and we conclude that the diagram that contains c separate connected pieces is proportional to N^c . From equation (4.16) we then get

$$\begin{aligned}
& \langle 0 | (\rho_p \rho_q) (\rho_p^\dagger \rho_q^\dagger) | 0 \rangle = \\
& = \begin{array}{c} \text{Diagram 1: } i \text{---} j \text{ with arcs } p \text{ (} i \rightarrow j \text{)} \text{ and } q \text{ (} j \rightarrow i \text{)} \\ \text{Diagram 2: } i \text{---} j \text{---} m \text{ with arcs } p \text{ (} i \rightarrow j \text{)} \text{ and } q \text{ (} j \rightarrow m \text{)} \\ \text{Diagram 3: } i \text{---} l \text{---} j \text{ with arcs } p \text{ (} i \rightarrow l \text{)} \text{ and } q \text{ (} j \rightarrow l \text{)} \\ \text{Diagram 4: } i \text{---} l \text{---} j \text{ with arcs } p \text{ (} i \rightarrow l \text{)} \text{ and } q \text{ (} l \rightarrow j \text{)} \end{array} \\
& + \begin{array}{c} \text{Diagram 5: } i \text{---} l \text{---} j \text{ with arcs } p \text{ (} i \rightarrow l \text{)} \text{ and } q \text{ (} j \rightarrow l \text{)} \\ \text{Diagram 6: } j \text{---} m \text{ with arcs } q \text{ (} j \rightarrow m \text{)} \end{array} + O(N) \\
& = \left(\begin{array}{c} \text{Diagram 1: } i \text{---} j \text{ with arcs } p \text{ (} i \rightarrow j \text{)} \\ \text{Diagram 2: } i \text{---} j \text{ with arcs } p \text{ (} i \rightarrow j \text{)} \end{array} \right) \times \left(\begin{array}{c} \text{Diagram 3: } i \text{---} j \text{ with arcs } q \text{ (} j \rightarrow i \text{)} \\ \text{Diagram 4: } i \text{---} j \text{ with arcs } q \text{ (} i \rightarrow j \text{)} \end{array} \right) + O(N) \\
& = N^2 (1 + (S(p) - 1))(1 + (S(q) - 1)) + O(N) = N^2 S(p) S(q) + O(N). \tag{4.17}
\end{aligned}$$

It is not hard to obtain the normalization of the n -phonon state using the same method:

$$\begin{aligned}
\langle 0 | (\rho_{\mathbf{p}_1} \cdots \rho_{\mathbf{p}_n})(\rho_{\mathbf{p}_1}^\dagger \cdots \rho_{\mathbf{p}_n}^\dagger) | 0 \rangle &= \prod_{m=1}^n \left(\begin{array}{c} \mathbf{p}_m \\ \circlearrowleft \\ i \end{array} + \begin{array}{c} \mathbf{p}_m \\ \text{---} \\ i \quad j \end{array} \right) + O(N^{n-1}) \\
&= N^n S(p_1) \cdots S(p_n) + O(N^{n-1}). \tag{4.18}
\end{aligned}$$

The energies of the Feynman phonon states are obtained from the identity

$$\langle 0 | A(H - E_0)B | 0 \rangle = \frac{1}{2m} \sum_{i=1}^N \langle 0 | (\nabla_i A) \cdot (\nabla_i B) | 0 \rangle, \tag{4.19}$$

where A and B are functions of particle coordinates, like $\rho_{\mathbf{p}_1} \cdots \rho_{\mathbf{p}_n}$, which commute with the potential. For one-phonon state we obtain

$$\begin{aligned}
\langle \mathbf{k} | H - E_0 | \mathbf{k} \rangle &= \frac{\langle 0 | \rho_{\mathbf{k}}(H - E_0)\rho_{\mathbf{k}}^\dagger | 0 \rangle}{\langle 0 | \rho_{\mathbf{k}}\rho_{\mathbf{k}}^\dagger | 0 \rangle} = \frac{1}{2mNS(k)} \sum_i \langle 0 | (\nabla_i \rho_{\mathbf{k}}) \cdot (\nabla_i \rho_{\mathbf{k}}^\dagger) | 0 \rangle \\
&= \frac{k^2}{2mNS(k)} \langle 0 | \overline{\rho_{\mathbf{k}}\rho_{\mathbf{k}}^\dagger} | 0 \rangle = \frac{k^2}{2mNS(k)} \begin{array}{c} \mathbf{k} \\ \circlearrowleft \\ i \end{array} = \frac{k^2}{2mS(k)}, \tag{4.20}
\end{aligned}$$

where the bar over the product of two ρ 's denotes that only the diagonal terms in the double sum are to be taken:

$$\overline{\rho_{\mathbf{a}}\rho_{\mathbf{b}}^\dagger} = \sum_{i=j} e^{i(\mathbf{b}\cdot\mathbf{r}_j - \mathbf{a}\cdot\mathbf{r}_i)} = \sum_i e^{i(\mathbf{b}-\mathbf{a})\cdot\mathbf{r}_i}. \tag{4.21}$$

Energy of the two-phonon state is

$$\begin{aligned}
\langle \mathbf{p}, \mathbf{q} | H - E_0 | \mathbf{p}, \mathbf{q} \rangle &= \frac{\langle 0 | (\rho_{\mathbf{p}}\rho_{\mathbf{q}})(H - E_0)(\rho_{\mathbf{p}}^\dagger\rho_{\mathbf{q}}^\dagger) | 0 \rangle}{\langle 0 | (\rho_{\mathbf{p}}\rho_{\mathbf{q}})(\rho_{\mathbf{p}}^\dagger\rho_{\mathbf{q}}^\dagger) | 0 \rangle} \\
&= \frac{1}{2mN^2S(p)S(q)} \sum_i \langle 0 | (\nabla_i(\rho_{\mathbf{p}}\rho_{\mathbf{q}})) \cdot (\nabla_i(\rho_{\mathbf{p}}^\dagger\rho_{\mathbf{q}}^\dagger)) | 0 \rangle \\
&= \frac{1}{2mN^2S(p)S(q)} \left\{ p^2 \langle 0 | \overline{(\rho_{\mathbf{p}}\rho_{\mathbf{q}})(\rho_{\mathbf{p}}^\dagger\rho_{\mathbf{q}}^\dagger)} | 0 \rangle + \right. \\
&\quad \left. + \mathbf{p} \cdot \mathbf{q} \left[\langle 0 | \overline{(\rho_{\mathbf{p}}\rho_{\mathbf{q}})(\rho_{\mathbf{p}}^\dagger\rho_{\mathbf{q}}^\dagger)} | 0 \rangle + \langle 0 | \overline{(\rho_{\mathbf{p}}\rho_{\mathbf{q}})(\rho_{\mathbf{p}}^\dagger\rho_{\mathbf{q}}^\dagger)} | 0 \rangle \right] + q^2 \langle 0 | \overline{(\rho_{\mathbf{p}}\rho_{\mathbf{q}})(\rho_{\mathbf{p}}^\dagger\rho_{\mathbf{q}}^\dagger)} | 0 \rangle \right\}
\end{aligned}$$

$$\begin{aligned}
&= \frac{1}{2mN^2 S(p)S(q)} \left[p^2 \left(\text{circle } i \text{ with } p \right) \left(\text{circle } j \text{ with } q + \text{arc } j \text{ to } k \text{ with } q \right) \right. \\
&\quad + 2p \cdot q \left(\text{arc } i \text{ to } j \text{ with } p-q + \text{arc } i \text{ to } j \text{ with } p + \text{arc } j \text{ to } m \text{ with } q \right. \\
&\quad \quad \left. + \text{arc } i \text{ to } m \text{ with } p + \text{arc } m \text{ to } j \text{ with } p-q + \text{arc } m \text{ to } i \text{ with } q + \text{arc } i \text{ to } j \text{ with } q-p + g_{ijk}^c \text{ terms} \right) \\
&\quad \left. + q^2 \left(\text{circle } i \text{ with } p + \text{arc } i \text{ to } j \text{ with } p \right) \left(\text{circle } k \text{ with } q \right) \right] \\
&= \frac{1}{2mN^2 S(p)S(q)} \left\{ N^2 [p^2 S(q) + q^2 S(p)] + O(N) \right\} \\
&= \frac{p^2}{2m S(p)} + \frac{q^2}{2m S(q)} + O(N^{-1}). \tag{4.22}
\end{aligned}$$

The generalization of this result to the case of n -phonon state is straightforward:

$$\langle \mathbf{p}_1, \dots, \mathbf{p}_n | H - E_0 | \mathbf{p}_1, \dots, \mathbf{p}_n \rangle = \sum_{i=1}^n \frac{p_i^2}{2m S(p_i)} + O(N^{-1}), \tag{4.23}$$

and we conclude that both the normalizations (4.18) and the energies (4.23) of Feynman phonons are determined⁶⁹ by the static structure function $S(q)$.

4.1.2 Off-diagonal CB matrix elements

In this subsection we examine the off-diagonal CB matrix elements of the unit operator

and the Hamiltonian. They are given by:

$$(\mathbf{p}_1, \dots, \mathbf{p}_n | \mathbf{q}_1, \dots, \mathbf{q}_m) = \frac{\langle 0 | (\rho_{\mathbf{p}_1} \cdots \rho_{\mathbf{p}_n}) (\rho_{\mathbf{q}_1}^\dagger \cdots \rho_{\mathbf{q}_m}^\dagger) | 0 \rangle}{N^{(n+m)/2} [S(p_1) \cdots S(p_n) S(q_1) \cdots S(q_m)]^{1/2}}, \quad (4.24)$$

$$\begin{aligned} (\mathbf{p}_1, \dots, \mathbf{p}_n | (H - E_0) | \mathbf{q}_1, \dots, \mathbf{q}_m) &= \frac{1}{2m} \sum_i \frac{\langle 0 | \nabla_i (\rho_{\mathbf{p}_1} \cdots \rho_{\mathbf{p}_n}) \cdot \nabla_i (\rho_{\mathbf{q}_1}^\dagger \cdots \rho_{\mathbf{q}_m}^\dagger) | 0 \rangle}{N^{(n+m)/2} [S(p_1) \cdots S(p_n) S(q_1) \cdots S(q_m)]^{1/2}} \\ &= \frac{1}{2m N^{(n+m)/2} [S(p_1) \cdots S(p_n) S(q_1) \cdots S(q_m)]^{1/2}} \\ &\times \sum_{i=1}^n \sum_{j=1}^m \mathbf{p}_i \cdot \mathbf{p}_j \langle 0 | \overline{(\rho_{\mathbf{p}_1} \cdots \rho_{\mathbf{p}_i} \cdots \rho_{\mathbf{p}_n}) \cdot (\rho_{\mathbf{q}_1}^\dagger \cdots \rho_{\mathbf{q}_j}^\dagger \cdots \rho_{\mathbf{q}_m}^\dagger)} | 0 \rangle. \end{aligned} \quad (4.25)$$

CB states $|\mathbf{p}_1, \dots, \mathbf{p}_n\rangle$ and $|\mathbf{q}_1, \dots, \mathbf{q}_m\rangle$ are eigenstates of the total momentum operator $\mathbf{P}_{tot} = \sum_{j=1}^N \frac{1}{i} \nabla_j$ with the eigenvalues $\sum_{i=1}^n \mathbf{p}_i$ and $\sum_{j=1}^m \mathbf{q}_j$ respectively. Thus the necessary condition for their overlap (4.24) to be non-vanishing is that $\sum_{i=1}^n \mathbf{p}_i = \sum_{j=1}^m \mathbf{q}_j$, i.e. that the momentum is conserved. The same is true for the CB matrix elements of the Hamiltonian (4.25), since \mathbf{P}_{tot} commutes with it. Anticipating our future needs, we set

$$\sum_{i=1}^n \mathbf{p}_i = \sum_{j=1}^m \mathbf{q}_j = \mathbf{k}, \quad (4.26)$$

the momentum transfer. It is plain that, since m and n are finite numbers, in the limit $k \rightarrow \infty$ at least one of the momenta \mathbf{p}_i and of \mathbf{q}_j must have a magnitude of order k in order to satisfy the above relation. Phonons whose momenta are of the order k are called "hard", as opposed to phonons with finite momenta (of order k^0) which are named "soft".

It can be shown that the matrix elements (4.24) and (4.25) vanish if the states $|\mathbf{p}_1, \dots, \mathbf{p}_n\rangle$ and $|\mathbf{q}_1, \dots, \mathbf{q}_m\rangle$ contain an unequal number of hard phonons. To demonstrate this we need to study the numerator of equation (4.24)

$$\langle 0 | (\rho_{\mathbf{p}_1} \cdots \rho_{\mathbf{p}_n}) (\rho_{\mathbf{q}_1}^\dagger \cdots \rho_{\mathbf{q}_m}^\dagger) | 0 \rangle \equiv \sum_{\substack{i_1 \neq \cdots \neq i_n \\ j_1 \neq \cdots \neq j_m}} \langle 0 | e^{-i(\mathbf{p}_1 \cdot \mathbf{r}_{i_1} + \cdots + \mathbf{p}_n \cdot \mathbf{r}_{i_n} - \mathbf{q}_1 \cdot \mathbf{r}_{j_1} - \cdots - \mathbf{q}_m \cdot \mathbf{r}_{j_m})} | 0 \rangle. \quad (4.27)$$

Let us assume that \mathbf{p}_1 and $\mathbf{q}_1 \sim \mathbf{k}$ while all other phonons are soft. If we write $\mathbf{p}_1 = \mathbf{k} + \mathbf{a}$ and $\mathbf{q}_1 = \mathbf{k} + \mathbf{b}$ where \mathbf{a} and \mathbf{b} are finite, we find that the exponent on the right-hand

side of the above equation contains the factor $e^{i\mathbf{k}\cdot\mathbf{r}_{i_1j_1}}$. If $i_1 \neq j_1$ the expectation value is proportional to $(S(k) - 1)$ which vanishes at large k . This is due to the fact that the static structure function $S(k)$ of a Bose liquid approaches unity exponentially fast as $k \rightarrow \infty$ even when the interatomic interactions are hard, like for example the Lenard-Jones (6,12) potential. We do not address here the problem of hard sphere gas whose $(S(k) - 1)$ does not go exponentially to zero at large k due to the singularity in the derivative of the pair distribution function $g(r)$ at $r = r_c$ the hard core radius. The $i_1 = j_1$ terms do not vanish, and we conclude that if \mathbf{p}_1 and \mathbf{q}_1 are the only hard phonons then

$$\langle 0 | (\rho_{\mathbf{p}_1} \cdots \rho_{\mathbf{p}_n})(\rho_{\mathbf{q}_1}^\dagger \cdots \rho_{\mathbf{q}_m}^\dagger) | 0 \rangle = \langle 0 | \overline{(\rho_{\mathbf{p}_1} \cdots \rho_{\mathbf{p}_n})(\rho_{\mathbf{q}_1}^\dagger \cdots \rho_{\mathbf{q}_m}^\dagger)} | 0 \rangle, \quad (4.28)$$

where we have used notation (4.21). Similarly, if $\mathbf{p}_1, \mathbf{p}_2, \mathbf{q}_1$ and \mathbf{q}_2 are the only hard phonons in CB states $|\mathbf{p}_1, \dots, \mathbf{p}_n\rangle$ and $|\mathbf{q}_1, \dots, \mathbf{q}_m\rangle$ then we find

$$\begin{aligned} & \langle 0 | (\rho_{\mathbf{p}_1} \cdots \rho_{\mathbf{p}_n})(\rho_{\mathbf{q}_1}^\dagger \cdots \rho_{\mathbf{q}_m}^\dagger) | 0 \rangle = \\ & \langle 0 | \overline{(\rho_{\mathbf{p}_1} \rho_{\mathbf{p}_2} \cdots \rho_{\mathbf{p}_n})(\rho_{\mathbf{q}_1}^\dagger \rho_{\mathbf{q}_2}^\dagger \cdots \rho_{\mathbf{q}_m}^\dagger)} | 0 \rangle + \langle 0 | \overline{(\rho_{\mathbf{p}_1} \rho_{\mathbf{p}_2} \cdots \rho_{\mathbf{p}_n})(\rho_{\mathbf{q}_1}^\dagger \rho_{\mathbf{q}_2}^\dagger \cdots \rho_{\mathbf{q}_m}^\dagger)} | 0 \rangle. \end{aligned} \quad (4.29)$$

In general, we conclude that the only terms of the multiple sum (4.27) that contribute to the overlap (4.24) are those where ρ 's and ρ^\dagger 's of hard phonons are paired together in the sense of equation (4.21). As a corollary it follows that the overlap of two CB states with an unequal number of hard phonons vanishes since then such pairing is impossible.

In our calculation of $S(\mathbf{k}, \omega)$ we need to consider only the CB states with one hard and any number of soft phonons. This is because the initial state $\rho_{\mathbf{k}}^\dagger | 0 \rangle$ in equation (2.9) belongs to the CB's (after it is properly normalized) and it has only one hard phonon. One hard phonon states are denoted by $|\mathbf{P}, \mathbf{p}_1, \dots, \mathbf{p}_n\rangle$, where

$$\mathbf{P} = \mathbf{k} - \mathbf{p}_1 - \cdots - \mathbf{p}_n, \quad (4.30)$$

and all lower case \mathbf{p}_i are of order "1", i.e. of order k^0 . Using equation (4.28) we obtain

$$(\mathbf{P}, \mathbf{p}_1, \dots, \mathbf{p}_n | \mathbf{Q}, \mathbf{q}_1, \dots, \mathbf{q}_m) = \frac{\langle 0 | \overline{(\rho_{\mathbf{P}} \rho_{\mathbf{p}_1} \cdots \rho_{\mathbf{p}_n})(\rho_{\mathbf{Q}} \rho_{\mathbf{q}_1}^\dagger \cdots \rho_{\mathbf{q}_m}^\dagger)} | 0 \rangle}{N^{(n+m+2)/2} [S(\mathbf{p}_1) \cdots S(\mathbf{p}_n) S(\mathbf{q}_1) \cdots S(\mathbf{q}_m)]^{1/2}}, \quad (4.31)$$

where we have taken into account that $S(P) = S(Q) = 1$ since $\mathbf{P}, \mathbf{Q} \sim \mathbf{k} \rightarrow \infty$. In particular, for $n = 1$ and $m = 0$ we obtain

$$\begin{aligned}
(\mathbf{k} - 1, 1 | \mathbf{k}) &= \frac{\langle 0 | \overline{(\rho_{\mathbf{k}-1} \rho_1) \rho_{\mathbf{k}}^\dagger} | 0 \rangle}{N^{3/2} \sqrt{S(l)}} = \frac{1}{N^{3/2} \sqrt{S(l)}} \begin{array}{c} 1 \\ \text{---} \text{---} \text{---} \\ i \quad \quad \quad j \end{array} \\
&= \frac{1}{\sqrt{N}} \frac{S(l) - 1}{\sqrt{S(l)}}. \tag{4.32}
\end{aligned}$$

As far as matrix elements of the Hamiltonian are concerned, we need to consider only the terms having $\mathbf{P} \cdot \mathbf{Q}$ in equation (4.25), which give contributions of order k^2 and k . The terms having $\mathbf{P} \cdot \mathbf{q}_j$ or $\mathbf{p}_i \cdot \mathbf{Q}$ contain $\overline{\rho_{\mathbf{P}} \rho_{\mathbf{q}_j}^\dagger}$ and $\overline{\rho_{\mathbf{P}} \rho_{\mathbf{Q}}^\dagger}$ terms respectively, i.e. they contain expectation values of $e^{i\mathbf{k} \cdot \mathbf{x}_{lm}}$ which vanish in the limit $k \rightarrow \infty$. Finally, the terms having $\mathbf{p}_i \cdot \mathbf{q}_j$ give contributions of order 1 which can be neglected. It then follows that:

$$\begin{aligned}
&(\mathbf{P}, \mathbf{p}_1, \dots, \mathbf{p}_n | (H - E_0) | \mathbf{Q}, \mathbf{q}_1, \dots, \mathbf{q}_m) = \\
&\frac{1}{2m} \left[k^2 - \mathbf{k} \cdot \left(\sum_{i=1, n} \mathbf{p}_i + \sum_{j=1, m} \mathbf{q}_j \right) \right] (\mathbf{P}, \mathbf{p}_1, \dots, \mathbf{p}_n | \mathbf{Q}, \mathbf{q}_1, \dots, \mathbf{q}_m) + O(k^0), \tag{4.33}
\end{aligned}$$

i.e. in the $k \rightarrow \infty$ limit the CB matrix elements of the Hamiltonian are proportional to those of the unit operator. In particular, from equations (4.32) and (4.33) we obtain

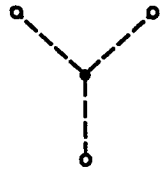
$$(\mathbf{k} - 1, 1 | (H - E_0) | \mathbf{k}) = -\frac{1}{\sqrt{N}} \frac{\mathbf{k} \cdot 1 (S(l) - 1)}{2m \sqrt{S(l)}} + O(k^0). \tag{4.34}$$

Finally, we want to calculate the off-diagonal two-phonon CB matrix element of the unit operator that is given by

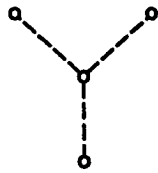
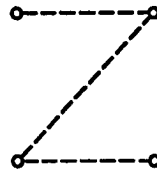
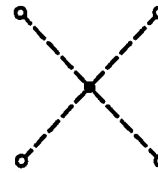
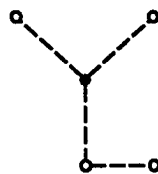
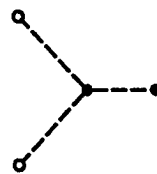
$$\begin{aligned}
(\mathbf{k} - 1, 1 | \mathbf{k} - \mathbf{m}, \mathbf{m}) &= \frac{\langle 0 | \overline{(\rho_{\mathbf{k}-1} \rho_1) (\rho_{\mathbf{k}-\mathbf{m}}^\dagger \rho_{\mathbf{m}}^\dagger)} | 0 \rangle}{N^2 \sqrt{S(l) S(m)}} \\
&= \frac{1}{N^2 \sqrt{S(l) S(m)}} \left[\langle 0 | (\rho_{\mathbf{m}-1} \rho_{\mathbf{m}-1}^\dagger) | 0 \rangle + \langle 0 | (\rho_{\mathbf{m}-1} \rho_1 \rho_{\mathbf{m}}^\dagger) | 0 \rangle \right]. \tag{4.35}
\end{aligned}$$

In order to calculate the second expectation value on the right-hand side of equation (4.35) we need an explicit expression for connected three-body distribution function g_{ijk}^c .

It is not known exactly, and we will use an approximate form, the so-called convolution approximation⁷⁰:

$$g_{ijk}^c \approx \rho \int d^3r_l h_{il} h_{jl} h_{kl} \equiv \text{Diagram} \quad (4.36)$$


The choice of convolution approximation will enable us to express all relevant CB and OCB matrix elements in term of the static structure function. It is straightforward to build approximate forms for the higher connected distribution functions that will have this same property. For example⁷¹:

$$g_{ijkl}^c \approx \text{Diagram 1} + \text{Diagram 2} + \text{Diagram 3} + \text{Diagram 4} + \text{Diagram 5} \quad (4.37)$$






etc. It can be easily checked that the convolution forms (4.36) and (4.37) satisfy the so-called sequential relation for the distribution functions

$$g_{a-1}(\mathbf{r}_1, \dots, \mathbf{r}_{a-1}) = \frac{\rho}{N-a+1} \int d^3r_a g_a(\mathbf{r}_1, \dots, \mathbf{r}_a) \quad (4.38)$$

that follows from the definition (4.5). On the other hand, in the presence of the strong short range repulsion the distribution functions g_a ought to vanish whenever position of any two particles coincide. In particular, we demand that

$$g_{iij} = 0, \quad (4.39)$$

which is not satisfied in the convolution approximation. The more detailed discussion of merits and shortcomings of the convolution approximation can be found in the ref. 34.

From equations (4.35) and (4.36) we get

$$\begin{aligned}
& (k-l, l | k-m, m) = \\
& = \frac{1}{N^2 \sqrt{S(l)S(m)}} \left(\begin{array}{c} \text{Diagram 1: } i \xrightarrow{1-m} j \\ \text{Diagram 2: } i \xrightarrow{l} j \xrightarrow{m} k \\ \text{Diagram 3: } i \xrightarrow{l} j \xrightarrow{1-m} k \\ \text{Diagram 4: } i \xrightarrow{m-l} j \xrightarrow{m} k \\ \text{Diagram 5: } i \xrightarrow{l} j \xrightarrow{1-m} k \end{array} \right) \\
& = \frac{1}{N \sqrt{S(l)S(m)}} \{ (S(|l-m|) - 1) + (S(l) - 1)(S(m) - 1) + (S(l) - 1)(S(|l-m|) - 1) + \\
& \quad + (S(m) - 1)(S(|l-m|) - 1) + (S(l) - 1)(S(m) - 1)(S(|l-m|) - 1) \} \\
& = \frac{1}{N \sqrt{S(l)S(m)}} \{ S(l)S(m)S(|l-m|) - S(l) - S(m) + 1 \}. \tag{4.40}
\end{aligned}$$

4.2 Orthogonalization of CB states

CB states are complete and normalized, but not mutually orthogonal. They can be used in the perturbation expansions, but require the special formalism that takes into the account their nonorthogonality, which is often called correlated-basis perturbation theory (CBPT)⁷². There has been an ample amount of work on this approach, and it was proved that the perturbation expansion is renormalizable, and the leading terms in the expansion of energy eigenvalues have been explicitly derived⁷³. Recently, low order CBPT was used in microscopic calculations on helium liquids^{55,74,75} and nuclear matter^{76,77}.

On the other hand, the clear analysis of the convergence properties of CBPT is yet

to be given. In particular, it is not clear whether the nonorthogonality spuriousities that are introduced when CBPT is truncated are negligible or not. Furthermore, the properly orthogonalized eigenvectors can not be easily extracted out from CBPT which is a major problem when quantities other than eigenvalues of the Hamiltonian are to be calculated.

In order to use normal perturbation theory, we have to orthogonalize the CB states. There are continuum many of them, so that it can not be achieved using the well known Gram-Schmidt procedure, which is described in subsection 4.2.1. It is possible to orthogonalize the CB states using the Löwdin transformation⁷⁸, whose definition and properties are discussed in subsection 4.2.2. Resulting orthogonal states, however, have higher energies than CB states; in particular, the ground state expectation value of the Hamiltonian is higher than E_0 , which is an unwanted property. Perturbative corrections move the energy down again, and both the increase in energy due to the Löwdin transform and decrease due to perturbative corrections are larger than the net displacement^{34,79}. In view of these difficulties, the orthogonal correlated-basis perturbation theory (OCBPT) was not the preferred tool for studies of quantum liquids.

Recently, however, the new orthogonalization scheme, free of the problems mentioned above, was proposed by Fantoni and Pandharipande³⁵. This new scheme is the subject of the subsection 4.2.3. The energies of the orthogonal CB (OCB) states obtained with this scheme are equal to those of CB states in the thermodynamic limit.

It is expected that OCBPT has better convergence than the nonorthogonal CBPT. Moreover OCBPT uses the well known simple perturbation expansions instead of the nonorthogonal perturbation theory. On the other hand, the computation of the matrix elements is more involved due to complexity of OCB states. The convergence of OCBPT is not expected to depend upon the specific nature of the bare interaction, i.e. if it has a hard core or not. For this reason we use it to study the scaling properties of the response at large k and ω .

4.2.1 Gram-Schmidt orthogonalization procedure

This procedure is well known and it is described in many texts on linear algebra, hence we quote it without the proof. If $|i\rangle$ ($i = 1, 2, \dots$) is an arbitrary nonorthogonal basis, then the vectors

$$|1\rangle_{GS} = \frac{1}{\sqrt{\langle 1|1\rangle}}|1\rangle, \quad (4.41)$$

$$|i\rangle_{GS} = \frac{|i\rangle - \sum_{j=1}^{i-1} |j\rangle_{GS} \langle GS(j|i)}{[\langle i|i\rangle - \sum_{j=1}^{i-1} |\langle GS(j|i)|^2]^{1/2}}, \quad i = 2, 3, \dots \quad (4.42)$$

form an ortho-normal basis. We note that the Gram-Schmidt procedure depends on the assumption that there are countably many vectors in the basis $|i\rangle$, and is not applicable to the CB states of equation (4.1) that depend on the continually varying momentum labels. Also, we note that the orthogonalization process is recursive and thus depends on the chosen order of vectors $|1\rangle, |2\rangle, \dots$, and different choices of the order yield different sets of orthogonal normalized vectors $|i\rangle_{GS}$.

4.2.2 Löwdin transformation and its properties

Löwdin has invented the orthogonalization procedure⁷⁸ that is both applicable to the arbitrarily large sets of states $|i\rangle$ and does not depend upon the chosen order to label the states. The procedure is defined as follows. Let $|i\rangle$ be an arbitrary nonorthogonal basis, and N_{ij} be its overlap matrix

$$N_{ij} \equiv \langle i|j\rangle, \quad (4.43)$$

and let all of the vectors $|i\rangle$ be normalized. Then the vectors

$$|i\rangle_L = \sum_j |j\rangle (N^{-1/2})_{ji} \quad (4.44)$$

form the orthogonal normalized basis, where $(N^{-1/2})_{ij}$ is the inverse square root of the overlap matrix (4.43).

We will prove the above statement under the assumption that the label i takes on discrete values only. The generalization to the case of continually varying i is straightforward, the sum in equation (4.44) is replaced by the appropriate integral. For the overlap of the Löwdin states we obtain

$$\begin{aligned} {}_L\langle i | j \rangle_L &= \left[\sum_m (N^{-1/2})_{mi}^* |m\rangle \right] \left[\sum_n |n\rangle (N^{-1/2})_{nj} \right] \\ &= \sum_{m,n} (N^{-1/2})_{im} N_{mn} (N^{-1/2})_{nj} = \delta_{ij}, \end{aligned} \quad (4.45)$$

where we have used the hermitean property of the overlap matrix

$$N_{ij}^* = N_{ji}. \quad (4.46)$$

Now, to finish the proof, we have to show that N_{ij} is a positive definite matrix, so that $(N^{-1/2})_{ij}$ exists. We will prove the equivalent statement that the determinants of all leading minors of the matrix N_{ij} are positive. We start this proof by recalling that the n -th leading minor of the matrix is its $n \times n$ submatrix situated in the upper left corner of the matrix. It is obviously constituted by the overlaps of the first n vectors $|i\rangle$. These n vectors form the base of the n -dimensional vector space, and can be expanded in terms of an other orthogonal basis $|j\rangle$ in this space as

$$|i\rangle = \sum_{j=1}^n |j\rangle c_{ji}. \quad (4.47)$$

We denote the n -th leading minor of the overlap matrix by $N_{n,ij}$ and obtain

$$\det |N_{n,ij}| = \det \left| \sum_{l=1}^n c_{li}^* c_{lj} \right| = \det |c_{ij}^*| \det |c_{ij}| = |\det |c_{ij}||^2 \geq 0. \quad (4.48)$$

The equality in expression (4.48) can not be reached since the matrix c_{ij} transforms one basis into another which guarantees that it is not singular (i.e. $\det |c_{ij}| \neq 0$), and we conclude that

$$\det |N_{n,ij}| > 0, \quad (4.49)$$

which finishes the proof of the existence of the matrix $(N^{-1/2})_{ij}$ and of the statement (4.44).

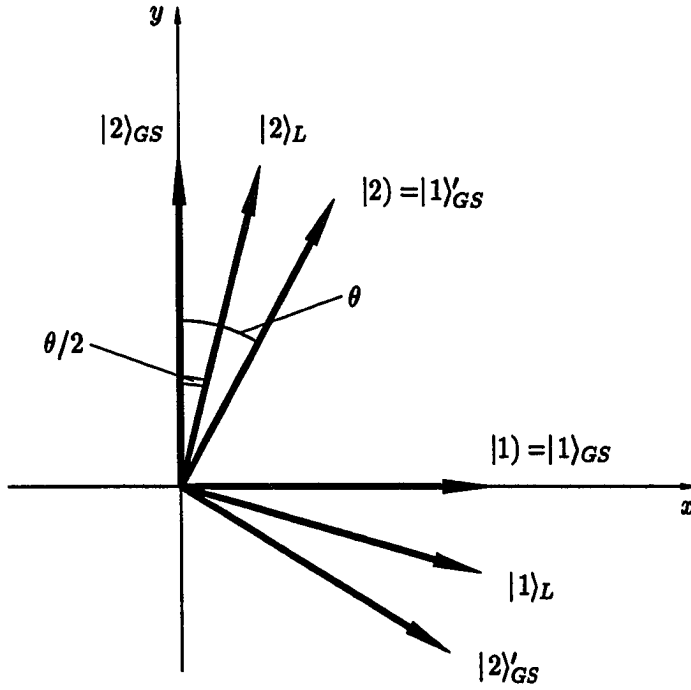


Figure 4.1: The two vector orthogonalization example ($\theta = 30^\circ$).

We can illustrate the differences between the Gram-Schmidt and Löwdin transforms by an example of the nonorthogonal basis that contain only two real vectors:

$$|1\rangle = \begin{bmatrix} 1 \\ 0 \end{bmatrix}, \quad |2\rangle = \begin{bmatrix} \sin \theta \\ \cos \theta \end{bmatrix} \quad (4.50)$$

The overlap matrix and its inverse square root are

$$N = \begin{bmatrix} 1 & \sin \theta \\ \sin \theta & 1 \end{bmatrix}, \quad N^{-1/2} = \frac{1}{\cos \theta} \begin{bmatrix} \cos \frac{\theta}{2} & -\sin \frac{\theta}{2} \\ -\sin \frac{\theta}{2} & \cos \frac{\theta}{2} \end{bmatrix}, \quad (4.51)$$

and we obtain the following Gram-Schmidt and Löwdin states:

$$|1\rangle_{GS} = \begin{bmatrix} 1 \\ 0 \end{bmatrix}, \quad |2\rangle_{GS} = \begin{bmatrix} 0 \\ 1 \end{bmatrix}, \quad (4.52)$$

$$|1\rangle_L = \begin{bmatrix} \cos \frac{\theta}{2} \\ -\sin \frac{\theta}{2} \end{bmatrix}, \quad |2\rangle_L = \begin{bmatrix} \sin \frac{\theta}{2} \\ \cos \frac{\theta}{2} \end{bmatrix}, \quad (4.53)$$

all of whom are shown in fig. 4.1.

As mentioned before, the nonorthogonal vectors $|i\rangle$ enter the Gram-Schmidt procedure in an asymmetric way since the vector $|1\rangle$ is singled out. If we renumerate them like $|1'\rangle \equiv |2\rangle$ and $|2'\rangle \equiv |1\rangle$, then the different set of orthogonal vectors

$$|1'\rangle_{GS} = \begin{bmatrix} \sin \theta \\ \cos \theta \end{bmatrix}, \quad |2'\rangle_{GS} = \begin{bmatrix} \cos \theta \\ -\sin \theta \end{bmatrix} \quad (4.54)$$

is obtained. On the contrary, the set $|1'\rangle$ and $|2'\rangle$ yields exactly the same Löwdin states since the overlap matrix N (equation (4.51)) does not change. Moreover, even the ordering of the Löwdin states is arbitrary since the matrix $N^{-1/2}$ is not unique for the given matrix N . In our example we could have chosen

$$N^{-1/2} = \frac{1}{\sin \theta} \begin{bmatrix} -\sin \frac{\theta}{2} & \cos \frac{\theta}{2} \\ \cos \frac{\theta}{2} & -\sin \frac{\theta}{2} \end{bmatrix}, \quad (4.55)$$

instead of $N^{-1/2}$ of equation (4.51), which would correspond to the exchange $|1\rangle_L \leftrightarrow |2\rangle_L$.

We also remark without the proof that Löwdin transformation has the variational property that the set of vectors $|i\rangle_L$ is the orthogonal basis that is the "closest" to the original set $|i\rangle$. More precisely, the quantity

$$\Delta^2 \equiv \|[(|i\rangle - \langle i|][|i\rangle - |i\rangle)]\|^2, \quad (4.56)$$

where $|i\rangle$ is an arbitrary orthogonal basis, reaches the minimum when $|i\rangle \equiv |i\rangle_L$.

The calculation of $N^{-1/2}$ is not easy, and becomes forbiddingly hard as the set $|i\rangle$ gets larger. To avoid these problems an approximate method of calculation of $N^{-1/2}$ was developed. The matrix N is divided into diagonal and off-diagonal parts:

$$N = 1 + \bar{N}, \quad (4.57)$$

$$\bar{N}_{ij} = N_{ij}(1 - \delta_{ij}), \quad (4.58)$$

and its inverse square root is found as the sum of the infinite series

$$N^{-1/2} = 1 - \frac{1}{2}\bar{N} + \frac{3}{8}(\bar{N})^2 - \dots, \quad (4.59)$$

where the coefficients in this expansion are the same as in the Taylor expansion of $(1+x)^{-1/2}$ around the point $x = 0$.

The expansion (4.59) is very useful in practice, but may fail to converge. More precisely, it diverges when the largest eigenvalue of \bar{N} exceeds 1. This possibility was overlooked by many authors, including the Löwdin himself, who defined the transform in terms of the expansion (4.59), instead of defining it in terms of $N^{-1/2}$ which, as we proved, always exist. We will encounter the situation when the series (4.59) diverges in chapter 6 where we calculate the deep inelastic response of the Fermi liquid at zero temperature. Here, we give an elementary example that involves only three real vectors

$$|1\rangle = \begin{bmatrix} 1 \\ 0 \\ 0 \end{bmatrix}, \quad |2\rangle = \frac{1}{\sqrt{2}} \begin{bmatrix} 1 \\ 1 \\ 0 \end{bmatrix}, \quad |3\rangle = \frac{1}{\sqrt{2}} \begin{bmatrix} 1 \\ 0 \\ 1 \end{bmatrix}. \quad (4.60)$$

The overlap matrix and its determinant are

$$N = \begin{bmatrix} 1 & 1/\sqrt{2} & 1/\sqrt{2} \\ 1/\sqrt{2} & 1 & 1/2 \\ 1/\sqrt{2} & 1/2 & 1 \end{bmatrix}, \quad \det|N| = \frac{1}{4}, \quad (4.61)$$

so that the inverse matrix is given by

$$N^{-1} = 4 \begin{bmatrix} 3/4 & -1/2\sqrt{2} & -1/2\sqrt{2} \\ -1/2\sqrt{2} & 1/2 & 0 \\ -1/2\sqrt{2} & 0 & 1/2 \end{bmatrix} = \begin{bmatrix} 3 & -\sqrt{2} & -\sqrt{2} \\ -\sqrt{2} & 2 & 0 \\ -\sqrt{2} & 0 & 2 \end{bmatrix}, \quad (4.62)$$

and

$$N^{-1/2} = \frac{\sqrt{5+2\sqrt{2}}}{\sqrt{2 \cdot 17}} \begin{bmatrix} 3\sqrt{2}-2 & -2 & -2 \\ -2 & \sqrt{2}-1+\sqrt{5-2\sqrt{2}} & \sqrt{2}-1-\sqrt{5-2\sqrt{2}} \\ -2 & \sqrt{2}-1-\sqrt{5-2\sqrt{2}} & \sqrt{2}-1+\sqrt{5-2\sqrt{2}} \end{bmatrix} \quad (4.63)$$

Next, we calculate the n -th power of the matrix

$$\bar{N} \equiv N - 1 = \begin{bmatrix} 0 & 1/\sqrt{2} & 1/\sqrt{2} \\ 1/\sqrt{2} & 0 & 1/2 \\ 1/\sqrt{2} & 1/2 & 0 \end{bmatrix}. \quad (4.64)$$

Using the ansatz

$$(\bar{N})^n = \begin{bmatrix} a_n & b_n & b_n \\ b_n & c_n & d_n \\ b_n & d_n & c_n \end{bmatrix} \quad (4.65)$$

and the obvious relation

$$(\bar{N})^{n+1} = \bar{N}(\bar{N})^n, \quad (4.66)$$

we obtain the following set of difference equations for the unknown quantities a_n , b_n , c_n , and d_n :

$$\left. \begin{aligned} a_{n+1} &= \sqrt{2}b_n \\ b_{n+1} &= \frac{1}{\sqrt{2}}a_n + \frac{1}{2}b_n \\ c_{n+1} &= \frac{1}{\sqrt{2}}b_n + \frac{1}{2}d_n \\ d_{n+1} &= \frac{1}{\sqrt{2}}b_n + \frac{1}{2}c_n \end{aligned} \right\}, \quad (4.67)$$

with the initial conditions

$$a_1 = 0, \quad b_1 = 1/\sqrt{2}, \quad c_1 = 0, \quad d_1 = 1/2. \quad (4.68)$$

The system (4.67), (4.68) is linear, and can be solved by usual methods. The solution is

$$\left. \begin{aligned} a_n &= \frac{2}{\sqrt{17}}(\lambda_1^{n-1} - \lambda_2^{n-1}) \\ b_n &= \sqrt{\frac{2}{17}}(\lambda_1^n - \lambda_2^n) \\ c_n &= \frac{1}{\sqrt{17}}(\lambda_1^{n+1} - \lambda_2^{n+1}) - \lambda_3^{n+1} \\ d_n &= \frac{1}{\sqrt{17}}(\lambda_1^{n+1} - \lambda_2^{n+1}) + \lambda_3^{n+1} \end{aligned} \right\}, \quad (4.69)$$

where

$$\lambda_{1,2} = \frac{1 \pm \sqrt{17}}{4}, \quad \lambda_3 = -\frac{1}{2}, \quad (4.70)$$

are the eigenvalues of the matrix \bar{N} , and we find that the series (4.59) is divergent due to the fact that the eigenvalue $\lambda_1 \approx 1.28$ is larger than 1.

In those instances when the series (4.59) fails to converge, it is still possible to find $N^{-1/2}$ by discretization and diagonalization of the operator N_{ij} . An other procedure for calculation of $N^{-1/2}$ is based on the observation that although series (4.59) is divergent when the largest eigenvalue λ_{\max} of \bar{N} exceeds 1, the series

$$N^{-1/2}(\alpha) = 1 - \frac{1}{2}\alpha\bar{N} + \frac{3}{8}(\alpha\bar{N})^2 - \dots, \quad (4.71)$$

converges for all $\alpha < 1/\lambda_{\max}$. After the series (4.71) is summed for several values of α the operator $N^{-1/2}$ is found by a rational (Padé) extrapolation^{80,81} to $\alpha = 1$.

4.2.3 Fantoni-Pandharipande scheme of orthogonalization

As we have already mentioned, it is impossible to orthogonalize CB states (4.1) using Gram-Schmidt procedure alone, while straightforward application of the Löwdin transform leads to difficulties due to the fact that Löwdin states have higher energies than the CB states. The Fantoni-Pandharipande orthogonalization scheme³⁵, which is free of these problems, is defined as follows. CB states (4.1) are orthogonalized recursively with respect to the number of phonons they contain. We start with the one phonon states $|\mathbf{p}\rangle$. They are orthogonal to the ground state $|0\rangle$ and to each other because of the momentum conservation, and can be included in the orthogonal basis without change. In fact, any two CB states with different total momentum are orthogonal to each other, which means that we can restrict our attention to the subset of CB states with the given total momentum \mathbf{k} without loss of generality. Thus the first state in OCB is

$$|\mathbf{k}\rangle = |\mathbf{k}\rangle. \quad (4.72)$$

The two-phonon states are orthogonalized in two steps. First, a partially orthogonal (PO)

set of two-phonon states is defined using the Gram-Schmidt procedure

$$|\mathbf{p}_1, \mathbf{p}_2\rangle = |\mathbf{p}_1, \mathbf{p}_2\rangle - |\mathbf{k}\rangle\langle\mathbf{k}|\mathbf{p}_1, \mathbf{p}_2\rangle. \quad (4.73)$$

It should be noted that this expression differs from usual Gram-Schmidt one (equation (4.35)) by the absence of the factor

$$[1 - |\langle\mathbf{k}|\mathbf{p}_1, \mathbf{p}_2\rangle|^2]^{-1/2} \quad (4.74)$$

which, it turns out, is equal to one in the thermodynamic limit³⁵. A two-phonon PO state $|\mathbf{p}_1, \mathbf{p}_2\rangle$ is orthogonal to one-phonon OCB state $|\mathbf{k}\rangle$ by construction, but it is not orthogonal to other two-phonon PO states $|\mathbf{q}_1, \mathbf{q}_2\rangle$. This is achieved in the second step by the Löwdin transformation:

$$|\mathbf{p}_1, \mathbf{p}_2\rangle = \sum_{\mathbf{q}_1, \mathbf{q}_2} |\mathbf{q}_1, \mathbf{q}_2\rangle (N^{-1/2})_{\mathbf{q}_1, \mathbf{q}_2; \mathbf{p}_1, \mathbf{p}_2}, \quad (4.75)$$

where, as before, $N^{-1/2}$ is the inverse square root of the overlap matrix N of the states that are being orthogonalized, in this case of the two-phonon PO states:

$$N_{\mathbf{q}_1, \mathbf{q}_2; \mathbf{p}_1, \mathbf{p}_2} \equiv \{\mathbf{q}_1, \mathbf{q}_2|\mathbf{p}_1, \mathbf{p}_2\rangle. \quad (4.76)$$

The same two step procedure is repeated for three-phonon states, four-phonon states, and so on.

In general, if the CB states up to and including $(n - 1)$ -phonon states have already been properly orthogonalized, the n -phonon states are orthogonalized by first obtaining a PO set of n -phonon states

$$|\mathbf{p}_1, \dots, \mathbf{p}_n\rangle \equiv |\mathbf{p}_1, \dots, \mathbf{p}_n\rangle - \sum_{m < n} \sum_{\mathbf{q}_1, \dots, \mathbf{q}_m} |\mathbf{q}_1, \dots, \mathbf{q}_m\rangle \langle\mathbf{q}_1, \dots, \mathbf{q}_m|\mathbf{p}_1, \dots, \mathbf{p}_n\rangle \quad (4.77)$$

that are orthogonal to all $(m < n)$ -phonon OCB states. These states are then mutually orthogonalized using Löwdin transform

$$|\mathbf{p}_1, \dots, \mathbf{p}_n\rangle = \sum_{\mathbf{q}_1, \dots, \mathbf{q}_n} |\mathbf{q}_1, \dots, \mathbf{q}_n\rangle (N^{-1/2})_{\mathbf{q}_1, \dots, \mathbf{q}_n; \mathbf{p}_1, \dots, \mathbf{p}_n}, \quad (4.78)$$

where $N^{-1/2}$ here denotes inverse square root of the overlap matrix N of the n -phonon PO states:

$$N_{\mathbf{q}_1, \dots, \mathbf{q}_n; \mathbf{p}_1, \dots, \mathbf{p}_n} \equiv \{\mathbf{q}_1, \dots, \mathbf{q}_n | \mathbf{p}_1, \dots, \mathbf{p}_n\}. \quad (4.79)$$

The methods for calculation of $N^{-1/2}$ were discussed in subsection 4.2.2. The simplest one is to sum the series (4.59), providing that it converges. In the case of n -phonon PO states $N^{-1/2}$ is given by

$$\begin{aligned} (N^{-1/2})_{\mathbf{q}_1, \dots, \mathbf{q}_n; \mathbf{p}_1, \dots, \mathbf{p}_n} &= \delta_{\mathbf{q}_1, \dots, \mathbf{q}_n; \mathbf{p}_1, \dots, \mathbf{p}_n} - \frac{1}{2} \overline{\{\mathbf{q}_1, \dots, \mathbf{q}_n | \mathbf{p}_1, \dots, \mathbf{p}_n\}} \\ &+ \frac{3}{8} \sum_{\mathbf{p}'_1, \dots, \mathbf{p}'_n} \overline{\{\mathbf{q}_1, \dots, \mathbf{q}_n | \mathbf{p}'_1, \dots, \mathbf{p}'_n\} \{\mathbf{p}'_1, \dots, \mathbf{p}'_n | \mathbf{p}_1, \dots, \mathbf{p}_n\}} - \dots \end{aligned} \quad (4.80)$$

where a bar on the matrix elements indicates that the diagonal matrix elements are to be omitted.

It is shown in ref. 35 that in the thermodynamic limit ($N, \Omega \rightarrow \infty$ while $\rho \equiv N/\Omega = \text{const}$) the Fantoni-Pandharipande orthogonalization scheme has the following properties:

- a) The diagonal matrix elements of the unit operator are preserved by the orthogonalization process, i.e. the OCB states are normalized as are the CB states.
- b) The diagonal matrix elements of the Hamiltonian are preserved, i.e. the OCB states have the same energies as the CB states.
- c) The off-diagonal matrix elements are not preserved. For example, the matrix elements of the unit operator vanish after the transformation.

These properties hold only for the OCB states with the finite number of phonons, which limits the applicability of Fantoni-Pandharipande scheme to very low (strictly speaking zero) temperature. At finite temperatures states with the number of phonons that is comparable to the number of particles in the system have to be taken into account, and the above properties are not applicable.

From here on the notation $|i\rangle, |j\rangle, \dots$ will be used only for OCB states that are obtained from CB states (4.1) using the Fantoni-Pandharipande scheme that we have just described. These may also be denoted by listing all momentum labels whenever appropriate.

At the end we mention that the original definition³⁵ of Fantoni-Pandharipande scheme, in which the PO states are defined as

$$|\mathbf{p}_1, \dots, \mathbf{p}_n\rangle' \equiv |\mathbf{p}_1, \dots, \mathbf{p}_n\rangle - \sum_{m < n} \sum_{\mathbf{q}_1, \dots, \mathbf{q}_m} |\mathbf{q}_1, \dots, \mathbf{q}_m\rangle (\mathbf{q}_1, \dots, \mathbf{q}_m | \mathbf{p}_1, \dots, \mathbf{p}_n) \quad (4.81)$$

instead of equation (4.77), is incorrect since these PO states with different number of phonons are not mutually orthogonal:

$$\langle \mathbf{p}_1, \dots, \mathbf{p}_n | \mathbf{q}_1, \dots, \mathbf{q}_m \rangle' \neq 0 \quad \text{for } n \neq m, \quad (4.82)$$

which can be verified by direct substitution.

4.3 OCB matrix elements in scaling limit

The OCB matrix elements of the unit operator are trivial since the OCB states are orthonormal, and we need to study the matrix elements of the Hamiltonian only. The diagonal OCB matrix elements of the Hamiltonian are the same as the CB matrix elements by construction, and using equation (4.23) we get

$$\langle \mathbf{p}_1, \dots, \mathbf{p}_n | H | \mathbf{p}_1, \dots, \mathbf{p}_n \rangle = \sum_{i=1}^n \frac{p_i^2}{2m S(p_i)}. \quad (4.83)$$

On the other hand, the off-diagonal OCB matrix elements of the Hamiltonian are different from the CB ones. We can generally write

$$| \mathbf{P}, \mathbf{p}_1, \dots, \mathbf{p}_n \rangle = \sum_{m \leq n} \sum_{\mathbf{q}_1, \dots, \mathbf{q}_m} \alpha(\mathbf{p}_1, \dots, \mathbf{p}_n, \mathbf{q}_1, \dots, \mathbf{q}_m) | \mathbf{Q}, \mathbf{q}_1, \dots, \mathbf{q}_m \rangle, \quad (4.84)$$

where the coefficients $\alpha(\mathbf{p}_1, \dots, \mathbf{p}_n, \mathbf{q}_1, \dots, \mathbf{q}_m)$ are obtained from the Gram-Schmidt and Löwdin transformations described in the subsection 4.2.3. From equations (4.84) and (4.33)

we obtain

$$\begin{aligned}
& \langle \mathbf{P}, \mathbf{p}_1, \dots, \mathbf{p}_n | H | \mathbf{P}', \mathbf{p}'_1, \dots, \mathbf{p}'_{n'} \rangle \\
&= \sum_{\substack{m \leq n \\ m' \leq n'}} \sum_{\substack{\mathbf{q}_1, \dots, \mathbf{q}_m \\ \mathbf{q}'_1, \dots, \mathbf{q}'_{m'}}} \alpha^*(\mathbf{p}_1, \dots, \mathbf{p}_n, \mathbf{q}_1, \dots, \mathbf{q}_m) \alpha(\mathbf{p}'_1, \dots, \mathbf{p}'_{n'}, \mathbf{q}'_1, \dots, \mathbf{q}'_{m'}) \\
&\quad \times \langle \mathbf{Q}, \mathbf{q}_1, \dots, \mathbf{q}_m | (H - E_0) | \mathbf{Q}', \mathbf{q}'_1, \dots, \mathbf{q}'_{m'} \rangle \\
&= \sum_{\substack{m \leq n \\ m' \leq n'}} \sum_{\substack{\mathbf{q}_1, \dots, \mathbf{q}_m \\ \mathbf{q}'_1, \dots, \mathbf{q}'_{m'}}} \frac{1}{2m} \left[k^2 - \mathbf{k} \cdot \left(\sum_{i=1}^m \mathbf{q}_i + \sum_{j=1}^{m'} \mathbf{q}'_j \right) \right] \\
&\quad \times \alpha^*(\mathbf{p}_1, \dots, \mathbf{p}_n, \mathbf{q}_1, \dots, \mathbf{q}_m) \alpha(\mathbf{p}'_1, \dots, \mathbf{p}'_{n'}, \mathbf{q}'_1, \dots, \mathbf{q}'_{m'}) \\
&\quad \times \langle \mathbf{Q}, \mathbf{q}_1, \dots, \mathbf{q}_m | \mathbf{Q}', \mathbf{q}'_1, \dots, \mathbf{q}'_{m'} \rangle + O(k^0). \tag{4.85}
\end{aligned}$$

The coefficient of the k^2 term is just the overlap $\langle \mathbf{P}, \mathbf{p}_1, \dots, \mathbf{p}_n | \mathbf{P}', \mathbf{p}'_1, \dots, \mathbf{p}'_{n'} \rangle$, which is zero for nondiagonal elements. Hence the leading term of the off-diagonal OCB matrix elements of the Hamiltonian is proportional to k :

$$\langle \mathbf{P}, \mathbf{p}_1, \dots, \mathbf{p}_n | H | \mathbf{P}', \mathbf{p}'_1, \dots, \mathbf{p}'_{n'} \rangle = O(k). \tag{4.86}$$

We conclude this subsection with the calculation of the one- to two-phonon OCB matrix element of the Hamiltonian $\langle \mathbf{k} - \mathbf{l}, \mathbf{l} | H | \mathbf{k} \rangle$. In order to do it we need to calculate the corresponding PO matrix elements. Using equations (4.77), (4.72) and (4.34) we find that the one- to two-phonon PO matrix element is given by (from here on we will omit the $O(k^0)$ terms):

$$\begin{aligned}
& \{ \mathbf{k} - \mathbf{l}, \mathbf{l} | (H - E_0) | \mathbf{k} \} \\
&= (\mathbf{k} - \mathbf{l}, \mathbf{l} | (H - E_0) | \mathbf{k}) - (\mathbf{k} - \mathbf{l}, \mathbf{l} | \mathbf{k}) (\mathbf{k} | (H - E_0) | \mathbf{k}) \\
&= -\frac{1}{2m} \mathbf{k} \cdot \mathbf{l} \frac{1}{\sqrt{N}} \frac{S(l) - 1}{\sqrt{S(l)}} \equiv -\frac{k}{m} \frac{1}{\sqrt{N}} \frac{\hat{\mathbf{k}} \cdot \hat{\mathbf{l}}}{2} \sqrt{f_0(l)}. \tag{4.87}
\end{aligned}$$

The OCB states are obtained from PO states using the Löwdin transformation for which the overlap of the two phonon PO states is needed. From equations (4.73), (4.72), (4.34)

and (4.40) it follows that the overlap of the two-phonon PO states is given by

$$\begin{aligned} \langle \mathbf{k} - \mathbf{l}, \mathbf{l} | \mathbf{k} - \mathbf{m}, \mathbf{m} \rangle &= (\mathbf{k} - \mathbf{l}, \mathbf{l} | \mathbf{k} - \mathbf{m}, \mathbf{m}) - (\mathbf{k} - \mathbf{l}, \mathbf{l} | \mathbf{k}) (\mathbf{k} | \mathbf{k} - \mathbf{m}, \mathbf{m}) \\ &= \frac{1}{N} \sqrt{S(l)S(m)} (S(|\mathbf{l} - \mathbf{m}|) - 1). \end{aligned} \quad (4.88)$$

The one to two-phonon OCB matrix element of the Hamiltonian can be calculated using PO matrix elements (4.87) and (4.88) and equation (4.75) as follows:

$$\begin{aligned} \langle \mathbf{k} - \mathbf{l}, \mathbf{l} | H | \mathbf{k} \rangle &= \\ &= \langle \mathbf{k} - \mathbf{l}, \mathbf{l} | (H - E_0) | \mathbf{k} \rangle - \frac{1}{2} \sum_{\mathbf{l}_1} \overline{\langle \mathbf{k} - \mathbf{l}, \mathbf{l} | \mathbf{k} - \mathbf{l}_1, \mathbf{l}_1 \rangle} \langle \mathbf{k} - \mathbf{l}_1, \mathbf{l}_1 | (H - E_0) | \mathbf{k} \rangle \\ &\quad + \frac{3}{8} \sum_{\mathbf{l}_1, \mathbf{l}_2} \overline{\langle \mathbf{k} - \mathbf{l}, \mathbf{l} | \mathbf{k} - \mathbf{l}_1, \mathbf{l}_1 \rangle} \overline{\langle \mathbf{k} - \mathbf{l}_1, \mathbf{l}_1 | \mathbf{k} - \mathbf{l}_2, \mathbf{l}_2 \rangle} \langle \mathbf{k} - \mathbf{l}_2, \mathbf{l}_2 | (H - E_0) | \mathbf{k} \rangle - \dots \\ &= -\frac{1}{\sqrt{N}} \frac{k}{2m} \left(\hat{\mathbf{k}} \cdot \mathbf{l} \frac{S(l) - 1}{\sqrt{S(l)}} - \frac{1}{2} \int \frac{d^3 l_1}{(2\pi)^3 \rho} \sqrt{S(l)S(l_1)} (S(|\mathbf{l} - \mathbf{l}_1|) - 1) \hat{\mathbf{k}} \cdot \mathbf{l}_1 \frac{S(l_1) - 1}{\sqrt{S(l_1)}} \right. \\ &\quad \left. + \frac{3}{8} \int \frac{d^3 l_1}{(2\pi)^3 \rho} \int \frac{d^3 l_2}{(2\pi)^3 \rho} \sqrt{S(l)S(l_1)} (S(|\mathbf{l} - \mathbf{l}_1|) - 1) \right. \\ &\quad \left. \times \sqrt{S(l_1)S(l_2)} (S(|\mathbf{l}_1 - \mathbf{l}_2|) - 1) \hat{\mathbf{k}} \cdot \mathbf{l}_2 \frac{S(l_2) - 1}{\sqrt{S(l_2)}} - \dots \right) \\ &= -\frac{1}{\sqrt{N}} \frac{k}{2m} \hat{\mathbf{k}} \cdot \hat{\mathbf{l}} \left[\sqrt{f_0(l)} + \sqrt{S(l)} \left(-\frac{1}{2} \int \frac{d^3 l_1}{(2\pi)^3 \rho} A(\mathbf{l}, \mathbf{l}_1) l_1 \frac{S(l_1) - 1}{S(l_1)} \right. \right. \\ &\quad \left. \left. + \frac{3}{8} \int \frac{d^3 l_1}{(2\pi)^3 \rho} A(\mathbf{l}, \mathbf{l}_1) \int \frac{d^3 l_2}{(2\pi)^3 \rho} A(\mathbf{l}_1, \mathbf{l}_2) l_2 \frac{S(l_2) - 1}{S(l_2)} - \dots \right) \right] \\ &\equiv -\frac{k}{m} \frac{1}{\sqrt{N}} \frac{\hat{\mathbf{k}} \cdot \hat{\mathbf{l}}}{2} \sqrt{f(l)}, \end{aligned} \quad (4.89)$$

where

$$\begin{aligned} f(l) &= \left[\sqrt{f_0(l)} + \sqrt{S(l)} \left(-\frac{1}{2} \int \frac{d^3 l_1}{(2\pi)^3 \rho} A(\mathbf{l}, \mathbf{l}_1) l_1 \frac{S(l_1) - 1}{S(l_1)} \right. \right. \\ &\quad \left. \left. + \frac{3}{8} \int \frac{d^3 l_1}{(2\pi)^3 \rho} A(\mathbf{l}, \mathbf{l}_1) \int \frac{d^3 l_2}{(2\pi)^3 \rho} A(\mathbf{l}_1, \mathbf{l}_2) l_2 \frac{S(l_2) - 1}{S(l_2)} - \dots \right) \right]^2, \end{aligned} \quad (4.90)$$

$$A(\mathbf{l}, \mathbf{m}) \equiv \hat{\mathbf{l}} \cdot \hat{\mathbf{m}} S(m) (S(|\mathbf{l} - \mathbf{m}|) - 1). \quad (4.91)$$

The function $f(l)$ is determined entirely by the static structure function $S(q)$. It

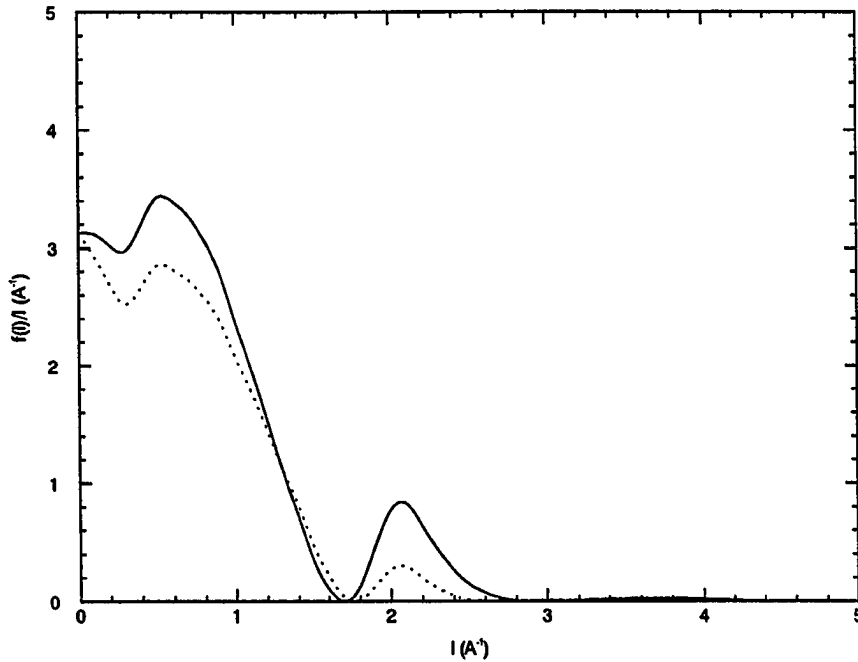


Figure 4.2: The function $f(l)/l$ (equation (4.90)) of liquid ${}^4\text{He}$ at equilibrium density and zero temperature calculated from $S(q)$ of ref. 81 with (solid line) and without (dotted line) Löwdin corrections.

contains a leading term

$$f_0(l) = l^2 \frac{(S(l) - 1)^2}{S(l)}, \quad (4.92)$$

and small corrections from the Löwdin orthogonalization of the two-phonon states. When $l \rightarrow 0$ the function $A(l, l_1)$ can be expanded in l and substituted in equation (4.90). The angular integral of the zeroth-order term of this expansion vanishes, and the bracket that multiplies $\sqrt{S(l)}$ in equation (4.92) is proportional to l . Thus, the function $f(l)$ is linear for small values of l and has the same slope as $f_0(l)$. The functions $f(l)$ and $f_0(l)$ computed using experimental⁸¹ $S(l)$ for liquid ${}^4\text{He}$ at low temperatures are shown in Figure 4.2.

We want to stress that the simple angular dependence of the one- to two-phonon matrix element (4.89) and the linearity of the function $f(l)$, which will both be crucial for the calculation of the scaling function $J(y)$ in chapter 5, are not the artifacts of the

convolution approximation that was used in the calculation of the overlap of two-phonon CB states (equation (4.40)), but rather a genuine property of the matrix element (4.89). Indeed, the three-body integral in equation (4.40) depends only on l , m , and $\hat{\mathbf{l}} \cdot \hat{\mathbf{m}}$ due to the isotropy of the liquid, and so does the overlap of the two-phonon PO states (4.88). This property alone fixes the angular dependence in equation (4.89), as is obvious from the derivation therein. An additional feature of the overlap (4.88) is that it vanishes when $l \rightarrow 0$ or $m \rightarrow 0$ since PO states with an unequal number of phonons are mutually orthogonal by construction, which explains the linearity of the function $f(l)$ at the origin.

4.4 OCBPT of $S(\mathbf{k}, \omega)$

The DSF $S(\mathbf{k}, \omega)$ (equation (2.9)) can be written as

$$S(\mathbf{k}, \omega) = -\frac{1}{\pi} \text{Im} D(\mathbf{k}, \omega) \quad (4.93)$$

where

$$D(\mathbf{k}, \omega) = \frac{1}{N} \langle 0 | \rho_{\mathbf{k}} [\omega - H + E_0 + i\eta]^{-1} \rho_{\mathbf{k}}^\dagger | 0 \rangle \quad (4.94)$$

is the density-density response function (DDRF), and η is a positive infinitesimal. The Hamiltonian of the system is divided into diagonal and off-diagonal parts with respect to OCB:

$$H = H_0 + H', \quad (4.95)$$

$$\langle i | H_0 | j \rangle = \delta_{ij} \langle i | H | i \rangle, \quad (4.96)$$

$$\langle i | H' | j \rangle = (1 - \delta_{ij}) \langle i | H | j \rangle, \quad (4.97)$$

and since OCB states $|i\rangle, |j\rangle$ are close to the exact eigenstates of the Hamiltonian, we expect H' to be small and treat it as a perturbation. The resolvent in DDRF can be expanded as:

$$\begin{aligned} D(\mathbf{k}, \omega) &= \frac{1}{N} \sum_{n=0}^{\infty} \langle 0 | \rho_{\mathbf{k}} [\omega - H_0 + E_0 + i\eta]^{-1} (H' [\omega - H_0 + E_0 + i\eta]^{-1})^n \rho_{\mathbf{k}}^\dagger | 0 \rangle \\ &= \sum_i X_0^*(i) G_0(i) X_0(i) + \sum_{i,j} X_0^*(i) G_0(i) H'_{ij} G_0(j) X_0(j) + \dots, \end{aligned} \quad (4.98)$$

where

$$X_0(i) = \frac{1}{\sqrt{N}} \langle i | \rho_{\mathbf{k}}^\dagger | 0 \rangle, \quad (4.99)$$

and

$$G_0(i) = \langle i | [\omega - H_0 + E_0 + i\eta]^{-1} | i \rangle \quad (4.100)$$

are energy denominators.

In general, matrix elements $X_0(i)$ can be formidable. However, if we use the Feynman phonon OCB states as the intermediate states $|i\rangle$, the state

$$| \mathbf{k} \rangle \equiv \frac{1}{\sqrt{N S(\mathbf{k})}} \rho_{\mathbf{k}}^\dagger | 0 \rangle, \quad (4.101)$$

is a member of OCB, and the matrix elements $X_0(i)$ become simply

$$X_0(i) = \sqrt{S(\mathbf{k})} \delta_{i,\mathbf{k}}. \quad (4.102)$$

In this case the expansion (4.98) can be further simplified to obtain

$$\begin{aligned} D(\mathbf{k}, \omega) &= S(\mathbf{k}) [G_0(\mathbf{k}) + G_0(\mathbf{k}) [\sum_i H'_{\mathbf{k}i} G_0(i) H'_{i\mathbf{k}}] G_0(\mathbf{k}) + \dots] \\ &= S(\mathbf{k}) [G_0(\mathbf{k}) + G_0(\mathbf{k}) \Sigma(\mathbf{k}, \omega) G_0(\mathbf{k}) + G_0(\mathbf{k}) \Sigma(\mathbf{k}, \omega) G_0(\mathbf{k}) \Sigma(\mathbf{k}, \omega) G_0(\mathbf{k}) + \dots] \\ &= S(\mathbf{k}) G_0(\mathbf{k}) + G_0(\mathbf{k}) \Sigma(\mathbf{k}, \omega) D(\mathbf{k}, \omega), \end{aligned} \quad (4.103)$$

where

$$\Sigma(\mathbf{k}, \omega) = \sum_i H'_{\mathbf{k}i} G_0(i) H'_{i\mathbf{k}} + \sum_{i,j} H'_{\mathbf{k}i} G_0(i) H'_{ij} G_0(j) H'_{j\mathbf{k}} + \dots \quad (4.104)$$

is the proper self energy (PSE). Finally, from equation (4.103) it follows that

$$D(\mathbf{k}, \omega) = \frac{S(\mathbf{k})}{G_0^{-1}(\mathbf{k}) - \Sigma(\mathbf{k}, \omega) + i\eta}, \quad (4.105)$$

which, together with equation (4.93), gives

$$S(\mathbf{k}, \omega) = -\frac{S(\mathbf{k})}{\pi} \frac{\text{Im} \Sigma(\mathbf{k}, \omega) - \eta}{(G_0^{-1}(\mathbf{k}) - \text{Re} \Sigma(\mathbf{k}, \omega))^2 + (\text{Im} \Sigma(\mathbf{k}, \omega) - \eta)^2}. \quad (4.106)$$

4.5 Scaling property of $S(\mathbf{k}, \omega)$

When k is large, $S(k) = 1$, and from equations (4.83) and (4.100) we obtain:

$$G_0(k) = [\omega - \frac{k^2}{2m} + i\eta]^{-1} = \frac{m}{k}(y + i\eta)^{-1}, \quad (4.107)$$

$$D(\mathbf{k}, \omega) = [\omega - \frac{k^2}{2m} - \Sigma(\mathbf{k}, \omega) + i\eta]^{-1}. \quad (4.108)$$

Moreover, it was proved in section 4.1 that only the states $|i\rangle$ that have one hard phonon with momentum of order k and one or more soft phonons with finite momenta contribute to $\Sigma(\mathbf{k}, \omega)$. These states are represented as:

$$|i\rangle = |\mathbf{k} - \mathbf{p}_1 - \dots - \mathbf{p}_{n-1}, \mathbf{p}_1, \dots, \mathbf{p}_{n-1}\rangle, \quad (4.109)$$

where $|\mathbf{p}_i|$ are finite, i.e. of order k^0 , and

$$\begin{aligned} G_0(i) &= [\omega - \frac{1}{2m}(\mathbf{k} - \mathbf{p}_1 - \dots - \mathbf{p}_{n-1})^2 + O(k^0) + i\eta]^{-1} \\ &= \frac{m}{k}g_0(i) + O(k^{-2}), \end{aligned} \quad (4.110)$$

$$g_0(i) = [y - \hat{k} \cdot (\mathbf{p}_1 + \dots + \mathbf{p}_{n-1}) + i\eta]^{-1}. \quad (4.111)$$

It was also proved in section 4.3 (c.f. equation (4.86)) that the off-diagonal matrix elements H'_{ij} between states having one hard phonon each are proportional to k/m , i.e.

$$H'_{ij} = \frac{k}{m}[h'_{ij} + O(k^{-1})] \quad (4.112)$$

where h'_{ij} is independent of k . From equations (4.104), (4.111) and (4.112) it follows that

$$\frac{m}{k}\Sigma(\mathbf{k}, \omega) = \Sigma_S(y) + O(k^{-1}), \quad (4.113)$$

$$\Sigma_S(y) = \sum_i h'_{\mathbf{k}i} g_0(i) h'_{i\mathbf{k}} + \sum_{i \neq j} h'_{\mathbf{k}i} g_0(i) h'_{ij} g_0(j) h'_{j\mathbf{k}} + \dots \quad (4.114)$$

Consequently

$$\frac{k}{m}D(\mathbf{k}, \omega) = D_S(y) + O(k^{-1}), \quad (4.115)$$

$$D_S(y) = [y - \Sigma_S(y) + i\eta]^{-1}, \quad (4.116)$$

so that

$$\frac{k}{m}S(\mathbf{k}, \omega) = J(y) + O(k^{-1}), \quad (4.117)$$

$$J(y) = -\frac{1}{\pi} \frac{\text{Im}\Sigma_S(y) - \eta}{(y - \text{Re}\Sigma_S(y))^2 + (\text{Im}\Sigma_S(y) - \eta)^2}, \quad (4.118)$$

i.e. $\frac{k}{m}S(\mathbf{k}, \omega)$ is function of y alone in the limit $k \rightarrow \infty$, and y -scaling is found to be an exact result.

We also obtain the useful relation

$$1 - yD_S(y) = \frac{-\Sigma_S(y)}{y - \Sigma_S(y) + i\eta} \quad (4.119)$$

from equation (4.116).

Chapter 5

Calculation of the scaling function of the Bose liquid at $T=0$

In this chapter we present the calculation of the zero temperature scaling function $J(y)$ of the Bose liquids in general, and of ${}^4\text{He}$ in particular. The material is organized as follows. In section 5.1 we derive an analytic expression for $J(y)$ using the Ward identity that is proved in section 5.2. The properties of this $J(y)$ are discussed in section 5.3, and numerical results on ${}^4\text{He}$ are given in section 5.4. Finally, in section 5.5 we give the brief summary of the theory of deep inelastic response of Bose liquids at zero temperature, i.e. of chapters 4 and 5.

5.1 Calculation of the scaling function

It was shown in chapter 4 that spectator phonons do not contribute to the matrix elements of OCB, i.e.

$$\langle \mathbf{p}_1, \dots, \mathbf{p}_n, \mathbf{q}_1, \dots, \mathbf{q}_m | H | \mathbf{p}'_1, \dots, \mathbf{p}'_{n'}, \mathbf{q}_1, \dots, \mathbf{q}_m \rangle = \langle \mathbf{p}_1, \dots, \mathbf{p}_n | H | \mathbf{p}'_1, \dots, \mathbf{p}'_{n'} \rangle \quad (5.1)$$

when the number of phonons $(n + m)$ and $(n' + m)$ is finite³⁵. Because of this property

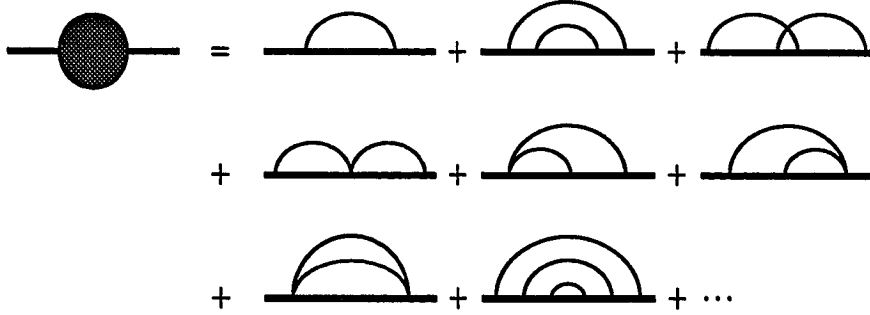


Figure 5.1: The expansion of the self-energy $\Sigma_S(y)$ (equation (4.114)). The thick line represents the hard phonon while the thin lines represent the soft phonons.

it is possible to consider the diagrammatic expansion of $\Sigma_S(y)$ (equation (4.114)) shown in fig. 5.1, where the thick line represents the hard phonon and thin lines represent soft phonons. An exact calculation of $\Sigma_S(y)$ is difficult because of the large number of different types of vertices, representing the matrix elements h'_{ij} , in this expansion. However, all the diagrams based on the vertex at which the hard phonon emits or absorbs a soft phonon, as illustrated in fig. 5.2, can be summed by the standard field theoretical methods, as will be shown below.

In section 4.3 it was shown that this basic one- to two-phonon vertex is given by

$$\frac{m}{k} \langle \mathbf{k} | H | \mathbf{k} - \mathbf{l}, \mathbf{l} \rangle \equiv \Gamma_0(l) + O(k^{-1}) = -\frac{1}{\sqrt{N}} \frac{\hat{\mathbf{k}} \cdot \hat{\mathbf{l}}}{2} \sqrt{f(l)} + O(k^{-1}). \quad (5.2)$$

The function $f(l)$ is determined entirely by the static structure function $S(q)$, and is also calculated in that section. We recall that $S(q)$ is the only input in our calculation of the scaling function, as opposed to other works where the ground state momentum distribution $n(q)$ is used.

Since we closely follow the calculation of electron self-energy in QED, it is natural to

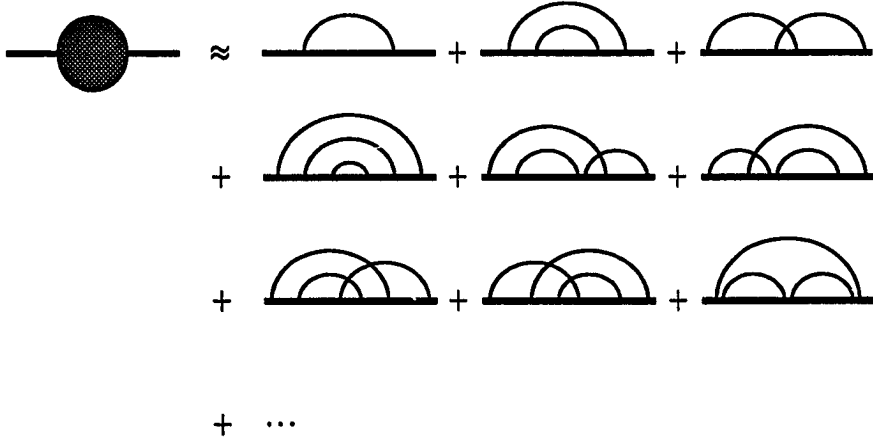


Figure 5.2: Diagrammatic representation of terms that include only the one- to two-phonon vertex: the proper self-energy $\Sigma_S(y)$.

use the same terminology whenever possible. Thus, the dressed vertex $\Gamma(\mathbf{l}, y)$ is defined as

$$\Gamma(\mathbf{l}, y) = \Gamma_0(l)[1 + \Lambda(\mathbf{l}, y)], \quad (5.3)$$

and it represents the sum of diagrams in fig. 5.3; $\Lambda(\mathbf{l}, y)$ is the vertex correction. The dressed hard phonon propagator $g(y)$ is shown in fig. 5.4, and the Dyson equation^{83,84} for the proper self energy is shown in fig. 5.5. Analytically it is written as

$$\begin{aligned} \Sigma_S(y) &= \sum_{\mathbf{l}} \Gamma(\mathbf{l}, y) g(y + \hat{\mathbf{k}} \cdot \mathbf{l}) \Gamma_0(l) \\ &= \sum_{\mathbf{l}} \left(-\frac{1}{\sqrt{N}} \frac{\hat{\mathbf{k}} \cdot \hat{\mathbf{l}}}{2} \sqrt{f(l)} \right) \frac{1 + \Lambda(\mathbf{l}, y)}{y + \hat{\mathbf{k}} \cdot \mathbf{l} - \Sigma_S(y + \hat{\mathbf{k}} \cdot \mathbf{l}) + i\eta} \left(-\frac{1}{\sqrt{N}} \frac{\hat{\mathbf{k}} \cdot \hat{\mathbf{l}}}{2} \sqrt{f(l)} \right) \\ &= \int \frac{d^3l}{(2\pi)^3 \rho} \frac{(\hat{\mathbf{k}} \cdot \hat{\mathbf{l}})^2 f(l) [1 + \Lambda(\mathbf{l}, y)]}{4[y + \hat{\mathbf{k}} \cdot \mathbf{l} - \Sigma_S(y + \hat{\mathbf{k}} \cdot \mathbf{l}) + i\eta]}. \end{aligned} \quad (5.4)$$

If we put $\Lambda(\mathbf{l}, y) \equiv 0$ in equation (5.4), we obtain the integral equation for the sum of all diagrams without intersecting soft phonon lines as is illustrated in fig. 5.6:

$$\Sigma'_S(y) = \int \frac{d^3l}{(2\pi)^3 \rho} \frac{(\hat{\mathbf{k}} \cdot \hat{\mathbf{l}})^2 f(l)}{4[y + \hat{\mathbf{k}} \cdot \mathbf{l} - \Sigma'_S(y + \hat{\mathbf{k}} \cdot \mathbf{l}) + i\eta]}. \quad (5.5)$$

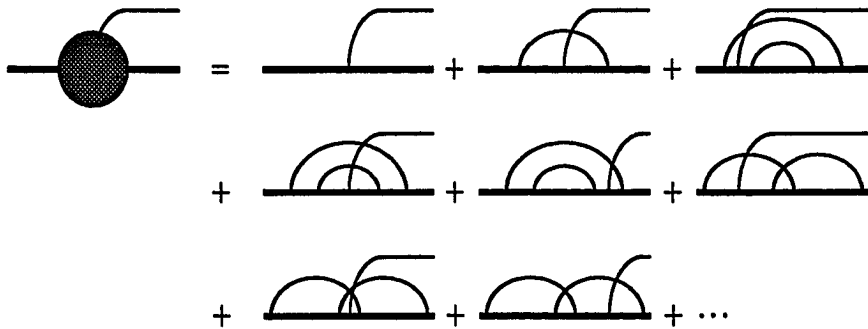


Figure 5.3: Diagrammatic representation of terms that include only the one- to two-phonon vertex: the dressed vertex $\Gamma(1, y)$.

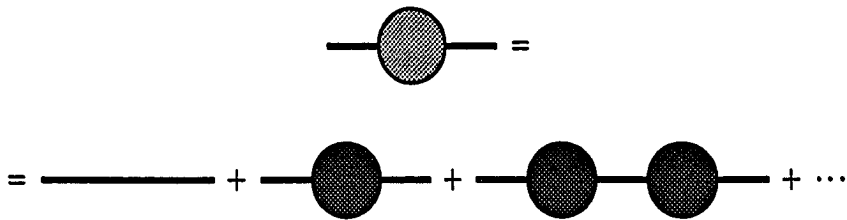


Figure 5.4: Diagrammatic representation of terms that include only the one- to two-phonon vertex: the dressed hard phonon propagator $g(y)$.

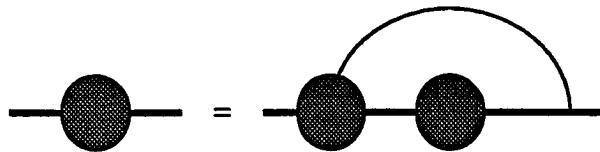


Figure 5.5: Diagrammatic representation of terms that include only the one- to two-phonon vertex: the Dyson equation.

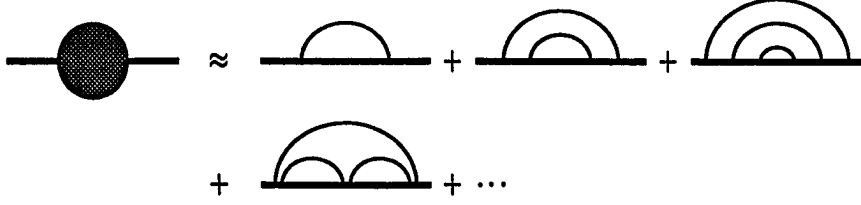


Figure 5.6: Diagrammatic representation of terms that include only the one- to two-phonon vertex: nonintersecting diagrams of $\Sigma'_S(y)$.

This integral equation for $\Sigma'_S(y)$ can be easily solved numerically by iteration.

To calculate $\Sigma_S(y)$ including the vertex correction we need another equation relating $\Sigma_S(y)$ to $\Lambda(\mathbf{l}, y)$. As mentioned in chapter 4, the number of hard phonons is conserved in this theory, and equals to one. This conservation is analogous to the charge conservation in QED, and it is not surprising that the identity

$$\hat{\mathbf{k}} \cdot \mathbf{l} \Lambda(\mathbf{l}, y) = \Sigma_S(y) - \Sigma_S(y + \hat{\mathbf{k}} \cdot \mathbf{l}), \quad (5.6)$$

analogous to the Ward identity of QED,^{59,60} holds. The proof of this identity is given in section 5.2. Equation (5.6) is expressed as

$$\hat{\mathbf{k}} \cdot \mathbf{l} [1 + \Lambda(\mathbf{l}, y)] = [y + \hat{\mathbf{k}} \cdot \mathbf{l} - \Sigma_S(y + \hat{\mathbf{k}} \cdot \mathbf{l})] - [y - \Sigma_S(y)] \quad (5.7)$$

and substituted into equation (5.4) to obtain

$$\begin{aligned} \Sigma_S(y) &= \int \frac{d^3 l}{(2\pi)^3 \rho} \frac{\hat{\mathbf{k}} \cdot \hat{\mathbf{l}} f(l) \{ [y + \hat{\mathbf{k}} \cdot \mathbf{l} - \Sigma_S(y + \hat{\mathbf{k}} \cdot \mathbf{l})] - [y - \Sigma_S(y)] \}}{4l [y + \hat{\mathbf{k}} \cdot \mathbf{l} - \Sigma_S(y + \hat{\mathbf{k}} \cdot \mathbf{l}) + i\eta]} \\ &= \int \frac{d^3 l}{(2\pi)^3 \rho} \hat{\mathbf{k}} \cdot \hat{\mathbf{l}} \frac{f(l)}{4l} - [y - \Sigma_S(y)] \int \frac{d^3 l}{(2\pi)^3 \rho} \frac{\hat{\mathbf{k}} \cdot \hat{\mathbf{l}} f(l)}{4l [y + \hat{\mathbf{k}} \cdot \mathbf{l} - \Sigma_S(y + \hat{\mathbf{k}} \cdot \mathbf{l}) + i\eta]} \\ &= -[y - \Sigma_S(y)] \int \frac{d^3 l}{(2\pi)^3 \rho} \frac{\hat{\mathbf{k}} \cdot \hat{\mathbf{l}} f(l)}{4l [y + \hat{\mathbf{k}} \cdot \mathbf{l} - \Sigma_S(y + \hat{\mathbf{k}} \cdot \mathbf{l}) + i\eta]}. \end{aligned} \quad (5.8)$$

Substituting this $\Sigma_S(y)$ into the right-hand side of equation (4.119) we obtain

$$1 - y D_S(y) = \int \frac{d^3 l}{(2\pi)^3 \rho} \frac{\hat{\mathbf{k}} \cdot \hat{\mathbf{l}} f(l)}{4l [y + \hat{\mathbf{k}} \cdot \mathbf{l} - \Sigma_S(y + \hat{\mathbf{k}} \cdot \mathbf{l}) + i\eta]}$$

$$\begin{aligned}
&= \int \frac{d^3l}{(2\pi)^3\rho} \hat{\mathbf{k}} \cdot \hat{\mathbf{l}} \frac{f(l)}{4l} D_S(y + \hat{\mathbf{k}} \cdot \mathbf{l}) \\
&= \frac{1}{16\pi^2\rho} \int_{-\infty}^{\infty} dl_z D_S(y + l_z) l_z F(l_z), \tag{5.9}
\end{aligned}$$

where

$$F(x) \equiv \int_0^{\infty} \rho d\rho \frac{f(\sqrt{\rho^2 + x^2})}{\rho^2 + x^2} = \int_{|x|}^{\infty} dt \frac{f(t)}{t}. \tag{5.10}$$

At small t the function $f(t)$ is linear in t so that $F(x)$ is finite and continuous at $x = 0$. Moreover it is real and decreasing since $f(t)$ is real and positive. Taking the real and imaginary parts of equation (5.9) we obtain

$$y \operatorname{Re} D_S(y) - 1 = \frac{1}{16\pi^2\rho} \int_{-\infty}^{\infty} dz (y - z) F(y - z) \operatorname{Re} D_S(z), \tag{5.11}$$

$$y \operatorname{Im} D_S(y) = \frac{1}{16\pi^2\rho} \int_{-\infty}^{\infty} dz (y - z) F(y - z) \operatorname{Im} D_S(z). \tag{5.12}$$

Equations (5.11) and (5.12) are of the convolution type, and can be solved by Fourier transform. Function $F(x)$ is absolutely integrable since the integral

$$\begin{aligned}
\int_{-\infty}^{\infty} dx |F(x)| &= \int_{-\infty}^{\infty} dx \int_0^{\infty} \rho d\rho \frac{f(\sqrt{\rho^2 + x^2})}{\rho^2 + x^2} = \frac{1}{2\pi} \int d^3r \frac{f(r)}{r^2} \\
&= 2 \int_0^{\infty} dx f(x) \tag{5.13}
\end{aligned}$$

is finite, which implies that its Fourier transform \tilde{F} is defined. We use the identity

$$i\tilde{f}'(s) = \int_{-\infty}^{\infty} dy e^{-iy^s} y f(y), \tag{5.14}$$

where prime denotes the differentiation of the function with respect to its argument, and introduce the notation

$$X(s) = \int_{-\infty}^{\infty} dy e^{-iy^s} \operatorname{Re} D_S(y) \tag{5.15}$$

$$Y(s) = \int_{-\infty}^{\infty} dy e^{-iy^s} \operatorname{Im} D_S(y), \tag{5.16}$$

to reduce the integral equations (5.11) and (5.12) into differential ones

$$X'(s) = a\tilde{F}'(s)X(s) - 2\pi i\delta(s) \tag{5.17}$$

$$Y'(s) = a\tilde{F}'(s)Y(s), \tag{5.18}$$

where $a = 1/16\pi^2\rho$. Equation (5.18) is linear homogeneous differential equation of the first order whose solution is

$$Y(s) = C_2 e^{a\tilde{F}(s)}, \quad (5.19)$$

where C_2 is an arbitrary constant. The equation (5.17) is not homogeneous, and we look for its solution in the form

$$X(s) = C(s) e^{a\tilde{F}(s)}, \quad (5.20)$$

where $C(s)$ is the function to be determined. Substitution of the ansatz (5.20) into equation (5.17) gives

$$\begin{aligned} C'(s) &= -2\pi i e^{-a\tilde{F}(s)}\delta(s) = -2\pi i e^{-a\tilde{F}(0)}\delta(s) \\ \therefore C(s) &= -2\pi i e^{-a\tilde{F}(0)}\theta(s) + C_1, \end{aligned} \quad (5.21)$$

and we obtain

$$X(s) = C_1 e^{a\tilde{F}(s)} - 2\pi i e^{a(\tilde{F}(s)-\tilde{F}(0))}\theta(s), \quad (5.22)$$

where C_1 is another arbitrary constant. Expressions (5.22) and (5.19) are general solutions of the equations (5.17) and (5.18) respectively.

In order to fix the values of arbitrary constants C_1 and C_2 we need some additional constraint on $X(s)$ and $Y(s)$. From equation (4.116) it is obvious that the function $D_S(z)$ viewed as the function of the complex variable z has no singularities in the upper half-plane ($\text{Re } z > 0$). Real and imaginary parts of such functions are connected by the dispersion relations^{85,86}

$$\text{Re}D_S(y) = \frac{1}{\pi}\wp \int_{-\infty}^{\infty} dy' \frac{\text{Im}D_S(y')}{y' - y} \quad (5.23)$$

$$\text{Im}D_S(y) = -\frac{1}{\pi}\wp \int_{-\infty}^{\infty} dy' \frac{\text{Re}D_S(y')}{y' - y}, \quad (5.24)$$

where \wp denotes the principal value of an integral. The Fourier transforms of $\text{Re}D_S(y)$ and $\text{Im}D_S(y)$, $X(s)$ and $Y(s)$, are also connected. Using the formula⁸⁷

$$\wp \int_{-\infty}^{\infty} dy \frac{e^{-iy s}}{y} = -i\pi \text{sgn}(s), \quad (5.25)$$

we obtain from dispersion relations (5.23) and (5.24) single relation

$$X(s) = i \operatorname{sgn}(s) Y(s), \quad (5.26)$$

which, together with equations (5.19) and (5.22), yields

$$C_1 - 2\pi i e^{-a\tilde{F}(0)} \theta(s) = i C_2 \operatorname{sgn}(s). \quad (5.27)$$

The last equation is equivalent to the system

$$C_1 = -iC_2, \quad C_1 - 2\pi i e^{-a\tilde{F}(0)} = iC_2, \quad (5.28)$$

which is obtained from it by substituting the values $s < 0$ and $s > 0$ respectively. The solutions of this system are

$$C_1 = -iC_2 = i\pi e^{-a\tilde{F}(0)}, \quad (5.29)$$

and we obtain

$$X(s) = -i\pi e^{a(\tilde{F}(s)-\tilde{F}(0))} \operatorname{sgn}(s), \quad (5.30)$$

$$Y(s) = -\pi e^{a(\tilde{F}(s)-\tilde{F}(0))}. \quad (5.31)$$

In the limit $s \rightarrow \pm\infty$ $\tilde{F}(s) \rightarrow 0$, and hence $X(s) \rightarrow \mp i\pi e^{-a\tilde{F}(0)}$, $Y(s) \rightarrow -\pi e^{-a\tilde{F}(0)}$. Thus, we have to be careful when inverting Fourier transforms. Using the formula (5.25) we obtain

$$\begin{aligned} \operatorname{Re}D_S(y) &= \int_{-\infty}^{\infty} \frac{ds}{2\pi} e^{isy} X(s) = -i\pi e^{-a\tilde{F}(0)} \int_{-\infty}^{\infty} \frac{ds}{2\pi} e^{isy} \operatorname{sgn}(s) (e^{a\tilde{F}(s)} - 1 + 1) \\ &= e^{-a\tilde{F}(0)} \left[\frac{1}{y} + \int_0^{\infty} ds \sin(sy) (e^{a\tilde{F}(s)} - 1) \right]. \end{aligned} \quad (5.32)$$

Similarly we find

$$\begin{aligned} \operatorname{Im}D_S(y) &= \int_{-\infty}^{\infty} \frac{ds}{2\pi} e^{isy} Y(s) = -\pi e^{-a\tilde{F}(0)} \int_{-\infty}^{\infty} \frac{ds}{2\pi} e^{isy} (e^{a\tilde{F}(s)} - 1 + 1) \\ &= -e^{-a\tilde{F}(0)} \left[\pi\delta(y) + \int_0^{\infty} ds \cos(sy) (e^{a\tilde{F}(s)} - 1) \right]. \end{aligned} \quad (5.33)$$

We note in passing that $\text{Re}D_S(y)$ is an odd function and $\text{Im}D_S(y)$ an even one. The expressions (5.32) and (5.33) can be written together as

$$\begin{aligned} D_S(y) &= e^{-a\bar{F}(0)} \left[\frac{1}{y} - i\pi\delta(y) + \int_0^\infty ds (\sin(sy) - i\cos(sy)) (e^{a\bar{F}(s)} - 1) \right] \\ &= e^{-a\bar{F}(0)} \left[\frac{1}{y + i\eta} - i \int_0^\infty ds e^{isy} (e^{a\bar{F}(s)} - 1) \right]. \end{aligned} \quad (5.34)$$

It is also possible to write down an explicit formula for the proper self energy $\Sigma_S(y)$ in terms of the function $\bar{F}(s)$, but we will not do it here. Instead, we return to our main goal, the calculation of the scaling function $J(y)$. Since $\text{Im}D_S(y) = -\pi J(y)$ it follows from equation (5.33) that

$$J(y) = C \left\{ \delta(y) + \int_{-\infty}^\infty \frac{ds}{2\pi} e^{isy} \left[\exp \left(a \int_{-\infty}^\infty dx e^{-ixs} F(x) \right) - 1 \right] \right\}, \quad (5.35)$$

where we have introduced the constant

$$C \equiv e^{-a\bar{F}(0)} = \exp \left(-2a \int_0^\infty dx F(x) \right) = \exp \left(-2a \int_0^\infty dl f(l) \right). \quad (5.36)$$

Formulae (5.35) and (5.36), together with (5.10) and (4.90), express the scaling function of the Bose liquid at zero temperature in terms of the static structure function $S(q)$. They are the main result of this chapter.

5.2 Proof of the Ward identity

The Ward identity (equation (5.6)) establishes the connection between the proper self-energy $\Sigma_S(y)$ and the vertex correction $\Lambda(l, y)$. The diagrams that contribute to the $\Sigma_S(y)$ are shown in fig. 5.2. If an external leg l is attached to any hard phonon propagator in any of the $\Sigma_S(y)$ diagrams, a diagram contributing to the $\Lambda(l, y)$ is obtained. In fact, all the diagrams that contribute to the $\Lambda(l, y)$ (shown in fig. 5.3) can be generated in this way from the $\Sigma_S(y)$ diagrams. Thus, there is one to one correspondence between the diagrams that contribute to $\Sigma_S(y)$ and the groups of diagrams that contribute to the $\Lambda(l, y)$ that

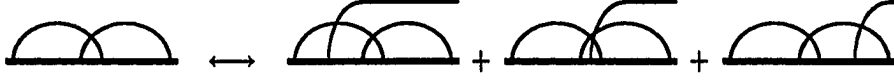


Figure 5.7: An example of the correspondence between $\Sigma_S(y)$ diagrams and groups of $\Lambda(l, y)$ diagrams.

have the same arrangement of the internal lines as the $\Sigma_S(y)$ diagram plus an additional external leg l attached to any hard phonon propagator. An example of this correspondence is shown in fig. 5.7.

The $\Sigma_S(y)$ diagrams can be enumerated by an index ν :

$$\Sigma_S(y) = \sum_{\nu} \Sigma_{S,\nu}(y). \quad (5.37)$$

The same enumeration scheme can be extended to the corresponding groups of the $\Lambda(l, y)$ diagrams:

$$\Lambda(l, y) = \sum_{\nu} \sum_{i_{\nu}} \Lambda_{\nu, i_{\nu}}(l, y), \quad (5.38)$$

where the indices i_{ν} enumerate the diagrams $\Lambda_{\nu, i_{\nu}}$ in the group ν , and all of these can be generated from the diagram $\Sigma_{S,\nu}$ by the procedure discussed above. We will prove the Ward identity (5.6) by showing that it holds for each group ν separately, i.e.

$$\hat{\mathbf{k}} \cdot \mathbf{l} \sum_{i_{\nu}} \Lambda_{\nu, i_{\nu}}(l, y) = \Sigma_{S,\nu}(y) - \Sigma_{S,\nu}(y + \hat{\mathbf{k}} \cdot \mathbf{l}). \quad (5.39)$$

We begin the proof of equation (5.39) by quoting the identity:

$$\hat{\mathbf{k}} \cdot \mathbf{l} [y + \hat{\mathbf{k}} \cdot \mathbf{m} + i\eta]^{-1} [y + \hat{\mathbf{k}} \cdot (\mathbf{m} + \mathbf{l}) + i\eta]^{-1} = [y + \hat{\mathbf{k}} \cdot \mathbf{m} + i\eta]^{-1} - [y + \hat{\mathbf{k}} \cdot (\mathbf{m} + \mathbf{l}) + i\eta]^{-1}. \quad (5.40)$$

From equations (4.111), (5.2) and (5.40) it follows that

$$\begin{aligned} \hat{\mathbf{k}} \cdot \mathbf{l} g_0(y + \hat{\mathbf{k}} \cdot \mathbf{m}) \Gamma_0(l) g_0(y + \hat{\mathbf{k}} \cdot (\mathbf{m} + \mathbf{l})) = \\ \Gamma_0(l) [g_0(y + \hat{\mathbf{k}} \cdot \mathbf{m}) - g_0(y + \hat{\mathbf{k}} \cdot (\mathbf{m} + \mathbf{l}))]. \end{aligned} \quad (5.41)$$

$$\hat{\mathbf{k}} \cdot \mathbf{l} \times \left(\begin{array}{c} \text{shaded oval} \\ \vdots \\ \text{---} \\ \begin{array}{ccc} \mathbf{k} & & \mathbf{k} - \mathbf{l} \\ | & & | \\ \mathbf{k} - \mathbf{m} & & \mathbf{k} - \mathbf{m} - \mathbf{l} \end{array} \end{array} \right) = \Gamma_0(\mathbf{l}) \times \left(\begin{array}{c} \text{shaded oval} \\ \vdots \\ \text{---} \\ \begin{array}{ccc} \mathbf{k} & & \mathbf{k} - \mathbf{l} \\ | & & | \\ \mathbf{k} - \mathbf{m} & \downarrow \mathbf{l} & \mathbf{k} - \mathbf{m} - \mathbf{l} \end{array} \end{array} \right) - \left(\begin{array}{c} \text{shaded oval} \\ \vdots \\ \text{---} \\ \begin{array}{ccc} \mathbf{k} & & \mathbf{k} - \mathbf{l} \\ | & & | \\ \mathbf{k} - \mathbf{m} & \mathbf{l} \downarrow & \mathbf{k} - \mathbf{m} - \mathbf{l} \end{array} \end{array} \right)$$

Figure 5.8: Graphical representation of equation (5.41). An arrow pointing from a vertex denotes an extraction of the momentum from the hard phonon propagator; shaded oval stands for an arbitrarily complex connection scheme of the internal lines.

Equation (5.41) has a simple graphical representation as is shown in fig. 5.8. An arrow pointing from a vertex denotes an extraction of the momentum from the hard phonon propagator, which is an artifact of the removed external leg \mathbf{l} . A shaded oval stands for an arbitrarily complex connection scheme of the internal lines.

Next, we consider the arbitrary group ν of the diagrams $\Lambda_{\nu,i}$ contributing to the vertex correction $\Lambda(\mathbf{l}, y)$. With the aid of equation (5.41) it is easy to demonstrate that equation (5.39) holds for an arbitrary ν as is done in fig. 5.9.

This finishes the proof of the Ward identity, since it was already shown that the validity of equation (5.39) for all ν 's implies equation (5.6).

$$\begin{aligned}
& \hat{k} \cdot l \Gamma_0(l) \sum_{i_\nu} \Lambda_{\nu, i_\nu}(l, y) = \\
& = \hat{k} \cdot l \times \left(\begin{array}{c} \text{Diagram 1} \\ \text{Diagram 2} \end{array} \right) \\
& = \Gamma_0(l) \times \left(\begin{array}{c} \text{Diagram 3} - \text{Diagram 4} + \dots \\ \text{Diagram 5} - \text{Diagram 6} \end{array} \right) \\
& = \Gamma_0(l) \times \left(\text{Diagram 7} - \text{Diagram 8} \right) \\
& = \Gamma_0(l) \left(\Sigma_{S, \nu}(y) - \Sigma_{S, \nu}(y + \hat{k} \cdot l) \right)
\end{aligned}$$

Figure 5.9: The proof of equation (5.39).

5.3 Discussion

We begin the analysis of the scaling function $J(y)$ (equation (5.35)) by evaluating it in the limit $y \rightarrow 0$. In this limit the function $F(y)$ (equation (5.10)) can be expanded as follows:

$$F(y \rightarrow 0) = F(0) - |y| \lim_{l \rightarrow 0} \frac{f(l)}{l} + O(y^2). \quad (5.42)$$

In section 4.3 it was shown that the slope of the $f(l)$ at the origin is the same as that of $f_0(l)$ (equation (4.92)) so that

$$\lim_{l \rightarrow 0} \frac{f(l)}{l} = \lim_{l \rightarrow 0} \frac{f_0(l)}{l} = \lim_{l \rightarrow 0} \frac{l}{S(l)} = 2mc, \quad (5.43)$$

where c is the sound velocity in the liquid, and we obtain

$$F(y \rightarrow 0) = F(0) - 2mc|y| + O(y^2). \quad (5.44)$$

The function $F(y)$ has a cusp at $y = 0$, and we will now show that as a consequence the scaling function $J(y)$ has a cusp at the origin in addition to the δ -function. In the theory of Fourier transforms⁸⁸ it is proved that for sufficiently smooth functions $\Phi(x)$:

$$\int_0^\infty dx \cos(sx)\Phi(x) = -\frac{\Phi'(0)}{s^2} + \frac{\Phi'''(0)}{s^4} - \frac{\Phi^{(V)}(0)}{s^6} + \dots \quad s \rightarrow \infty. \quad (5.45)$$

Thus, the Fourier transform of the function $F(x)$ is

$$\tilde{F}(s \rightarrow \infty) = 2 \int_0^\infty dx \cos(sx)F(x) = \frac{4mc}{s^2} + O\left(\frac{1}{s^4}\right), \quad (5.46)$$

so that the integrand of equation (5.35) becomes

$$e^{a\tilde{F}(s)} - 1 = \frac{4amc}{s^2} + O\left(\frac{1}{s^4}\right) = \frac{1}{4\pi^2\rho} \frac{mc}{s^2} + O\left(\frac{1}{s^4}\right) \quad s \rightarrow \infty. \quad (5.47)$$

From equations (5.35), (5.45), and (5.47) it follows that

$$J(y \rightarrow 0) = C\delta(y) + \frac{1}{4\pi^2\rho} [A - B|y|], \quad (5.48)$$

where the constant C is given by equation (5.36), and the constants A and B are given by

$$A = 4\pi\rho C \int_0^\infty ds \left[\exp\left(\frac{1}{8\pi^2\rho} \int_0^\infty dx \cos(sx)F(x)\right) - 1 \right], \quad (5.49)$$

$$B = C \frac{mc}{2}. \quad (5.50)$$

The scaling function in IA (equation (2.24)) exhibits the same small y behavior with the coefficients

$$C_{IA} = n_c, \quad A_{IA} = \int_0^\infty dq qn(q), \quad B_{IA} = \lim_{q \rightarrow 0} qn(q). \quad (5.51)$$

Using the well-known expression for the strength of the $1/q$ singularity of the momentum distribution $n(q)$ at zero temperature⁸⁹ we obtain

$$B_{IA} = n_c \frac{mc}{2}, \quad (5.52)$$

and find that

$$\frac{B}{C} = \frac{B_{IA}}{C_{IA}}, \quad (5.53)$$

i.e. the ratio B/C in our theory is identical to that in IA.

Next, we want to discuss the origin of the δ -function peak at $y = 0$. In general, the presence of the δ -function in DSF means that probe couples to a long-lived state with a given energy and momentum. The inverse lifetime of this excitation is given by the imaginary part of the self energy: $\tau^{-1} \sim \text{Im}\Sigma(\mathbf{k}, \omega)$, and it is expected to be proportional to k on the basis of the semi-classical value $\tau \sim \rho v \sigma$ where ρ is the density, $v \equiv k/m$ the velocity and σ the average two-body scattering cross section. The $\text{Im}\Sigma(\mathbf{k}, \omega)$ depends upon y , and it is of order k when $y \neq 0$. However, in the present calculation the $\text{Im}\Sigma(\mathbf{k}, \omega)$ at $y = 0$ does not have a term of order k , and hence the δ -function at $y = 0$ in the $J(y)$.

The origin of the y dependence of the lifetime can be easily seen in the contribution of the second order diagram, i.e. the first diagram of fig. 5.2. In second order, an off-shell Feynman phonon with momentum \mathbf{k} and energy $\omega = k^2/2m + ky/m$ can decay into two

Feynman phonons of momenta $\mathbf{k} - \mathbf{l}$ and \mathbf{l} , thus acquiring a lifetime given by⁴⁶

$$\frac{1}{\tau} = 2\pi \int \frac{d^3l}{(2\pi)^3 \rho} |\langle \mathbf{k} - \mathbf{l}, \mathbf{l} | H | \mathbf{k} \rangle|^2 \delta \left(\omega - \frac{(\mathbf{k} - \mathbf{l})^2}{2m} - \frac{l^2}{2m S(l)} \right). \quad (5.54)$$

Using equation (5.2) we obtain

$$\frac{1}{\tau} = \frac{1}{4(2\pi)^2 \rho} \frac{k}{m} \int d^3l (\hat{\mathbf{k}} \cdot \hat{\mathbf{l}})^2 f(l) \delta(y + \hat{\mathbf{k}} \cdot \mathbf{l} + O(k^{-1})). \quad (5.55)$$

When $y \neq 0$ we get $\tau \sim k^{-1}$ as expected from semi-classical arguments, but when $y = 0$ (on-shell Feynman phonon) the situation is completely different. In that case the energy-conserving δ -function forces the cosine $\hat{\mathbf{k}} \cdot \hat{\mathbf{l}}$ to be of the order k^{-1} which makes the integrand of the equation (5.55) small, and we find that on-shell Feynman phonon has a long lifetime $\tau \sim k$ in this order.

The $\Sigma_S(y)$ of equation (5.8) has the properties:

$$\text{Re}\Sigma_S(-y) = -\text{Re}\Sigma_S(y), \quad (5.56)$$

$$\text{Im}\Sigma_S(-y) = \text{Im}\Sigma_S(y), \quad (5.57)$$

$$\Sigma_S(0) = 0. \quad (5.58)$$

The solution of the simpler integral equation (5.5), obtained by summing diagrams of fig. 5.6, also satisfies the symmetry properties (5.56) and (5.57), however

$$\text{Im}\Sigma'_S(0) \neq 0. \quad (5.59)$$

Hence, the scaling function $J(y)$ obtained from the $\Sigma'_S(y)$ does not have a δ -function at $y = 0$. The approximation $\Sigma'_S(y)$ is bad since there is an exact cancellation between the summed and the omitted diagrams at $y = 0$. This cancellation occurs order by order in loopwise expansion of $\Sigma_S(y)$. We will demonstrate it on a two-loop level, i.e. we will show that the sum of the second and the third diagrams on fig. 5.2 vanish at $y = 0$. We denote

this sum $\Sigma_S^{(2)}(y)$ and obtain:

$$\begin{aligned}
\Sigma_S^{(2)}(0) &= \\
&= \int \frac{d^3 l}{(2\pi)^3 \rho} \frac{d^3 m}{(2\pi)^3 \rho} \frac{(\hat{\mathbf{k}} \cdot \hat{\mathbf{l}})^2 (\hat{\mathbf{k}} \cdot \hat{\mathbf{m}})^2 f(l) f(m)}{16(\hat{\mathbf{k}} \cdot \mathbf{l} + i\eta)[\hat{\mathbf{k}} \cdot (\mathbf{l} + \mathbf{m}) + i\eta]} \left(\frac{1}{\hat{\mathbf{k}} \cdot \mathbf{l} + i\eta} + \frac{1}{\hat{\mathbf{k}} \cdot \mathbf{m} + i\eta} \right) \\
&= \int \frac{d^3 l}{(2\pi)^3 \rho} \frac{d^3 m}{(2\pi)^3 \rho} \frac{\hat{\mathbf{k}} \cdot \mathbf{m} f(l) f(m)}{16 l^2 m^2 [\hat{\mathbf{k}} \cdot (\mathbf{l} + \mathbf{m}) + i\eta]} (\hat{\mathbf{k}} \cdot \mathbf{l} + \hat{\mathbf{k}} \cdot \mathbf{m}) \\
&= \int \frac{d^3 l}{(2\pi)^3 \rho} \frac{d^3 m}{(2\pi)^3 \rho} \frac{\hat{\mathbf{k}} \cdot \mathbf{m} f(l) f(m)}{16 l^2 m^2} = 0. \tag{5.60}
\end{aligned}$$

In the present calculation it was possible to sum all the diagrams containing one- to two-phonon vertex (fig. 5.2), and thus preserve this cancellation. If, for some reason, the $J(y)$ has to be approximated by a subset of diagrams, then it appears that the correct way to do it is to sum the diagrams order by order in the interaction rather than to sum infinite subsets of diagrams like $\Sigma'_S(y)$.

In our calculation of the scaling function $J(y)$, we have taken into account only the diagrams containing one- to two-phonon vertex. We can estimate the validity of this approximation by calculating the sum rules (2.80)-(2.82). The y^0 sum rule (2.80) is satisfied since from equation (5.35) it follows that

$$\int_{-\infty}^{\infty} dy J(y) = e^{-a\tilde{F}(0)} \left[1 + \int_{-\infty}^{\infty} \frac{ds}{2\pi} 2\pi \delta(s) (e^{a\tilde{F}(s)} - 1) \right] = 1. \tag{5.61}$$

The y sum rule (2.81) is satisfied since $J(y)$ is an even function of y , and for the y^2 (kinetic energy) sum rule we obtain

$$\begin{aligned}
\frac{2m}{3} E_k &= \int_{-\infty}^{\infty} dy y^2 J(y) = C \int_{-\infty}^{\infty} \frac{ds}{2\pi} (e^{a\tilde{F}(s)} - 1) \int_{-\infty}^{\infty} dy y^2 e^{iys} \\
&= -C \int_{-\infty}^{\infty} ds (e^{a\tilde{F}(s)} - 1) \delta''(s) = -C \left[\frac{d^2}{ds^2} e^{a\tilde{F}(s)} \right]_{s=0} \\
&= -C \left[a\tilde{F}''(0) + (a\tilde{F}'(0))^2 \right] e^{a\tilde{F}(0)} = -\frac{1}{16\pi^2 \rho} \int_{-\infty}^{\infty} dy (-iy)^2 F(y) \\
&= \frac{1}{24\pi^2 \rho} \int_0^{\infty} dl l^2 f(l), \tag{5.62}
\end{aligned}$$

where we have used the fact that $F(y)$ is a symmetric function which implies $\tilde{F}'(0) = 0$.

However, since equation (5.35) is not exact, the right-hand side of equation (5.62) may be

different from $2mE_k/3$, and the difference is a measure of the importance of the neglected one- to many- phonon diagrams.

Finally, we want to show that in the uniform limit ($|g(r) - 1| \ll 1$) the scaling function $J(y)$ (equation (4.35)) equals to the $J_{IA}(y)$. The uniform limit³⁴ is the situation where the radial distribution function is very near to unity:

$$g(r) = 1 - \alpha G(s), \quad s \equiv (\alpha\rho)^{1/3} r, \quad G(0) = 1, \quad (5.63)$$

where α is a small parameter. Physically, it corresponds to the dense ($\rho \rightarrow \infty$) systems with regular interaction, although it can be realized even in dilute ($\rho \rightarrow 0$) systems provided that the potential is sufficiently weak. The static structure function is given by³⁴

$$S(q) = 1 - F(p), \quad p \equiv (\alpha\rho)^{-1/3} q, \quad F(0) = 1. \quad (5.64)$$

Since $S(q)$ depends only on p , each integration over momenta gives an additional power of α . Thus, to the lowest order in α , the Löwdin corrections in equation (4.90) vanish and the function $f(l)$ becomes:

$$f_U(l) = \frac{l^2(S(l) - 1)^2}{S(l)} = 4l^2 n(l). \quad (5.65)$$

The above relation between $S(l)$ and $n(l)$ in the uniform limit is derived in ref. 34. Using it the scaling function in the uniform limit becomes

$$J_U(y) = C_U \delta(y) + \frac{1}{16\pi^2 \rho} \int_{|y|}^{\infty} dl \frac{f_U(l)}{l} = C_U \delta(y) + \frac{1}{4\pi^2 \rho} \int_{|y|}^{\infty} dq q n(q), \quad (5.66)$$

where

$$C_U = 1 - \frac{1}{8\pi^2 \rho} \int_0^{\infty} dl f_U(l) = 1 - \int \frac{d^3 q}{(2\pi)^3 \rho} n(q) \quad (5.67)$$

is the fraction of particles in the condensate, as in $J_{IA}(y)$.

5.4 Numerical results

In this section we will apply the theory developed in section 5.2 to the liquid ⁴He at zero temperature. The vertex function $f(l)$ given by equation (4.90) was calculated in

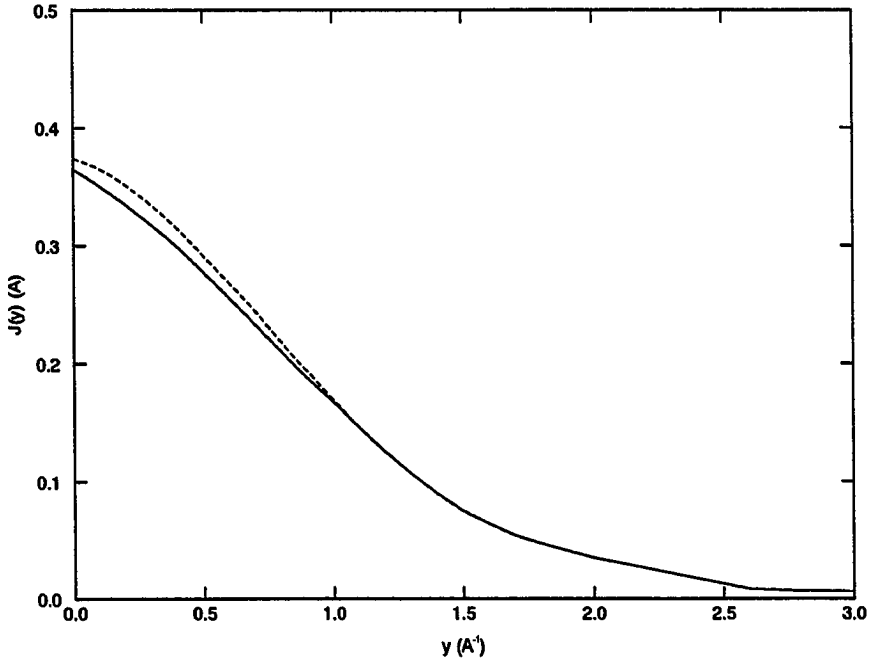


Figure 5.10: The scaling functions of liquid ${}^4\text{He}$ at equilibrium density and zero temperature. Solid line: $J(y)$ of equation (5.35) obtained using $f(l)$ of fig. 4.2; dotted line: $J_{IA}(y)$ generated from $n(q)$ of ref. 68. The δ -function peaks at $y = 0$ with the respective strengths of 0.15 and 0.092 are implied.

section 4.3 and shown in fig. 4.2. As was already mentioned, the only input needed in this computation is the static structure function $S(q)$. It can be seen that the Löwdin correction (i.e. the difference between $f(l)$ and $f_0(l)$) is small, but it is nevertheless significant since the scaling function $J(y)$ (equation (5.35)) and the strength of the δ -function peak (equation (5.36)) depend exponentially on $f(l)$.

Using this $f(l)$ in equations (5.35) and (5.36) we obtain $C = 0.15$, and the $J(y)$ that is shown in fig. 5.10. For comparison, $J_{IA}(y)$ generated from the variational $n(q)$ (ref. 68) that has the condensate fraction $n_c = 0.092$ is also shown. In order to test the sensitivity of the calculated $J(y)$ to changes in the input, we have computed it using the Monte Carlo $S(q)$ from ref. 61, and obtained essentially the same result. In particular, in this case $C =$

0.14 which is to be compared with $n_c = 0.11$ in the Monte Carlo calculation of ref. 61.

Finally, using the value $E_k = 14.8\text{K}$ from ref. 68 and $f(l)$ from fig. 4.2, we find that

$$\frac{3}{2mE_k} \frac{1}{24\pi^2\rho} \int_0^\infty dl l^2 f(l) = 0.97. \quad (5.68)$$

As was argued in section 5.3, the closeness of this value to 1 suggests that diagrams involving one- to many-phonon vertices have contributions much smaller than those of diagrams containing one- to two-phonon vertex only. However, the numerical value $1 - 0.97 = 0.03$ of the error has to be taken only as an estimate since the experimental $S(q)$ and theoretical E_k are used to obtain it.

5.5 Conclusions

In this and the previous chapter we have presented the calculation of the $S(\mathbf{k}, \omega)$ of a Bose liquid at $T = 0$ in the asymptotic limit $k, \omega \rightarrow \infty$, at $y \equiv \frac{m}{k}(\omega - k^2/2m) = \text{const}$, using OCB formalism. The orthogonalized Feynman phonon states are used to construct the OCB. It is found that y -scaling is exact in $k \rightarrow \infty$ limit, i.e. $\frac{m}{k}S(\mathbf{k}, \omega)$ is a function of y alone. It is also found that the dominant physical process is emission and absorption of soft phonons (i.e. phonons whose momenta are $\ll k$) by the hard phonon that is generated by the recoiling atom.

In order to obtain the scaling function $J(y)$ an approximation that amounts to allowing soft phonons to be emitted or absorbed only one at the time is introduced (c.f. figs. 5.2-5.6). The resulting theory is solved using field-theoretical methods without further approximations, and the closed expression for $J(y)$ is obtained (c.f. equations (5.35), (5.36), (5.10) and (4.90)). The only input needed is the static structure function $S(q)$ of the system.

It is found that $J(y)$ has a δ -function peak at $y = 0$, whose strength is connected with the slope $\left. \frac{dJ(y)}{dy} \right|_{y=0}$ in the same fashion as in the IA (equation (5.53)). In the case of the liquid ^4He this strength is equal to 0.15, which is to be compared with the corresponding

value of ~ 0.1 in the IA that is obtained from the theoretical calculations of the momentum distribution⁶⁸. The plot of the calculated $J(y)$ vs. $J_{IA}(y)$ for $y \neq 0$ is given in fig. 5.10.

Finally, the validity of the approximation made in neglecting processes that involve simultaneous emissions and/or absorptions of multiple phonons, is tested in two ways. First, the kinetic energy sum rule for $J(y)$ is evaluated (equation (5.62)). Its numerical closeness to the theoretical value suggests that the neglected processes are not important. Second, it is verified that in the exactly solvable uniform limit ($g(r) - 1 \ll 1$) $J(y)$ reduces to the IA as it should.

Chapter 6

Correlated basis theory of $S(\mathbf{k}, \omega)$ for Fermi systems

The OCB theory of the deep inelastic response of Bose liquids was presented in chapters 4 and 5. In this chapter we present its generalization to the case of Fermi liquids. The CB states suitable for Fermi systems are defined and discussed in section 6.1. In section 6.2 we examine the CB matrix elements of the unit operator and the Hamiltonian. Finally, in section 6.3 the OCB perturbation expansion of $S(\mathbf{k}, \omega)$ is considered, and its y -scaling property is proved.

6.1 The choice of the CB states

The n -particle n -hole CB states for Fermi systems are given by^{34,35}

$$|\mathbf{p}_1, \dots, \mathbf{p}_n; \mathbf{h}_1, \dots, \mathbf{h}_n\rangle \equiv \frac{G|\mathbf{p}_1, \dots, \mathbf{p}_n; \mathbf{h}_1, \dots, \mathbf{h}_n\rangle}{[\mathbf{p}_1, \dots, \mathbf{p}_n; \mathbf{h}_1, \dots, \mathbf{h}_n | G^\dagger G |\mathbf{p}_1, \dots, \mathbf{p}_n; \mathbf{h}_1, \dots, \mathbf{h}_n\rangle]^{1/2}}, \quad (6.1)$$

where the correlation operator G is defined as^{90,91}

$$G = F(\mathbf{R})F_{BF}, \quad (6.2)$$

where

$$F(\mathbf{R}) \equiv \prod_{\substack{i,j \\ i < j \leq N}} f_2(r_{ij}) \prod_{\substack{i,j,k \\ i < j < k \leq N}} f_3(r_{ij}, r_{jk}, r_{ki}) \dots \quad (6.3)$$

is an operator that depends upon the positions of the particles $\mathbf{R} \equiv (\mathbf{r}_1, \dots, \mathbf{r}_N)$ only, and

$$F_{BF} \equiv \prod_{\substack{i,j \\ i < j \leq N}} f_{BF}(ij) \quad (6.4)$$

are Feynman-Cohen backflow⁹² correlations. The non-interacting particle-hole states $| \]$ of the ideal Fermi gas are Slater determinants

$$\Phi(\mathbf{R}) = \det |\phi_i(\mathbf{r}_j)| = \det |e^{i\mathbf{q}_i \cdot \mathbf{r}_j}|. \quad (6.5)$$

The spin functions are suppressed for brevity. The effect of the backflow operator on the determinant can be expressed as

$$F_{BF}\Phi(\mathbf{R}) = \Phi(\mathbf{R}') = \det |\phi_i(\mathbf{r}'_j)|, \quad (6.6)$$

where

$$\mathbf{r}'_i = \mathbf{r}_i + \sum_{j(\neq i)} \eta(r_{ij})\mathbf{r}_{ij}, \quad (6.7)$$

and $\eta(r)$ is a function that is determined variationally.

Comparison of the Fermi CB states (6.1) to the Feynman phonons (4.3) that were used in the Bose case shows two main differences. First, the Fermi gas states $\Phi(\mathbf{R})$ can not be expressed as a product of the non-interacting ground state $\Phi_0(\mathbf{R})$ and the sum of $e^{i\mathbf{q}_i \cdot \mathbf{r}_j}$ factors or their products. Thus, it is impossible to express the Fermi CB states in the form of some simple factor multiplying the exact ground state, as was the case with the Feynman phonons. As a consequence, the CB (variational) ground state $|0\rangle$ is not equal to the true ground state $|\bar{0}\rangle$ of the system. Second, the backflow plays an important role in the Fermi systems since it accounts for the large ($\sim 20\%$) part of the variational ground

state energy, as was found in the case of liquid ^3He .⁹⁰ In contrast, the backflow correlations in Bose systems play the role only in description of excited states⁹² and can be neglected when the total moment of excitations is large.

The CB matrix element of the operator O is given by

$$(\mathbf{p}_1, \dots, \mathbf{h}_n | O | \mathbf{p}'_1, \dots, \mathbf{h}'_{n'}) = \int d^{3N} R \Phi_{\mathbf{p}_1, \dots, \mathbf{h}_n}^*(\mathbf{R}') F^*(\mathbf{R}) O F(\mathbf{R}) \Phi_{\mathbf{p}'_1, \dots, \mathbf{h}'_{n'}}^D(\mathbf{R}'), \quad (6.8)$$

where Φ^D denotes the so-called direct term:

$$\Phi^D(\mathbf{R}) = \prod_i \phi_i(\mathbf{r}_i). \quad (6.9)$$

At zero temperature both n and n' are finite which implies that most of the momentum labels in Φ^* and Φ^D in equation (6.8) are the same. Let \mathbf{q} be one such moment corresponding to the orbital $\phi_i(\mathbf{r}_i)$ in Φ^D . The determinant $\Phi_{\mathbf{p}_1, \dots, \mathbf{h}_n}^*(\mathbf{R}')$ is a sum of $N!$ terms of the form $(-1)^P \prod_j \phi_j(\mathbf{r}_{P(j)})$ corresponding to the different permutations P . If in one of these terms an orbital ϕ_i has an argument other than \mathbf{r}_i (i.e. $P(i) \neq i$ for that particular permutation) then we say that in this term the momentum \mathbf{q} is exchanged, and the term $e^{i\mathbf{q}(\mathbf{r}_i - \mathbf{r}_{P(i)})}$ appear in the integrand of the matrix element (6.8). On the other hand, permutations with $P(i) = i$ do not exchange the momentum \mathbf{q} , and exponential terms cancel out.

When the total momentum k of a CB state is large, and at least one of the particle momenta \mathbf{p}_i is hard (i.e. of order $\sim k$), then the terms in the matrix element (6.8) that contain exchanges of the hard momentum contain factors of the type $e^{\mathbf{k} \cdot \mathbf{r}_{ij}}$, and are exponentially small in the limit $k \rightarrow \infty$. In particular, there must be an equal number of hard momenta in $[\mathbf{p}_1, \dots, \mathbf{h}_n]$ and $[\mathbf{p}'_1, \dots, \mathbf{h}'_{n'}]$ states in order for matrix element to be non-vanishing. On the other hand, the initial state $\rho_{\mathbf{k}}^\dagger | \bar{0} \rangle$ in $S(\mathbf{k}, \omega)$ contains one hard momentum, and we conclude that only the intermediate states with one hard momentum are allowed. Moreover, since the terms in which it is exchanged are vanishingly small, it is not necessary to antisymmetrize the CB states with respect to the particle carrying hard momentum.

Similarly, the analysis of the matrix element $\langle i|\rho_{\mathbf{k}}^\dagger|\bar{0}\rangle$ shows that the index of the particle carrying the hard momentum should not be included in the backflow operator F_{BF} since it would give rise to the factor of the type $e^{\mathbf{k}\cdot(\mathbf{r}_1-\mathbf{r}'_1)}$ causing the matrix element to vanish in the $k \rightarrow \infty$ limit. Thus, we conclude that the CB states suitable for studying of the deep inelastic response of Fermi liquids are given by

$$|\mathbf{P} + \mathbf{h}, \mathbf{p}_1 + \mathbf{h}_1, \dots, \mathbf{p}_n + \mathbf{h}_n; \mathbf{h}, \mathbf{h}_1, \dots, \mathbf{h}_n\rangle, \quad (6.10)$$

where

$$\mathbf{P} = \mathbf{k} - \mathbf{p}_1 - \dots - \mathbf{p}_n \quad (6.11)$$

is the hard particle momentum and equations (6.4) and (6.5) are modified to read

$$F_{BF} = \prod_{\substack{i,j \\ 1 < i < j \leq N}} f_{BF}(ij), \quad (6.12)$$

$$\Phi(\mathbf{R}) = \phi_{\mathbf{P}+\mathbf{h}}(\mathbf{r}_1) \det |\phi_i(\mathbf{r}_j)|, \quad 1 < i < j \leq N, \quad (6.13)$$

$$\phi_{\mathbf{P}+\mathbf{h}}(\mathbf{r}) = e^{i(\mathbf{P}+\mathbf{h})\cdot\mathbf{r}}. \quad (6.14)$$

6.2 CB matrix elements and their properties

We first consider the diagonal CB matrix elements of the Hamiltonian. It can be shown that they are given by³⁵

$$\langle i|H|i\rangle = \langle 0|H|0\rangle + \sum_{p_i} e_v(p_i) - \sum_{h_i} e_v(h_i), \quad (6.15)$$

where $e_v(p_i)$ and $e_v(h_i)$ are variational energies of the particle and hole states respectively. At large momenta \mathbf{P} the energy $e_v(\mathbf{P} + \mathbf{h})$ approaches free particle dispersion relation⁷⁶, and we obtain

$$\langle i|H|i\rangle = \frac{(\mathbf{P} + \mathbf{h})^2}{2m} + O(k^0) = \frac{k^2}{2m} - \frac{\mathbf{k}}{m} \hat{\mathbf{k}} \cdot (\mathbf{p}_1 + \dots + \mathbf{p}_n - \mathbf{h}) + O(k^0). \quad (6.16)$$

Next, we want to find the k -dependence of the off-diagonal CB matrix elements of the Hamiltonian. They are given by

$$\begin{aligned}
& (i|H|j) = \\
& = \int d^{3N}R \phi_{\mathbf{P}+\mathbf{h}}^*(\mathbf{r}_1) \Phi_{\mathbf{p}_1+\mathbf{h}_1, \dots, \mathbf{h}_n}^*(\mathbf{r}'_2, \dots, \mathbf{r}'_N) F^*(\mathbf{R}) \\
& \quad \times \left(-\frac{1}{2m} \sum_i \nabla_i^2 + \sum_{i<j} v_{ij} \right) F(\mathbf{R}) \phi_{\mathbf{P}'+\mathbf{h}'}(\mathbf{r}_1) \Phi_{\mathbf{p}'_1+\mathbf{h}'_1, \dots, \mathbf{h}'_n}^D(\mathbf{r}'_2, \dots, \mathbf{r}'_N) \\
& = \frac{1}{2m} \sum_i \int d^{3N}R \nabla_i \left[\phi_{\mathbf{P}+\mathbf{h}}^*(\mathbf{r}_1) \Phi_{\mathbf{p}_1+\mathbf{h}_1, \dots, \mathbf{h}_n}^*(\mathbf{r}'_2, \dots, \mathbf{r}'_N) F^*(\mathbf{R}) \right] \\
& \quad \cdot \nabla_i \left[F(\mathbf{R}) \phi_{\mathbf{P}'+\mathbf{h}'}(\mathbf{r}_1) \Phi_{\mathbf{p}'_1+\mathbf{h}'_1, \dots, \mathbf{h}'_n}^D(\mathbf{r}'_2, \dots, \mathbf{r}'_N) \right] \\
& \quad + \int d^{3N}R \phi_{\mathbf{P}+\mathbf{h}}^*(\mathbf{r}_1) \Phi_{\mathbf{p}_1+\mathbf{h}_1, \dots, \mathbf{h}_n}^*(\mathbf{r}'_2, \dots, \mathbf{r}'_N) F^*(\mathbf{R}) \\
& \quad \times \sum_{i<j} v_{ij} F(\mathbf{R}) \phi_{\mathbf{P}'+\mathbf{h}'}(\mathbf{r}_1) \Phi_{\mathbf{p}'_1+\mathbf{h}'_1, \dots, \mathbf{h}'_n}^D(\mathbf{r}'_2, \dots, \mathbf{r}'_N). \tag{6.17}
\end{aligned}$$

In the limit $k \rightarrow \infty$ the leading term in equation (6.17) is the one in which the derivatives operate on the hard momentum orbitals $\phi_{\mathbf{P}+\mathbf{h}}$ and $\phi_{\mathbf{P}'+\mathbf{h}'}$, and we obtain

$$\begin{aligned}
& (i|H|j) = \\
& = \frac{(\mathbf{P} + \mathbf{h}) \cdot (\mathbf{P}' + \mathbf{h}')}{2m} \sum_i \int d^{3N}R \phi_{\mathbf{P}+\mathbf{h}}^*(\mathbf{r}_1) \Phi_{\mathbf{p}_1+\mathbf{h}_1, \dots, \mathbf{h}_n}^*(\mathbf{r}'_2, \dots, \mathbf{r}'_N) F^*(\mathbf{R}) \\
& \quad \times F(\mathbf{R}) \phi_{\mathbf{P}'+\mathbf{h}'}(\mathbf{r}_1) \Phi_{\mathbf{p}'_1+\mathbf{h}'_1, \dots, \mathbf{h}'_n}^D(\mathbf{r}'_2, \dots, \mathbf{r}'_N) + O(k^0) \\
& = \frac{1}{2m} \left[k^2 - \mathbf{k} \cdot \left(\sum_{i=1, n} \mathbf{p}_i + \sum_{j=1, n'} \mathbf{p}'_j - \mathbf{h} - \mathbf{h}' \right) \right] (i|j) + O(k^0), \tag{6.18}
\end{aligned}$$

Thus, for large k , the off-diagonal CB matrix elements of the Hamiltonian are proportional to the corresponding matrix elements of the unit operator. We want to stress that this conclusion is valid only because the matrix element of the potential (second term on the right-hand side of equation (6.17)) is finite, even when the potential contains hard-core, because the CB states have proper short range correlations built in thru the operator $F(\mathbf{R})$. In analogous derivation in Bose systems, this issue did not arise since Feynman phonons

contain the exact ground state wave function which implies the identity (4.19).

6.3 OCBPT of $S(\mathbf{k}, \omega)$ for Fermi systems and its y -scaling property

The OCB states are obtained from the CB ones using the Fantoni-Pandharipande orthogonalization procedure defined in subsection 4.2.3. The diagonal matrix elements are preserved in this procedure and, using equation (6.16), we find

$$\langle i | H | i \rangle = (i | H | i) = \frac{k^2}{2m} - \frac{k}{m} \hat{\mathbf{k}} \cdot (\mathbf{p}_1 + \cdots + \mathbf{p}_n - \mathbf{h}) + O(k^0) \quad (6.19)$$

On the other hand, in section 4.3 it was demonstrated that if the off-diagonal CB matrix element of the Hamiltonian is proportional to the corresponding overlap as in equation (6.18), then the off-diagonal OCB matrix element is of the form

$$\langle i | H | j \rangle = O(k). \quad (6.20)$$

The proof presented there used only the properties of the Fantoni-Pandharipande procedure and not the explicit form of the CB states, and is equally applicable here.

OCBPT of $S(\mathbf{k}, \omega)$ for Bose systems was developed in section 4.3. The initial stages of that development are applicable to the Fermi systems as well. Thus in order to calculate DSF $S(\mathbf{k}, \omega)$ and DDRF $D(\mathbf{k}, \omega)$ (equations (4.93)-(4.94)) we divide the Hamiltonian of the system into the diagonal and the off-diagonal parts with the respect to OCB (equations (4.95)-(4.97)) and perform the resolvent expansion (equations (4.98)-(4.100)). Since the state $\rho_{\mathbf{k}}^\dagger | 0 \rangle$ is a member of Feynman phonons OCB and, as a consequence $X_0(i) \sim \delta_{i,\mathbf{k}}$, further simplification of the expansion (4.98) was possible in the Bose case. In contrast, in the Fermi case we have to keep all $X_0(i)$'s in the expression (4.98). However, they have to satisfy sum-rule

$$\sum_i |X_0(i)|^2 = \frac{1}{N} \langle \bar{0} | \rho_{\mathbf{k}} \rho_{\mathbf{k}}^\dagger | \bar{0} \rangle = S(k) \rightarrow 1, \quad \text{when } k \rightarrow \infty, \quad (6.21)$$

and we expect only a few classes of states $|i\rangle$ to be important. For example, since the operator $\rho_{\mathbf{k}}^\dagger$ can be expressed as

$$\rho_{\mathbf{k}}^\dagger = \sum_{\mathbf{q}} a_{\mathbf{k}+\mathbf{q}}^\dagger a_{\mathbf{q}}, \quad (6.22)$$

where a^\dagger and a denote creation and annihilation operators of the ideal gas states, we expect that the main contribution comes from the particle-hole states

$$|i\rangle = |\mathbf{k} + \mathbf{h}, \mathbf{h}\rangle. \quad (6.23)$$

Even though the Fermi case is more complicated than the Bose one, it is still possible to sum the series (4.98) to all orders with the following Dyson-like equations⁹³:

$$D(\mathbf{k}, \omega) = \sum_i X_0^*(i) G_0(i) X(i), \quad (6.24)$$

where $X(i)$ is dressed $\rho_{\mathbf{k}}^\dagger$ matrix element

$$X(i) = X_0(i) - \sum_j H'_{ij} G_0(j) X(j). \quad (6.25)$$

We now proceed to prove that $S(\mathbf{k}, \omega)$ of the Fermi systems scales in the limit $k \rightarrow \infty$.

From equations (4.100) and (6.19) we find

$$\begin{aligned} G_0(i) &\equiv \langle i | [\omega - H_0 + E_0 + i\eta]^{-1} | i \rangle \\ &= [\omega - \frac{k^2}{2m} + \frac{k}{m} \hat{\mathbf{k}} \cdot (\mathbf{p}_1 + \cdots + \mathbf{p}_n - \mathbf{h}) + O(k^0) + i\eta]^{-1} \\ &= \frac{m}{k} g_0(i) + O(k^{-2}), \end{aligned} \quad (6.26)$$

where

$$g_0(i) = [y - \hat{\mathbf{k}} \cdot (\mathbf{p}_1 + \cdots + \mathbf{p}_n - \mathbf{h}) + i\eta]^{-1}, \quad (6.27)$$

and from equation (6.20) we obtain

$$H'_{ij} = \frac{k}{m} h'_{ij} + O(k^0). \quad (6.28)$$

It was argued in section 6.1 that the CB matrix element $\langle i | \rho_{\mathbf{k}}^\dagger | \bar{0} \rangle$ is of the order $O(k^0)$ since k -dependencies of the exponent in $\rho_{\mathbf{k}}^\dagger$ and in $\phi_{\mathbf{p}+\mathbf{h}}^*(\mathbf{r}_1)$ cancel each other. The OCB matrix

elements $X_0(i)$ are linear combinations of the above CB matrix elements and thus are also of the order $O(k^0)$:

$$X_0(i) \equiv \frac{1}{\sqrt{N}} \langle i | \rho_{\mathbf{k}}^\dagger | \bar{0} \rangle = O(k^0). \quad (6.29)$$

Finally, using equations (6.24)-(6.25) and (6.28)-(6.29) we obtain

$$\frac{k}{m} D(\mathbf{k}, \omega) = D_S(y) + O(k^{-1}), \quad (6.30)$$

where

$$D_S(y) = \sum_i X_0^*(i) g_0(i) X(i), \quad (6.31)$$

$$X(i) = X_0(i) - \sum_j h'_{ij} g_0(j) X(j), \quad (6.32)$$

which implies that $\frac{k}{m} S(\mathbf{k}, \omega)$ for the Fermi systems y -scales in the limit $k \rightarrow \infty$:

$$\frac{k}{m} S(\mathbf{k}, \omega) = J(y) + O(k^{-1}), \quad (6.33)$$

$$J(y) = -\frac{1}{\pi} \text{Im} \sum_i X_0^*(i) g_0(i) X(i). \quad (6.34)$$

From equation (6.34) it follows that the scaling function $J(y)$ of the Fermi system is determined by the functions $X(i)$ which are, in turn, determined by the off-diagonal OCB matrix elements of the Hamiltonian h'_{ij} and the functions $X_0(i)$ (equation (6.32)). Calculation of these matrix elements is coupled with considerable technical difficulties. For example, they depend upon twice the number of momentum labels than their Bose counterparts which raises the dimensionality of the integrals used in their evaluation. Also, the Löwdin expansion (equation (4.59)) is divergent when applied to liquid ^3He CB states, and alternative techniques of performing the Löwdin transform, discussed in the subsection 4.2.2, must be used instead. In light of these remarks, the calculation of the scaling function $J(y)$ of the Fermi systems remains a challenging problem.

Bibliography

- [1] R.A. Cowley and A.D.B. Woods, *Can. J. Phys.* **49**, 177(1971).
- [2] P. Martel, E.C. Svensson, A.D.B. Woods, V.F. Sears, and R.A. Cowley, *J. Low Temp. Phys.* **23**, 285(1976).
- [3] A.D.B. Woods and V.F. Sears, *Phys. Rev. Lett.* **39**, 415(1977).
- [4] V.F. Sears, E.C. Svensson, P. Martel, and A.D.B. Woods, *Phys. Rev. Lett.* **49**, 415(1982).
- [5] H.A. Mook, *Phys. Rev. Lett.* **32**, 1167(1974).
- [6] H.A. Mook, *Phys. Rev. Lett.* **51**, 1454(1983).
- [7] P.E. Sokol, K. Skold, D.L. Price, and R. Kelb, *Phys. Rev. Lett.* **54**, 909(1985).
- [8] H.A. Mook, *Phys. Rev. Lett.* **55**, 2452(1985).
- [9] H.R. Glyde and E.C. Svensson in *Methods in Experimental Physics* Vol.23 part B, ed. D.L. Price and K. Skold, Academic Press, 1987.
- [10] T.R. Sosnick, W.M. Snow, P.E. Sokol, and R.N. Silver, *Europhys. Lett.* **9** 707(1989).
- [11] P.E. Sokol in *Momentum Distributions*, ed. R.N. Silver and P.E. Sokol, Plenum Press, 1989.
- [12] G.B. West, *Phys. Rep.* **18C**, 263(1975).
- [13] P.C. Hohenberg and P.M. Platzman, *Phys. Rev.* **152**, 198(1966).
- [14] L.J. Rodriguez, H.A. Gerch, and H.A. Mook, *Phys. Rev.* **A9**, 2085(1974).
- [15] G. Reiter and R.N. Silver, *Phys. Rev. Lett.* **54**, 1047(1985).
- [16] R.N. Silver and G. Reiter, *Phys. Rev.* **B35**, 3647(1987).
- [17] R.N. Silver, *Phys. Rev.* **B37**, 3794(1988).
- [18] R.N. Silver, *Phys. Rev.* **B38**, 2283(1988).
- [19] R.N. Silver, *Phys. Rev.* **B39**, 4022(1989).

- [20] R.N. Silver in *Momentum Distributions*, ed. R.N. Silver and P.E. Sokol, Plenum Press, 1989.
- [21] P.M. Platzman and N. Tzoar, Phys. Rev. **B30**, 6397(1984).
- [22] C. Carraro, Ph.D. thesis, Caltech, 1990 (unpublished).
- [23] C. Carraro and S.E. Koonin, Phys. Rev. **B41**, 6741(1990).
- [24] C. Carraro and S.E. Koonin, Phys. Rev. Lett. **65**, 2792(1990).
- [25] H.A. Gerch and L.J. Rodriguez, Phys. Rev. **A8**, 905(1973).
- [26] A.S. Rinat and R. Rosenfelder, Phys. Lett. **B193**, 411(1987).
- [27] A.S. Rinat, Phys. Rev. **B36**, 5171(1987).
- [28] A.S. Rinat, Phys. Rev. **B40**, 6625(1989).
- [29] A.S. Rinat and M.F. Taragin, Phys. Rev. **B41**, 4247(1990).
- [30] J.J. Weinstein and J.W. Negele, Phys. Rev. Lett. **49**, 1016(1982).
- [31] V.F. Sears, Phys. Rev. **185**, 200(1969).
- [32] V.F. Sears, Phys. Rev. **B30**, 44(1984).
- [33] S. Stringari, Phys. Rev. **B35**, 2038(1987).
- [34] E. Feenberg, *Theory of Quantum Liquids*, Academic Press, 1969.
- [35] S. Fantoni and V.R. Pandharipande, Phys. Rev. **C37**, 1697(1988).
- [36] A. Belić and V.R. Pandharipande, Phys. Rev. **B39**, 2696(1989).
- [37] A. Belić and V.R. Pandharipande, to be published in Phys. Rev. **B45**.
- [38] A. Belić and V.R. Pandharipande, to be published.
- [39] M. Born, Z. Physik **38**, 803(1926).
- [40] M. Born and J.P. Oppenheimer, Ann. Phys. **84**, 457(1928).
- [41] H. Geiger and E. Marsden, Proc. Roy. Soc. **A82**, 495(1909).
- [42] J. Franck and G. Hertz, Verh. Dtsch. Phys. Ges. **16**, 512(1914).
- [43] E. M. Lyman, A. O. Hanson and M. B. Scott, Phys. Rev. **84**, 525(1951).
- [44] J. J. Aubert et al. (EMC), Phys. Lett. **123B**, 275(1983).
- [45] E. Fermi, Ricerca Sci. **7**, 13(1936).
- [46] E. Fermi, *Nuclear Physics*, U. of Chicago press, 1950, p.142.

- [47] L. Van Hove, Phys. Rev. **95**, 249(1954).
- [48] J.D. Bjorken, Phys. Rev. **179**, 1547(1969).
- [49] J. Kuti and V.F. Weisskopf, Phys. Rev. **D4**, 3418(1971).
- [50] R.P. Feynman, *Photon-Hadron Interactions*, Addison-Wesley, 1989.
- [51] J. Glimm and A. Jaffe, *Quantum Physics A Functional Integral Point of View*, Springer-Verlag, 1981.
- [52] G. Molière, Z. Naturforsch. **2**, 133(1947).
- [53] B.A. Lippmann and J. Schwinger, Phys. Rev. **79**, 469(1950).
- [54] R.P. Feynman, Phys. Rev. **94**, 262(1954).
- [55] E. Manousakis and V.R. Pandharipande, Phys. Rev. **B33**, 150(1986).
- [56] E. Manousakis, Ph.D. thesis, U. of Illinois, 1985 (unpublished).
- [57] A. Bijl, Physica **7**, 869(1940).
- [58] R. Jastrow, Phys. Rev. **98**, 1479(1955).
- [59] J.C. Ward, Phys. Rev. **78**, 1834(1950).
- [60] Y. Takahashi, Nuov. Cim. **6**, 370(1957).
- [61] P.A. Whitlock, D.M. Ceperley, G.V. Chester, and M.H. Kalos, Phys. Rev. B **19**, 5598(1979).
- [62] M.H. Kalos, M.A. Lee, P.A. Whitlock, and G.V. Chester, Phys. Rev. B **24**, 115(1981).
- [63] J.G. Kirkwood, J. Chem. Phys. **3**, 300(1935).
- [64] R.A. Aziz, V.P.S. Nain, J.S. Carley, W.L. Taylor, and G.T. McConville, J. Chem. Phys. **70**, 4330(1979).
- [65] W.L. McMillan, Phys. Rev. **138**, 442(1965).
- [66] F.J. Pinski and C.E. Campbell, Phys. Lett. **79B**, 23(1978).
- [67] Q.N. Usmani, S. Fantoni, and V.R. Pandharipande, Phys. Rev. **B26**, 6123(1982).
- [68] E. Manousakis, V.R. Pandharipande, and Q.N. Usmani, Phys. Rev. **B31**, 7022(1985); *ibid.* **B43**, 13587(1991).
- [69] F.Y. Wu, J. Low Temp. Phys. **9**, 177(1972).
- [70] H.W. Jackson and E. Feenberg, Rev. Mod. Phys. **34**, 686(1962).
- [71] F.Y. Wu and M.K. Chien, J. Math. Phys. **11**, 1912(1970).

- [72] E. Krotscheck and J.W. Clark, Nucl. Phys. **A328**, 73(1979).
- [73] S. Fantoni, Phys. Rev. **B29**, 2544(1984).
- [74] E. Krotscheck and R.A. Smith, Phys. Rev. **B27**, 4222(1983).
- [75] A. Fabrocini et al., Phys. Rev. **B33**, 6057(1986).
- [76] S. Fantoni, B.L. Friman, and V.R. Pandharipande, Nucl. Phys. **A339**, 51(1983).
- [77] S. Fantoni and V.R. Pandharipande, Nucl. Phys. **A427**, 473(1984).
- [78] P.O. Löwdin, J. Chem. Phys. **18**, 365(1950).
- [79] C.W. Woo, Phys. Rev. **151**, 138(1966).
- [80] H. Padé, Ann. Ecole Super. Normale **9**, Suppl., 1(1892).
- [81] G.A. Baker in *Advances in Theoretical Physics*, ed. K.A. Brueckner, Vol.1, pp 1-58, Academic Press, New York.
- [82] H.N. Robkoff and R.B. Hallock, Phys. Rev. **B25**, 1572(1982).
- [83] F.J. Dyson, Phys. Rev. **75**, 1736(1949).
- [84] J. Schwinger, Proc. Nat. Acad. Sci. **37**, 452(1951); *ibid.* **37**, 455(1951).
- [85] H. Kramers, Atti. Congr. Intern. Fisici (Como) **2**, 545(1927).
- [86] R. Kronig, J. Amer. Opt. Soc. **12**, 547(1926).
- [87] V.S. Vladimirov, *Equations of the Mathematical Physics*, Marcel Dekker, 1971.
- [88] M.J. Lighthill, *Introduction to Fourier Analysis and Generalised Functions*, Cambridge University Press, 1959.
- [89] J. Gavoret and P. Nozières, Ann. Phys. (NY) **28**, 349(1964).
- [90] E. Manousakis, S. Fantoni, V.R. Pandharipande, and Q.N. Usmani, Phys. Rev. **B28**, 3770(1983).
- [91] K.E. Schmidt, M.A. Lee, M.H. Kalos, and G.V. Chester, Phys. Rev. Lett. **47**, 807(1981).
- [92] R.P. Feynman and M. Cohen, Phys. Rev. **102**, 1189(1956).
- [93] S. Fantoni and V.R. Pandharipande, Nucl. Phys. **A473**, 234(1987).

Vita

Aleksandar Belić was born on April 22, 1962 in Belgrade, Yugoslavia. He graduated from Fifth Belgrade Gymnasium in May of 1980. He enrolled in University of Belgrade in September of 1981, and received Diploma in Physics in July of 1985. He then entered the graduate college of the University of Illinois in August 1985, and received an M. S. degree in 1987.